



*Citation for published version:*

Raithby, P, Bagherzadeh, M, Mahmoudi, H, Ataie, S, Bahjati, M, Kia, R & Vaccaro, L 2019, 'Synthesis and characterization of a new zwitterionic palladium complex as an environmentally friendly catalyst for the Heck-Mizoroki coupling reaction in GVL', *Journal of Molecular Catalysis A: Chemical*, vol. 474, 110406. <https://doi.org/10.1016/j.mcat.2019.110406>

*DOI:*

[10.1016/j.mcat.2019.110406](https://doi.org/10.1016/j.mcat.2019.110406)

*Publication date:*

2019

*Document Version*

Peer reviewed version

[Link to publication](#)

*Publisher Rights*

CC BY-NC-ND

**University of Bath**

**Alternative formats**

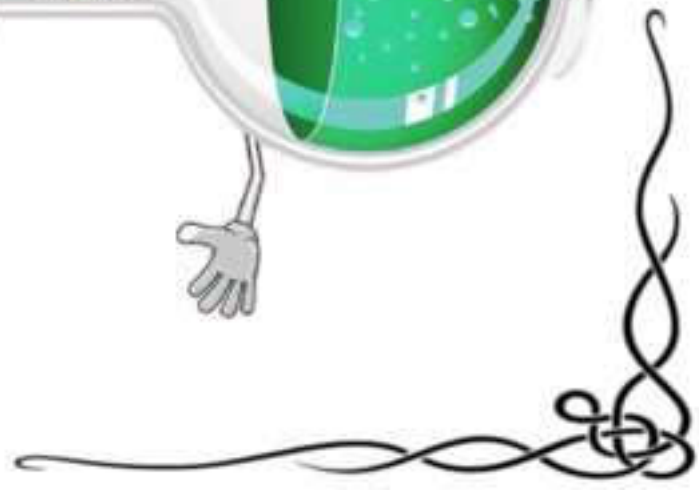
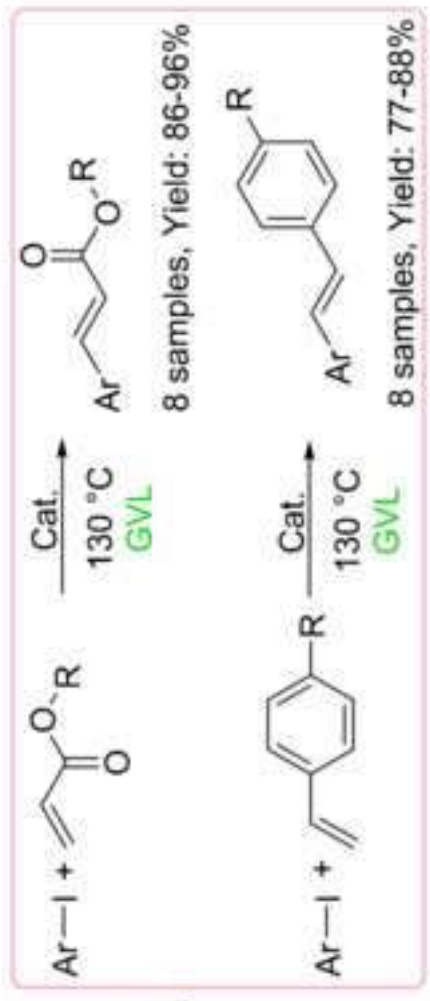
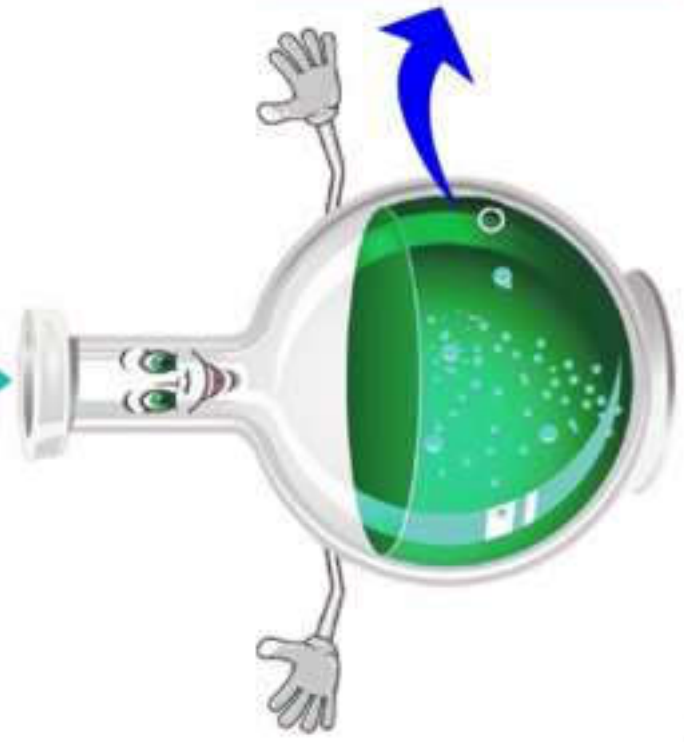
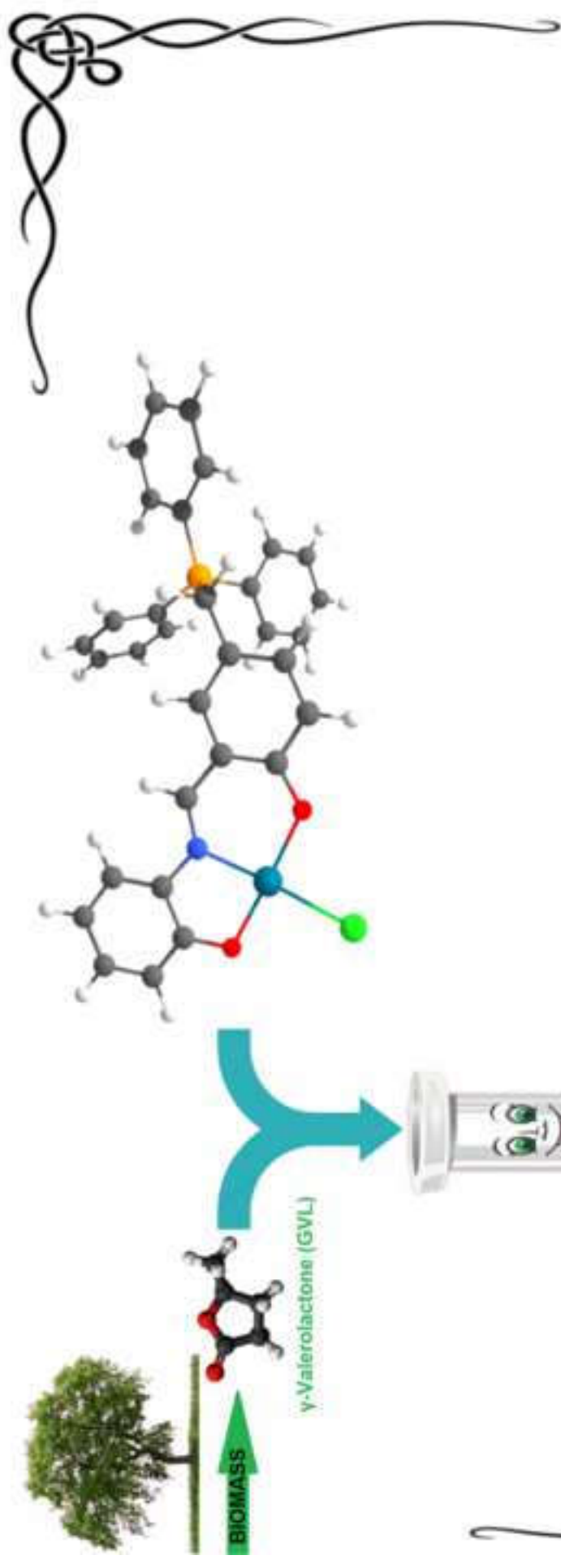
If you require this document in an alternative format, please contact:  
[openaccess@bath.ac.uk](mailto:openaccess@bath.ac.uk)

**General rights**

Copyright and moral rights for the publications made accessible in the public portal are retained by the authors and/or other copyright owners and it is a condition of accessing publications that users recognise and abide by the legal requirements associated with these rights.

**Take down policy**

If you believe that this document breaches copyright please contact us providing details, and we will remove access to the work immediately and investigate your claim.



## Synthesis and Characterization of a new Zwitterionic Palladium Complex as an Environmentally Friendly Catalyst for the Heck-Mizoroki Coupling Reaction

Mojtaba Bagherzadeh,<sup>\*a</sup> Hamed Mahmoudi,<sup>a</sup> Saeed Ataie,<sup>a</sup> Mohammad Bahjati,<sup>a</sup> Reza Kia<sup>a</sup>, Paul R. Raithby<sup>b</sup> and Luigi Vaccaro<sup>\*c</sup>

<sup>a</sup> Chemistry Department, Sharif University of Technology, Tehran, P.O. Box 11155-3516, Iran

<sup>b</sup> Chemistry Department, University of Bath, Bath, BA2 7AY, UK

<sup>c</sup> Green SOC – Dipartimento di Chimica Biologia e Biotecnologie, Università degli Studi di Perugia, I-06123, Perugia, Italy;

E-mail: luigi.vaccaro@unipg.it

### Highlights

- Synthesis of a palladium (II)/Shiff base catalytic system.
- Use of green solvent GVL
- Heck-Mizoroki reaction performed with high efficiency and with up to to 96% yield.
- TOF up to 4000/h

## Synthesis and Characterization of a new Zwitterionic Palladium Complex as an Environmentally Friendly Catalyst for the Heck-Mizoroki Coupling Reaction in GVL

Mojtaba Bagherzadeh,<sup>\*a</sup> Hamed Mahmoudi,<sup>a</sup> Saeed Ataie,<sup>a</sup> Mohammad Bahjati,<sup>a</sup> Reza Kia<sup>a</sup>, Paul R. Raithby<sup>b</sup> and Luigi Vaccaro<sup>\*c</sup>

<sup>a</sup> Chemistry Department, Sharif University of Technology, Tehran, P.O. Box 11155-3516, Iran

<sup>b</sup> Chemistry Department, University of Bath, Bath, BA2 7AY, UK

<sup>c</sup> Green SOC – Dipartimento di Chimica Biologia e Biotecnologie, Università degli Studi di Perugia, I-06123, Perugia, Italy;

E-mail: luigi.vaccaro@unipg.it

**Abstract.** A new zwitterionic Palladium (II) complex has been synthesized by the one-pot mixing of Pd(OAc)<sub>2</sub>, 2-aminophenol and (3-formyl-4-hydroxy-5-methylbenzyl) triphenylphosphonium chloride, in refluxing ethanol. The metal complex formed was characterized by <sup>1</sup>H NMR, <sup>13</sup>C NMR, <sup>31</sup>P NMR and X-ray crystallographic technique and its efficiency tested as a homogeneous pre-catalyst in Heck-Mizoroki cross coupling reaction using  $\gamma$ -Valerolactone (GVL) as a biomass-derived green medium. All the products were obtained in good to excellent yields.

**Keywords:** Cross-coupling reactions, Heck-Mizoroki coupling, Zwitterionic complex, Green chemistry

### 1. Introduction

The palladium-catalyzed coupling reactions have confirmed as one of the most efficient synthetic tools for carbon-carbon bonds with precision reliability [1]. Among them, Heck-Mizoroki reaction has been widely applied and still are attracting the attention of researchers who are aiming at finely tune their efficiency and applications [2]. Indeed, this reaction allows the widely general preparation of valuable compounds that find applications in a variety of fields such as in the synthesis of natural products, agrochemicals, pharmaceutical intermediates, and innovative materials [3] Most of the efforts for improving the efficiency of this reaction is directed towards the identification of effective catalytic systems that may allow defining faster milder reaction conditions [4].

Among the transition metals with catalytic ability in the carbon-carbon coupling reactions, palladium is still one of the most effective and widely employed [1f, 5]. In addition, the use of adequate ligands can strongly affect the catalytic performance of the metal [6]. Our interest has been often directed towards the preparation of Schiff base type ligands which have proven to be effective in the creation of a good  $\pi$ -conjugated electron system and in addition not less importantly, can be accessed with highly reliable synthetic procedures [7] The design and preparation of effective ligands may lead to effective palladium catalysts that do not need any co-catalyst or additives still allowing to define a protocol operating under mild conditions.

The natural sources, no more have enough potential to satisfy demands for various types of compounds in fine chemical and drug industries, and in this cumbersome circumstance, applying effective synthetic procedures can effectively and efficiently help the situation [8].

Heck-Mizoroki reaction (firstly introduced by Tsutomu Mizoroki [9] and described by Richard F. Heck [10] about half a century ago) which introduces a palladium-catalyzed carbon-carbon bond forming reaction, has been proved as a assorted gadget in synthetic chemistry for creation of compounds and resourceful procedure in the procurement of fine chemicals, natural products, agrochemicals and pharmaceutical intermediates as well as for materials chemistry [3g, 11].

The solvent used as a reaction medium represents another parameter that obviously influences the efficiency of a catalytic system. In addition, nowadays solvents play a crucial in shaping the overall chemical and environmental efficiency of synthetic protocols as they are directly related to critical safety, and toxicity issues. Among these aspects, the EHS (Environmental, Health, and Safety aspects) are the most important. Unfortunately, most of the organic solvents generally used in the design and synthesis of novel catalytic systems for cross-coupling protocols are toxic information on their behavior in safer solvents and conditions are not accessible [12]. Since many years we have been investigating the use of safer solvents as an alternative to classic wasteful and toxic reaction media generally used in cross-coupling protocols [1d, 13]. We have found that gamma-valerolactone (GVL), is a very effective non-toxic biomass-derived solvent alternative to replace the use of classic polar aprotic solvents such as DMF, DMA, and NMP. It is a valuable chemical deriving from - manipulation of lignocellulosic biomasses [14], possessing interesting physical properties [15].

Therefore, we have directed our investigation towards the design and synthesis of a palladium/Schiff base catalytic system specifically aiming at the evaluation of its efficiency in GVL. In this work, the novel zwitterionic palladium (II) Schiff Base complex **1** was synthesized and characterized by different techniques including its DFT computational study. We tested the zwitterionic complex **1** as a catalyst in the Heck-Mizoroki coupling reaction in GVL as a green medium (Figure 1).

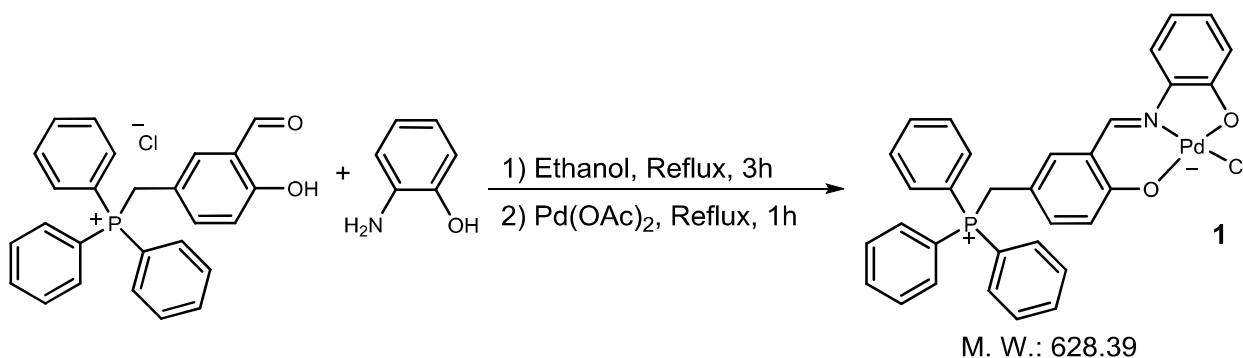


**Figure 1.** Synthesis of zwitterionic complex **1**

## 2. Experimental

### 2.1 Materials and methods

5-(Chloromethyl)-2-hydroxybenzaldehyde and (3-Formyl-4-hydroxy-5-methylbenzyl) triphenylphosphonium chloride was synthesized according to the previously published procedures [16]. All other chemicals and solvents were purchased from Merck and Sigma-Aldrich companies and were used without further purification. Elemental analyses for carbon, hydrogen, and nitrogen (CHN) were performed on a leco truspec elemental analyzer. FT-IR spectra were obtained employing KBr pellets on a Bruker Tensor 27 FT-IR spectrophotometer. The NMR spectra were recorded at room temperature with a Bruker FT-NMR 400 MHz ( $^1\text{H}$  at 400 MHz,  $^{13}\text{C}$  at 100.6 MHz and  $^{31}\text{P}$  at 162 MHz) spectrometer in  $\text{CDCl}_3$  or  $\text{DMSO-d}_6$ . The progress of catalytic reactions was performed by an Agilent Technologies 6890 N gas chromatography, equipped with a 19091J-236 HP-5, 5% phenyl methyl siloxane capillary column.

## 2.2 X-ray Crystallography

Single crystals of the complex suitable for X-ray diffraction analysis were grown by an ethanolic solution of the complex. X-ray intensity data were collected using the full sphere routine by  $\phi$  and  $\omega$  scans strategy on the Agilent *SuperNova* dual wavelength EoS S2 diffractometer with mirror monochromated Cu  $K\alpha$  radiation ( $\lambda = 1.54184 \text{ \AA}$ ). For the data collections, the crystal was cooled to 150 K using an Oxford diffraction Cryojet low-temperature attachment. The data reduction, including an empirical absorption correction using spherical harmonics, implemented in *SCALE3 ABSPACK* scaling algorithm [17], was performed using the *CrysAlisPro* software package [18]. The crystal structure of the complex was solved by direct methods using the online version of *AutoChem 2.0* in conjunction with *OLEX2* [19] suite of programs implemented in the *CrysAlis* software, and then refined by full-matrix least-squares (*SHELXL-97*) [20] on  $F^2$ . The non-hydrogen atoms were refined anisotropically. All of the hydrogen atoms were positioned geometrically in idealized positions and refined with the riding model approximation, with  $U_{\text{iso}}(\text{H}) = 1.2$  or  $1.5 U_{\text{eq}}(\text{C})$ . For the molecular graphics, the program *SHELXTL* [21] was used. All geometric calculations were carried out using the *PLATON* software [22]. One of the water molecules (O1W) is not fully occupied and was disordered over a center of inversion.

## 2.3 Synthesis of zwitterionic complex 1

To a refluxing and stirring solution of 1.5 mmol (3-Formyl-4-hydroxy-5-methylbenzyl) triphenylphosphonium chloride in 20 mL Ethanol, a solution of 2-Aminophenol (1.5 mmol in 20 mL Ethanol) was added dropwise. After 3h, 1.5 mmol  $\text{Pd}(\text{OAc})_2$  in 100 mL Ethanol was added to the above solution. As soon as, adding the Pd precursor to the solution, a green-brown powder was precipitated. After 1 h the precipitation has been completed and the complex was separated by filtration and washed with hot ethanol to remove unreacted materials and dry in air. (679 mg, 72% yield). Anal. Calc. for  $\text{PdO}_2\text{NCIPC}_{32}\text{H}_{25}$ : C 61.16, H 4.01, N 2.23%. found: C 61.23, H 4.01, N 2.22%.  $^1\text{H}$  NMR (400 MHz, DMSO)  $\delta$ : 8.30 (s, 1H), 7.93 – 7.85 (m, 3H), 7.82 – 7.52 (m, 13H), 7.33 – 7.18 (m, 1H), 6.99 – 6.88 (m, 1H), 6.69 (m, 3H), 6.47 (m, 1H), 5.16 – 4.90 (d,  $^2J_{\text{PH}}=14.23$  Hz, 2H).  $^{13}\text{C}$  NMR (101 MHz, DMSO)  $\delta$ : 167.67 (s), 162.42 (d,  $J_{\text{PC}}=1.91$  Hz), 145.34 (s), 139.33(s), 136.79 (s), 136.73 (d,  $J_{\text{PC}}=2.53$  Hz), 134.96 (d,  $J_{\text{PC}}=2.53$  Hz), 134.05 (d,  $J_{\text{PC}}=9.68$  Hz), 130.10 (d,  $J_{\text{PC}}=12.22$  Hz), 128.79 (s), 121.41 (d,  $J_{\text{PC}}=2.32$  Hz), 120.91 (s), 118.05 (d,  $J_{\text{PC}}=84.77$  Hz), 118.00 (s), 115.96 (s), 113.63 (s), 111.84 (d,  $J_{\text{PC}}=8.44$  Hz), 27.55 (d,  $J_{\text{PC}}=45.54$  Hz).  $^{31}\text{P}$  NMR (162 MHz, DMSO)  $\delta$ : 21.54 (s).

## 2.4 General procedure for Catalytic Heck Cross-coupling reaction

In a 4 mL screw-capped vial equipped with magnetic stirrer, 0.5 mmol Aryl halide, 0.75 mmol Alkene, 1.5 mmol bases,  $3.2 \times 10^{-2}$  mol% of catalyst **1** (using stock solution prepared by dissolving 0.002 g,  $3.18 \times 10^{-3}$  mmol complex **1** in 10 mL solvent) was mixed with together and temperature raised to 130 °C. After 90 min, the system was cooled to room temperature and 2 mL of n-Hexane was added to the system. The liquid extraction was performed by adding water (3×2 mL) to extracting the GVL. Finally, the product (**3** or **4**) was obtained by distillation of n-Hexane. Final purification of the catalytic product was performed by using flash chromatography.

### 3. Results and discussion

#### 3.1 Synthesis and characterization

Zwitterionic complex **1** was synthesized by the addition of Pd(OAc)<sub>2</sub> to a refluxing solution of (3-Formyl-4-hydroxy-5-methylbenzyl) triphenylphosphonium chloride and 2-aminophenol in ethanol (Fig. 1).

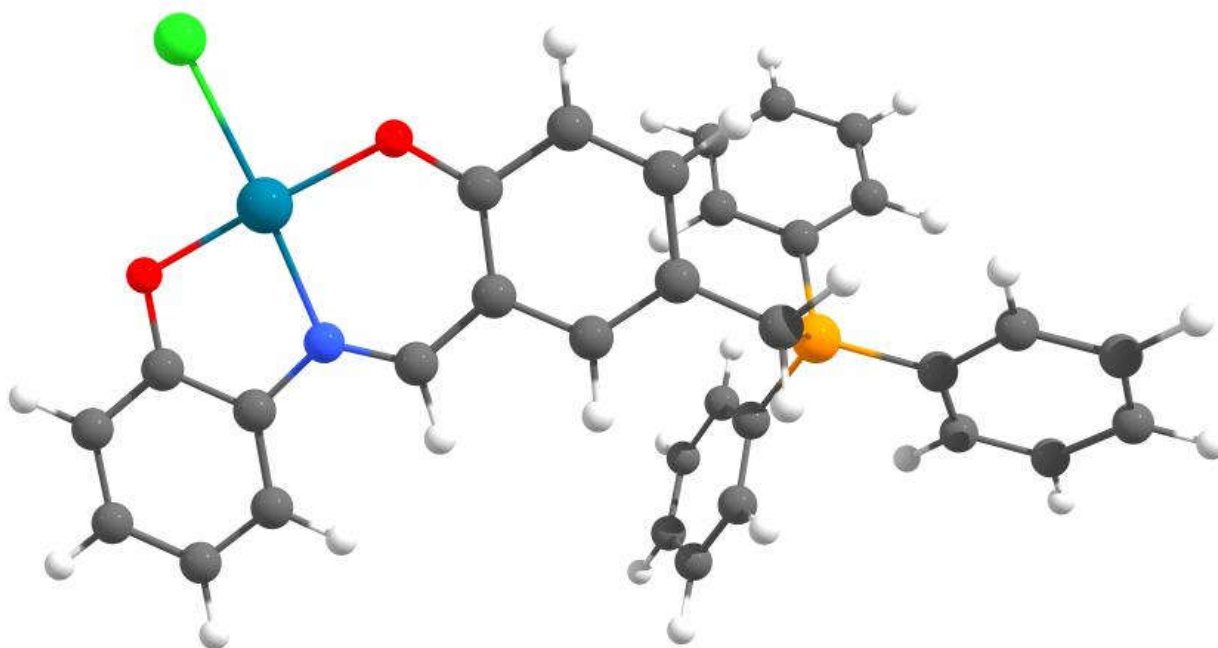
A singlet resonance at  $\delta=8.30$  ppm appears in the <sup>1</sup>H NMR spectrum of zwitterionic complex **1** (Fig. S3, supporting information), which is designated to the hydrogen of Schiff-base group (H5, Fig S3). Three sets of multiple resonances between  $\delta=7.61$ -7.91 ppm are assigned to hydrogens of phenyl phosphonium rings. The signal between  $\delta=7.87$ -7.91 ppm can be allocated to para-hydrogen of phenyl phosphonium rings, and also the pattern of this resonance looks like an incomplete triplet, due to the long-range coupling of these hydrogens with phosphor and other hydrogens. The resonance of Meta and Ortho positions of phenyl phosphonium rings are appeared at  $\delta=7.72$ -7.77 ppm and  $\delta=7.65$ -7.70 ppm respectively, and they are also merged together. As shown in the <sup>1</sup>H-<sup>1</sup>H COSY NMR spectrum (Fig. S6), these three sets of signals are correlated together. According to <sup>1</sup>H-<sup>1</sup>H COSY NMR spectrum, two sets of the doublet pattern can be observed at  $\delta= 7.79$  and  $\delta= 6.64$  ppm and they are assigned to H6 and H9, respectively. Other two sets of resonance with a triplet pattern at  $\delta= 6.46$  and  $\delta= 6.94$  ppm can be assigned to H7 and H8 hydrogens, respectively. The H6-H9 hydrogens are correlated together, as observed in the <sup>1</sup>H-<sup>1</sup>H COSY NMR spectrum. The resonance of H3 and H4 are appeared at  $\delta= 6.67$  and  $\delta= 6.62$  ppm respectively. These two hydrogens are merge and correlated together and they split each other into doublet signals. Another signal at  $\delta= 7.29$  ppm is related to H2 and this hydrogen is correlated with benzylic hydrogen as shown in the <sup>1</sup>H-<sup>1</sup>H COSY NMR spectrum. At last, the resonance of benzylic hydrogens is appeared at  $\delta=5.03$  ppm which has a doublet pattern with <sup>2</sup>J<sub>PH</sub>=14.23 Hz.

As well as, <sup>13</sup>C NMR, <sup>1</sup>H-<sup>13</sup>C HSQC, and <sup>1</sup>H-<sup>13</sup>C HMBC analyses are performed to confirm these assignments (Fig. S4, S7, S8). And also, a resonance at  $\delta=21.54$  ppm in <sup>31</sup>P NMR of complex **1** (Fig. S5) confirmed that just one type of phosphorus atom exists in the complex structure and the chemical shift of this signal is in the range of phosphonium salt chemical shifts [22].

#### 3.3 DFT studies

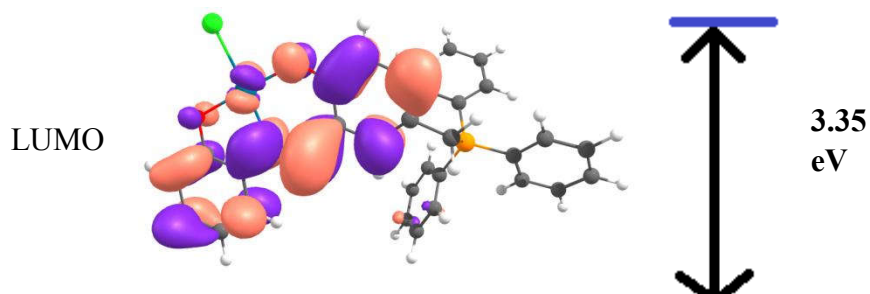
Full geometry optimization was performed in ethanol (CPCM model) for zwitterionic complex **1** in DFT B3LYP level with 6-311++g(d,p) basis set for all ligands atoms and LANL2DZ for Palladium by using Gaussian 09 package [23]. After optimization, the absence of negative frequency in the calculated vibrational spectrum showed that complex **1** was in the minimum energy level.

Optimized structure of **1** is shown in Fig. 2. (Details of optimized bonds lengths and angles are illustrated in table S3 and S4 in supporting information).



**Figure 2.** Optimized structure of zwitterionic complex **1**

The contour map of frontier molecular orbitals of **1** is shown in Fig. 3, Fig. S1 and the energy and composition of them are shown in Table S5. In general, it is very important to understand the nature of frontier molecular orbitals, because they play a vital role in both chemical activity and electronic transitions of the complex. These data confirm that zwitterionic complex **1** has a closed-shell structure. According to Fig. 3, and table S5, for complex **1**, the HOMO and LUMO orbitals are distributed over the ligand and only 3% of these two frontier molecular orbitals is located on the palladium. The large energy gap between HOMO and LUMO (3.35 eV) illustrates the low chemical activity and kinetic stability of this complex [24].





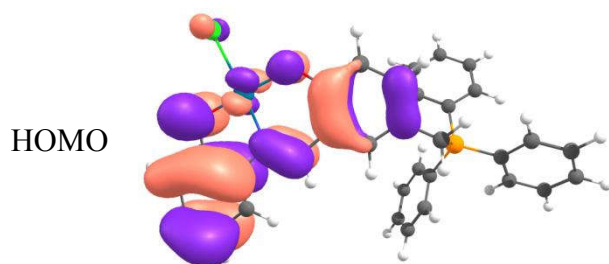


**Figure 3.** Contour map of the HOMO and LOMO orbitals of zwitterionic complex **1**

### 3.4. X-ray Crystal Structure

The solid-state structure of complex **1** was determined by X-ray crystallography and the ORTEP of the complex was shown with their atom-labeling scheme in Fig. 4. Details of data collection and refinement parameters are given in Table 1. Selected bond lengths and angles are listed in Table S1. The details of the intermolecular interactions are summarized in Table 2.

**Table 1.** Crystal data and refinement parameters of complex **1**

Empirical formula	<a href="#">C32H31NO5PClPd</a> . 0.53 H <sub>2</sub> O
Formula mass	<a href="#">691.94</a>
Crystal size (mm)	<a href="#">0.08</a> × <a href="#">0.03</a> × <a href="#">0.02</a>
Color	red
Crystal system	triclinic
Space group	<a href="#">P-1</a>
$\vartheta_{\max}$ (°)	73.03
$a$ (Å)	<a href="#">10.6165(4)</a>
$b$ (Å)	11.0509(3)
$c$ (Å)	<a href="#">14.6958(6)</a>
$\alpha$ (°)	<a href="#">89.951(3)</a>
$\beta$ (°)	76.172(3)
$\gamma$	(°) 63.400(3)
$V$ (Å <sup>3</sup> )	1485.73(10)
$Z$	2
$D_{\text{calc}}$ (Mg/m <sup>3</sup> )	<a href="#">1.547</a>
$\mu$	(mm <sup>-1</sup> ) 6.740
$F(000)$	707
Index ranges	-10 ≤ $h$ ≤ 13 -12 ≤ $k$ ≤ 13 -17 ≤ $l$ ≤ 18
No. of measured reflns.	17529
No. of independent reflns./ $R_{\text{int}}$	5883/ <a href="#">0.034</a>
No. of observed reflns. $I > 2\sigma(I)$	5510
No. of parameters	379
Goodness-of-fit (GOF)	1.034

$R_1$ (observed data)	0.0269
$wR_2$ (all data) <sup>a</sup>	0.0669

a)  $w=1/[\sigma^2(F_o^2)+(0.0310P)^2+0.6995P]$  where  $P=(F_o^2+2F_c^2)/3$

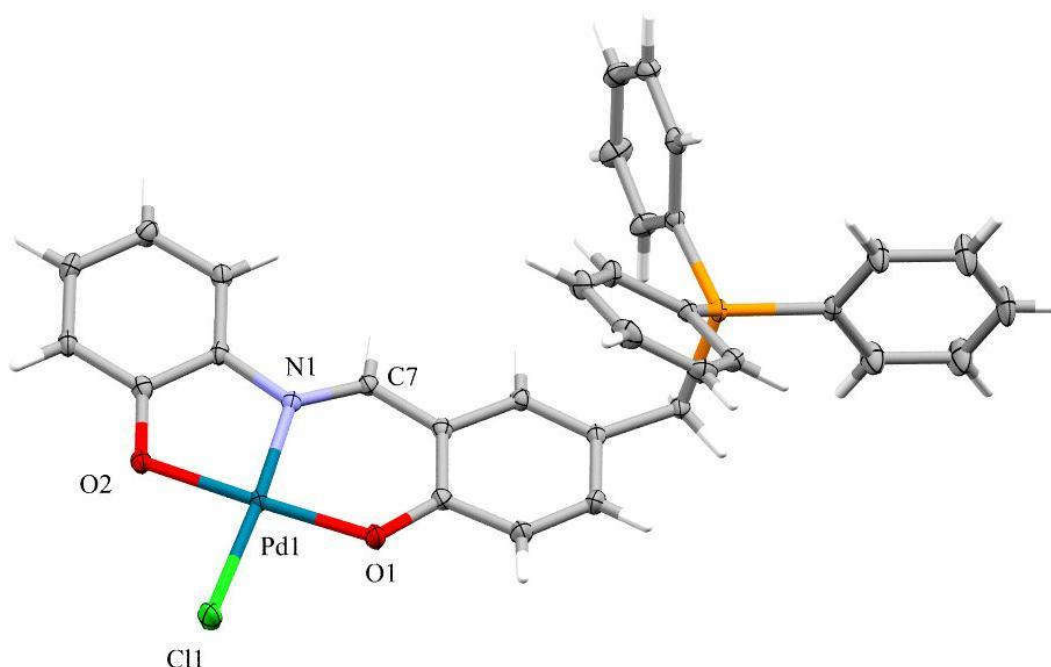


**Figure 4.** The ORTEP of complex 1 with selected atom numbering and ellipsoids with 40% probability [Pd1—Cl1 = 2.3283(7) Å; Pd1—N1 = 1.9661(19) Å; Pd1—O1 = 1.9666(17) Å; Pd1—O2 = 1.9929(17) Å; O1—Pd1—O2 = 178.32(8) °; Cl1—Pd1—N1 = 176.32(6) °]. The water molecules were omitted for clarity.

**Table 2.** The details of the intermolecular interactions in complex 1

D—H <sup>⋯</sup> A	H—A	D <sup>⋯</sup> A	D—H <sup>⋯</sup> A
O2W—H1W2 <sup>⋯</sup> Cl1	2.48	3.230(3)	147
O2W—H2W2 <sup>⋯</sup> O1W	2.01	2.804(8)	155
O2W—H2W2 <sup>⋯</sup> O1W	2.14	2.773(7)	131
O3W—H1W3 <sup>⋯</sup> O2W	2.09	2.933(4)	167
O3W—H2W3 <sup>⋯</sup> Cl1	2.70	3.425(3)	145
O4W—H2W4 <sup>⋯</sup> O2	1.97	2.731(3)	148
C14—H14B <sup>⋯</sup> O3W	2.44	3.343(3)	155
C19—H19 <sup>⋯</sup> O1	2.58	3.221(3)	126

The details of the hydrogen bonding interactions are listed in Table 2. The geometry around the Pd atom is a square-planar involving the chlorine atom and a tridentate OON donor ligand. The Pd atom is coplanar to the least-squares plane of O1, O2, N1, and Cl1 atoms with a slight deviation of 0.007(1) Å. The interesting feature of the crystal packing is the connection of the neighboring molecules through a cluster of water molecules (Fig. 5) along the *b*-axis.

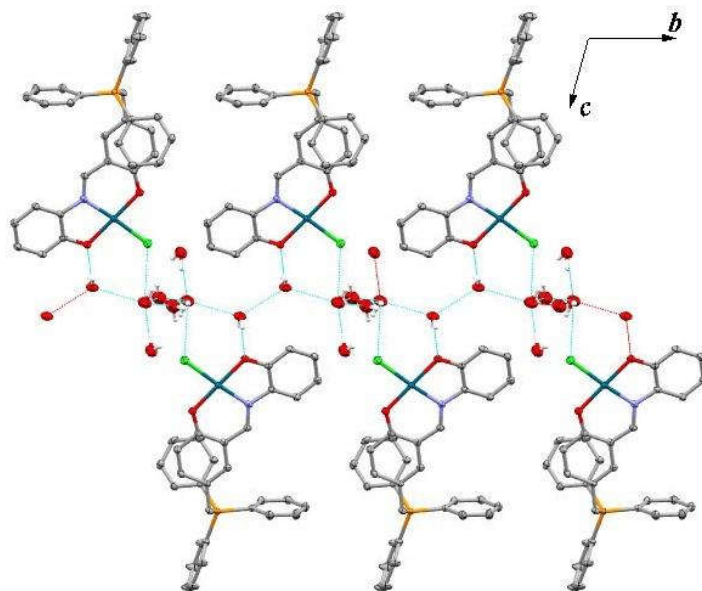


**Figure 5** Part of the crystal packing viewed down the *a*-axis, showing the connection of the neighboring molecules into a one-dimensional infinite chain through water cluster formation along the *b*-axis. All H-atoms were omitted for clarity except for water molecules. On the other hand, intermolecular  $\pi\cdots\pi$  and C—H $\cdots$ O interactions form a one-dimensional infinite chain of molecules along the *a*-axis (Fig. 6).

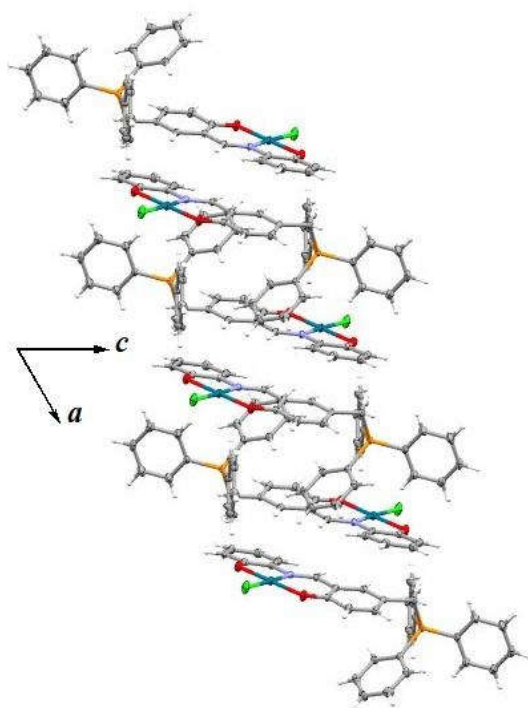


**Figure 6** Part of the crystal packing viewed down the *b*-axis, showing the connection of the neighboring molecules into a one-dimensional infinite chain through the intermolecular  $\pi\cdots\pi$  and C—H...O interactions along the *a*-axis.

### 3.5 Catalytic efficiency of complex 1

In order to understand the catalytic potential of zwitterionic complex **1**, the Heck coupling was tested, and representative iodobenzene (**2a**) and methyl acrylate (**3a**) were selected to optimize the reaction conditions (Table 3). The efficiency of the process was evaluated by GC conversion and isolated yield of product **3a**, but also by turnover frequency (TOF).

**Table 3.** parameter optimization for the Heck- Mizoroki coupling reaction

entry	mol % cat	Volume of stock solution <sup>a</sup>	Base	GVL Volume	Temp.	Time h	Conv <sup>b</sup>	TOF <sup>c</sup> 1/h
1	$5.4 \times 10^{-3}$	85 $\mu$ L	KOAc	2 mL	130 $^{\circ}$ C	24	14%	108
2	$3.2 \times 10^{-2}$	500	KOAc	1.5 mL	130 $^{\circ}$ C	24	43%	56
3	$6.4 \times 10^{-2}$	1000	KOAc	1 mL	130 $^{\circ}$ C	24	51%	33
4	$6.4 \times 10^{-2}$	1000	TEA	1 mL	130 $^{\circ}$ C	1.5	>99%	1031
5	$6.4 \times 10^{-2}$	1000	TEA	0 mL	130 $^{\circ}$ C	1.5	>99%	1031
6	<b><math>3.2 \times 10^{-2}</math></b>	<b>500</b>	<b>TEA</b>	<b>0 mL</b>	<b>130 <math>^{\circ}</math>C</b>	<b>1.5</b>	<b>&gt;99%</b>	<b>2062</b>
7	$1.6 \times 10^{-2}$	250	TEA	0 mL	130 $^{\circ}$ C	1.5	93%	3875
8	$8.0 \times 10^{-3}$	125	TEA	0 mL	130 $^{\circ}$ C	1.5	49%	4083

<sup>a</sup>; The Stock solution was prepared by dissolving of 0.002 gr ( $3.18 \times 10^{-3}$  mmol) of complex in 10 mL of solvent.

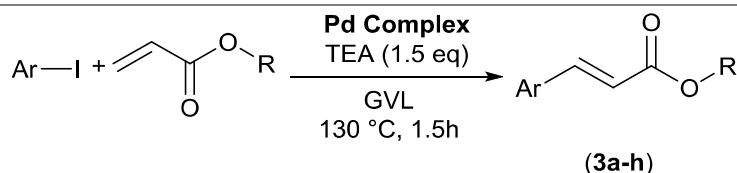
<sup>b</sup>; Reaction conditions: 0.5 mmol iodobenzene, 0.75 mmol methyl acrylate, 1.5 mmol base.

<sup>c</sup>; TOF=(mmol substrate/mmol Cat) $\times$ Conversion/Time (h)

At this latter purpose, a stock solution of complex **1** was prepared in GVL at a concentration of  $3.18 \times 10^{-4}$  M. The system was initially evaluated with the KOAc as a base, but after 24 hours even with an increase in catalyst content, no acceptable conversion was obtained (Table 3, entries 1-3). In order to solve this problem, the base was replaced with TEA, which increased the conversion to 99% in just 1.5 hours (entry 4). Also, to reduce the amount of waste from the reaction, the amount of solvent was reduced and only the solvent in the stock solution was used, which did not make a difference in the conversion of reaction (entry 5). In the end, the amount of catalyst was reduced and the catalytic system showed tremendous performance in a lower amount of catalyst, which increased the TOF of reaction (entries 6-8).

To verify the efficiency of zwitterionic complex **1** in Heck reaction, the reactions were investigated by using a series of aryl iodides and alkyl acrylates (Table 4) or styrenes (Table 5), under optimized condition (same as entry 6 in table 3) in 1.5 h. According to results demonstrated in Table 4 and 5, high to quantitative conversions and good to excellent yields of isolated products are considerable for different derivatives of **3** and **4** compounds. In the reaction of aryl iodides with styrenes (Table 5), a trace amount of the germinal isomer **4'** and the homo-coupling product was detected. For this issue, all products were purified by column chromatography.

**Table 4.** Heck-Mizoroki coupling of aryl iodide with alkyl acrylates in the presence of zwitterionic complex **1**<sup>a</sup>



Entry	Ar	R	Product	Conv% <sup>b</sup>	Yield% <sup>c</sup>	TOF <sup>d</sup>
1	Ph	-Me	3a	>99	89	2062
2	4-CH <sub>3</sub> -C <sub>6</sub> H <sub>4</sub>	-Me	3b	93	86	1938
3	4-OCH <sub>3</sub> -C <sub>6</sub> H <sub>4</sub>	-Me	3c	97	91	2021
4	4'-COCH <sub>3</sub> -C <sub>6</sub> H <sub>4</sub>	-Me	3d	>99	90	2062
5	Ph	-nBu	3e	>99	88	2062
6	4-CH <sub>3</sub> -C <sub>6</sub> H <sub>4</sub>	-nBu	3f	96	87	2000
7	4-OCH <sub>3</sub> -C <sub>6</sub> H <sub>4</sub>	-nBu	3g	98	93	2042
8	4'-COCH <sub>3</sub> -C <sub>6</sub> H <sub>4</sub>	-nBu	3h	99	96	2062

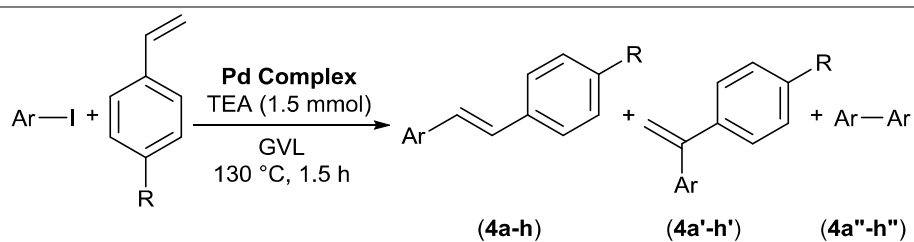
<sup>a</sup>; Reaction conditions: aryl iodide 0.5 mmol, alkyl acrylates 0.75 mmol, TEA 1.5 mmol, catalyst **1**  $3.2 \times 10^{-2}$  mol % (500  $\mu$ L of stock solution in GVL), 130 °C, and 1.5 h.

<sup>b</sup>; Measured by GC analyses.

<sup>c</sup>; Isolated yield of the pure product after flash chromatography.

<sup>d</sup>; TOF=(mmol substrate/mmol Cat)×Conversion/Time (h)

**Table 5.** Heck-Mizoroki coupling of aryl iodide with different styrenes in the presence of zwitterionic complex **1**<sup>a</sup>



Entry	Ar	R	Product	Conv% <sup>b</sup>	Yield% <sup>c</sup>	4/4'/4'' <sup>b</sup>	TOF <sup>d</sup>
1	Ph	-H	4a	>99	83	87/13/0	2062
2	4-CH <sub>3</sub> -C <sub>6</sub> H <sub>4</sub>	-H	4b	94	78	85/15/0	1958
3	4-OCH <sub>3</sub> -C <sub>6</sub> H <sub>4</sub>	-H	4c	98	80	84/16/0	2042
4	4'-COCH <sub>3</sub> -C <sub>6</sub> H <sub>4</sub>	-H	4d	>99	85	89/9/2	2062
5	Ph	-Cl	4e	97	86	91/9/0	2021
6	4-CH <sub>3</sub> -C <sub>6</sub> H <sub>4</sub>	-Cl	4f	93	84	86/14/0	1938
7	4-OCH <sub>3</sub> -C <sub>6</sub> H <sub>4</sub>	-Cl	4g	>99	88	89/11/0	2062
8	4'-COCH <sub>3</sub> -C <sub>6</sub> H <sub>4</sub>	-Cl	4h	>99	77	83/10/7	2062

---

<sup>a</sup>; Reaction conditions: aryl iodide 0.5 mmol, styrenes 0.75 mmol, TEA 1.5 mmol, catalyst **1**  $3.2 \times 10^{-2}$  mol % (500  $\mu$ L of stock solution in GVL), 130 °C, and 1.5 h.

<sup>b</sup>; Measured by GC analyses.

<sup>c</sup>; Isolated yield of the pure product after flash chromatography.

<sup>d</sup>; TOF=(mmol substrate/mmol Cat) $\times$ Conversion/Time (h)

---

#### 4. Conclusion

In summary, a new zwitterionic Pd (II) Schiff base complex was synthesized and fully characterized, by various technics. Also, DFT studies were performed on this complex and the nature of frontier molecular orbitals was obtained. Afterward, the complex was used as a homogeneous catalyst in Heck cross-coupling reaction. The importance of this catalytic system is related to using GVL as a green and renewable medium. The catalytic system showed remarkable activity in GVL for Heck coupling of various substrates and the catalyst successfully showed high potential in the green coupling of iodobenzene to methyl acrylate with the turnover frequency more than 4000/h.

#### Acknowledgments

M.B. acknowledges the research council of the Sharif University of Technology for the research funding of this work. RK is thankful to Bath University for a visiting lectureship. PRR is grateful to the Engineering and Physical Sciences Research Council (EPSRC) for continued funding (EP/K004956/1). The Università degli Studi di Perugia and MIUR are acknowledged for financial support to the project AMIS, through the program “Dipartimenti di Eccellenza - 2018-2022”.

#### Supporting Information

Crystallographic data for the structural analysis has been deposited in the Cambridge Crystallographic Data Centre, CCD No. 1895502. Full characterization data and Additional data for the computational study are available in the electronic supporting information.

#### References

1. a) M. Bagherzadeh, M. Amini, A. Ellern and L. Keith Woo, *Inorg. Chim. Acta*, 2011, DOI: 10.1016/j.ica.2011.10.040; b) M. Bagherzadeh, F. Ashouri, L. Hashemi and A. Morsali, *Inorg. Chem. Commun.*, 2014, **44**, 10-14; c) N. Khadir, G. Tavakoli, A. Assoud, M. Bagherzadeh and D. M. Boghaei, *Inorg. Chim. Acta*, 2016, **440**, 107-117; d) F. Valentini, H. Mahmoudi, L. A. Bivona, O. Piermatti, M. Bagherzadeh, L. Fusaro, C. Aprile, A. Marrocchi and L. Vaccaro, *ACS Sustainable Chemistry & Engineering*, 2019, DOI: 10.1021/acssuschemeng.8b06502; e) S. E. Hooshmand, B. Heidari, R. Sedghi and R. S. Varma, *Green chem.*, 2019, **21**, 381-405; f) Yin and J. Liebscher, *Chem. Rev.*, 2007, **107**, 133-173; g) J. Sołoducho, K. Olech, A. Świst, D. Zając and J. Cabaj, *Advances in Chemical Engineering and Science*, 2013, **3**, 19-32; h) L. A. Bivona, F. Giacalone, L. Vaccaro, C. Aprile and M. Gruttadauria, *ChemCatChem*, 2015, **7**, 2526-2533; i) V. Kozell, M. McLaughlin, G. Strappaveccia, S. Santoro, L. A. Bivona, C. Aprile, M. Gruttadauria and L. Vaccaro, *ACS Sustainable Chemistry & Engineering*, 2016, **4**, 7209-7216; j) A. S. Guram, X. Wang, E. E. Bunel, M. M. Faul, R. D. Larsen and M. J. Martinelli, *J. Org. Chem.*, 2007, **72**, 5104-5112.
2. a) M. Gholinejad, A. Neshat, F. Zareh, C. Nájera, M. Razeghi and A. Khoshnood, *Appl. Catal., A*, 2016, **525**, 31-40; b) H. M. Savanur, R. G. Kalkhambkar and K. K. Laali, *Appl. Catal., A*, 2017, **543**, 150-161; c) S. Ramírez-Rave, D. Morales-Morales and J.-M. Grévy, *Inorg. Chim. Acta*, 2017, **462**, 249-255; d) C. I. Ezugwu, B. Mousavi, M. A. Asraf, Z. Luo and F. Verpoort, *J. Catal.*, 2016, **344**, 445-454; e) M. B. Ibrahim, B. El

Ali, I. Malik and M. Fettouhi, *Tetrahedron Lett.*, 2016, **57**, 554-558; f) C. Maaliki, Y. Chevalier, E. Thiery and J. Thibonnet, *Tetrahedron Lett.*, 2016, **57**, 3358-3362; g) Z. M. Chen, C. S. Nervig, R. J. DeLuca and M. S. Sigman, *Angew. Chem.*, 2017, **129**, 6751-6754; h) Anuradha, S. Kumari, S. Layek and D. D. Pathak, *New J. Chem.*, 2017, **41**, 5595-5604; i) M. Bagherzadeh, N.-a. Mousavi, M. Zare, S. Jamali, A. Ellern and L. K. Woo, *Inorg. Chim. Acta*, 2016, **451**, 227-232; j) V. Kozell, T. Giannoni, M. Nocchetti, R. Vivani, O. Piermatti and L. Vaccaro, *Catalysts*, 2017, **7**, 186; k) D. Astruc, *Inorg. Chem.*, 2007, **46**, 1884-1894; l) H.-J. Xu, Y.-Q. Zhao and X.-F. Zhou, *J. Org. Chem.*, 2011, **76**, 8036-8041; m) C. Petrucci, M. Cappelletti, O. Piermatti, M. Nocchetti, M. Pica, F. Pizzo and L. Vaccaro, *J. Mol. Catal. A: Chem.*, 2015, **401**, 27-34; n) C. Pavia, F. Giacalone, L. A. Bivona, A. M. P. Salvo, C. Petrucci, G. Strappaveccia, L. Vaccaro, C. Aprile and M. Gruttadauria, *J. Mol. Catal. A: Chem.*, 2014, **387**, 57-62; o) C. Pavia, E. Ballerini, L. A. Bivona, F. Giacalone, C. Aprile, L. Vaccaro and M. Gruttadauria, *Adv. Synth. Catal.*, 2013, **355**, 2007-2018.

3. a) N. Arsalani, A. Akbari, M. Amini, E. Jabbari, S. Gautam and K. H. Chae, *Catal. Lett.*, 2017, **147**, 1086-1094; b) I. Bucsi, Á. Mastalir, Á. Molnár, K. L. Juhász and A. Kunfi, *Struct. Chem.*, 2017, **28**, 501-509; c) P. Wang, G.-Y. Wang, W.-L. Qiao and Y.-S. Feng, *Catal. Lett.*, 2016, **146**, 1792-1799; d) R. K. Dhungana, B. Shrestha, R. Thapa-Magar, P. Basnet and R. Giri, *Org. Lett.*, 2017, **19**, 2154-2157; e) X. Li, X. Gong, Z. Li, H. Chang, W. Gao and W. Wei, *RSC Adv.*, 2017, **7**, 2475-2479; f) J. Xiao, Z. Lu and Y. Li, *Industrial & Engineering Chemistry Research*, 2015, **54**, 790-797; g) H. Mahmoudi, F. Valentini, F. Ferlin, L. A. Bivona, I. Anastasiou, L. Fusaro, C. Aprile, A. Marrocchi and L. Vaccaro, *Green chem.*, 2019, **21**, 355-360; h) C. Petrucci, G. Strappaveccia, F. Giacalone, M. Gruttadauria, F. Pizzo and L. Vaccaro, *ACS Sustainable Chemistry & Engineering*, 2014, **2**, 2813-2819.

4. a) R. K. Sharma, M. Yadav, R. Gaur, R. Gupta, A. Adholeya and M. B. Gawande, *ChemPlusChem*, 2016, **81**, 1312-1319; b) G. Strappaveccia, E. Ismalaj, C. Petrucci, D. Lanari, A. Marrocchi, M. Drees, A. Facchetti and L. Vaccaro, *Green chem.*, 2015, **17**, 365-372.

5. Á. Molnár, *Chem. Rev.*, 2011, **111**, 2251-2320.

6. a) M. Bagherzadeh, S. Ataie, H. Mahmoudi and J. Janczak, *Inorg. Chem. Commun.*, 2017, **84**, 63-67; b) M. Bagherzadeh, H. Mahmoudi, M. Amini, S. Gautam and K. H. Chae, *Sci. Iran*, 2018, **25**, 1335-1343.

7. a) Y.-M. Cui, L. Qiao, Y. Li, Q. Wang, W. Chen and W.-X. Yan, *Transition Met. Chem.*, 2017, **42**, 51-56; b) H. Houjou, M. Ito and K. Araki, *Inorg. Chem.*, 2009, **48**, 10703-10707. c) M. Bagherzadeh, H. Mahmoudi, S. Ataie, M. Hafezi-Kahnamouei, S. Shahrokhian, G. Bellachioma, L. Vaccaro, *Inorg. Chim. Acta*, 2019, **492**, 213-220.

8. N. Vucetic, P. Virtanen, A. Nuri, I. Mattsson, A. Aho, J.-P. Mikkola and T. Salmi, *J. Catal.*, 2019, **371**, 35-46.

9. T. Mizoroki, K. Mori and A. Ozaki, *Bull. Chem. Soc. Jpn.*, 1971, **44**, 581-581.

10. R. F. Heck and J. Nolley Jr, *J. Org. Chem.*, 1972, **37**, 2320-2322.

11. a) X. Chen, K. M. Engle, D. H. Wang and J. Q. Yu, *Angew. Chem. Int. Ed.*, 2009, **48**, 5094-5115; b) J. Magano and J. R. Dunetz, *Chem. Rev.*, 2011, **111**, 2177-2250; c) D. Lopez-Tejedor, B. de las Rivas and J. Palomo, *Molecules*, 2018, **23**, 2358; d) F. R. Fortea-Pérez, M. L. E. I. Moubtassim, D. Armentano, G. De Munno, M. Julve and S.-E. Stiriba, *Inorganic Chemistry Frontiers*, 2018, **5**, 2148-2156; e) J. Choi and G. C. Fu, *Science*, 2017, **356**, eaaf7230.

12. F. M. Kerton, in *Encyclopedia of Inorganic and Bioinorganic Chemistry*, 2016, DOI: doi:10.1002/9781119951438.eibc2417.

13. a) L. Vaccaro, M. Curini, F. Ferlin, D. Lanari, A. Marrocchi, O. Piermatti and V. Trombettoni, *Journal*, 2018, **90**, 21; b) E. Ismalaj, G. Strappaveccia, E. Ballerini, F. Elisei, O. Piermatti, D. Gelman and L. Vaccaro,



- ACS Sustainable Chemistry & Engineering*, 2014, **2**, 2461-2464; c) G. Strappaveccia, L. Luciani, E. Bartollini, A. Marrocchi, F. Pizzo and L. Vaccaro, *Green chem.*, 2015, **17**, 1071-1076; d) A. Marrocchi, P. Adriaensens, E. Bartollini, B. Barkakaty, R. Carleer, J. Chen, D. K. Hensley, C. Petrucci, M. Tassi and L. Vaccaro, *Eur. Polym. J.*, 2015, **73**, 391-401; e) D. Rasina, A. Kahler-Quesada, S. Ziarelli, S. Warratz, H. Cao, S. Santoro, L. Ackermann and L. Vaccaro, *Green chem.*, 2016, **18**, 5025-5030; f) S. Santoro, F. Ferlin, L. Luciani, L. Ackermann and L. Vaccaro, *Green chem.*, 2017, **19**, 1601-1612; g) S. Santoro, A. Marrocchi, D. Lanari, L. Ackermann and L. Vaccaro, *Chemistry—A European Journal*, 2018, **24**, 13383-13390; h) L. Vaccaro, M. Curini, F. Ferlin, D. Lanari, A. Marrocchi, O. Piermatti and V. Trombettoni, *Pure Appl. Chem.*, 2018, **90**, 21-33; i) F. Ferlin, L. Luciani, O. Viteritti, F. Brunori, O. Piermatti, S. Santoro and L. Vaccaro, *Frontiers in chemistry*, 2018, **6**; j) L. Luciani, E. Goff, D. Lanari, S. Santoro and L. Vaccaro, *Green chem.*, 2018, **20**, 183-187; k) F. Ferlin, L. Luciani, S. Santoro, A. Marrocchi, D. Lanari, A. Bechtoldt, L. Ackermann and L. Vaccaro, *Green chem.*, 2018, **20**, 2888-2893; l) E. Petricci, C. Risi, F. Ferlin, D. Lanari and L. Vaccaro, *Scientific reports*, 2018, **8**, 10571.
14. a) J. Q. Bond, D. M. Alonso, D. Wang, R. M. West and J. A. Dumesic, *Science*, 2010, **327**, 1110-1114; b) G. W. Huber and A. Corma, *Angew. Chem. Int. Ed.*, 2007, **46**, 7184-7201.
15. N. K. Oklu and B. C. E. Makhubela, *Inorg. Chim. Acta*, 2018, **482**, 460-468.
16. a) C. Li-Juan, M. Fu-Ming and L. Guang-Xing, *Catal. Commun.*, 2009, **10**, 981-985; b) R. I. Kureshy, K. J. Prathap, T. Roy, N. C. Maity, N.-u. H. Khan, S. H. R. Abdi and H. C. Bajaj, *Adv. Synth. Catal.*, 2010, **352**, 3053-3060.
- 17 R. Clark and J. Reid, *Acta Crystallogr. Sect. A: Found. Crystallogr.*, 1995, **51**, 887-897.
- 18 *SuperNova Eos S2 System: Empirical absorption correction*, CrysAlis-Software package, Oxford Diffraction Ltd, 2011.
- 19 a) O. V. Dolomanov, L. J. Bourhis, R. J. Gildea, J. A. Howard and H. Puschmann, *J. Appl. Crystallogr.*, 2009, **42**, 339-341; b) 2012.
- 20 G. M. Sheldrick, *Acta Crystallogr. Sect. A: Found. Crystallogr.*, 2008, **64**, 112-122.
- 21 A. L. Spek, *Acta Crystallogr. Sect. D. Biol. Crystallogr.*, 2009, **65**, 148-155.
- 22 V. P. Balema, J. W. Wiench, M. Pruski and V. K. Pecharsky, *Chem. Commun.*, 2002, DOI: <http://dx.doi.org/10.1039/B111515D>, 724-725.
23. G. W. T. M. J. Frisch, H. B. Schlegel, G. E. Scuseria, , J. R. C. M. A. Robb, G. Scalmani, V. Barone, B. Mennucci, , H. N. G. A. Petersson, M. Caricato, X. Li, H. P. Hratchian, , J. B. A. F. Izmaylov, G. Zheng, J. L. Sonnenberg, M. Hada, , K. T. M. Ehara, R. Fukuda, J. Hasegawa, M. Ishida, T. Nakajima, , O. K. Y. Honda, H. Nakai, T. Vreven, J. A. Montgomery, Jr., , F. O. J. E. Peralta, M. Bearpark, J. J. Heyd, E. Brothers, , V. N. S. K. N. Kudin, R. Kobayashi, J. Normand, , A. R. K. Raghavachari, J. C. Burant, S. S. Iyengar, J. Tomasi, , N. R. M. Cossi, J. M. Millam, M. Klene, J. E. Knox, J. B. Cross, , C. A. V. Bakken, J. Jaramillo, R. Gomperts, R. E. Stratmann, , A. J. A. O. Yazyev, R. Cammi, C. Pomelli, J. W. Ochterski, , K. M. R. L. Martin, V. G. Zakrzewski, G. A. Voth, , J. J. D. P. Salvador, S. Dapprich, A. D. Daniels, , J. B. F. O. Farkas, J. V. Ortiz, J. Cioslowski, and a. D. J. Fox, *Gaussian 09, Revision A.01*, Gaussian, Inc., Wallingford CT, 2009.
24. J.-i. Aihara, *J. Phys. Chem. A*, 1999, **103**, 7487-7495.

**Supporting Information**

**for**

**Synthesis and Characterization of a new Zwitterionic Palladium Complex as an  
Environmentally Friendly Catalyst for the Heck-Mizoroki Coupling Reaction in GVL**

Mojtaba Bagherzadeh,<sup>\*a</sup> Hamed Mahmoudi,<sup>a</sup> Saeed Ataie,<sup>a</sup> Mohammad Bahjati,<sup>a</sup> Reza Kia<sup>a</sup>, Paul

R. Raithby<sup>b</sup> and Luigi Vaccaro<sup>\*c</sup>

<sup>a</sup> *Chemistry Department, Sharif University of Technology, Tehran, P.O. Box 11155-3516, Iran*

<sup>b</sup> *Chemistry Department, University of Bath, Bath, BA2 7AY, UK*

<sup>c</sup> *Green SOC – Dipartimento di Chimica Biologia e Biotecnologie, Università degli Studi di*

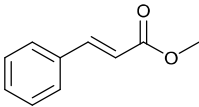
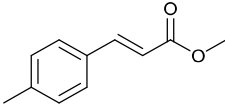
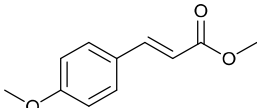
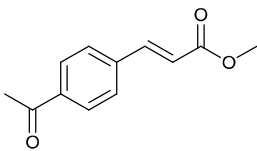
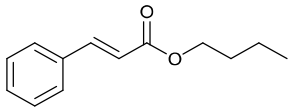
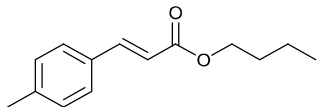
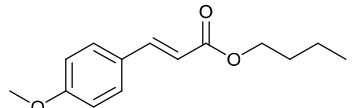
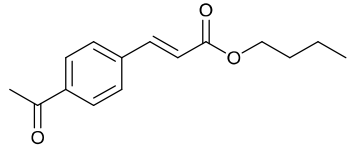
*Perugia, I-06123, Perugia, Italy*

[luigi.vaccaro@unipg.it](mailto:luigi.vaccaro@unipg.it)

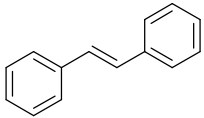
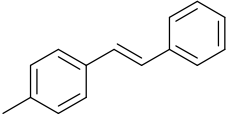
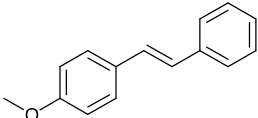
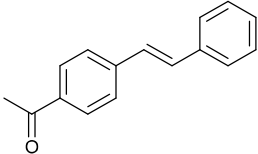
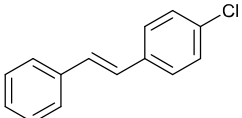
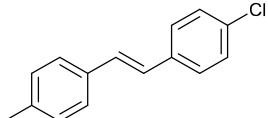
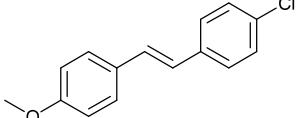
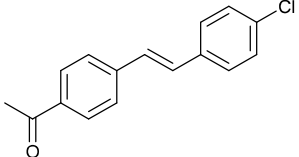
**Table of contents**

Additional experimental data	Pages 2-3
Additional calculated data	Pages 4-7
Additional spectroscopic data	Pages 8-45

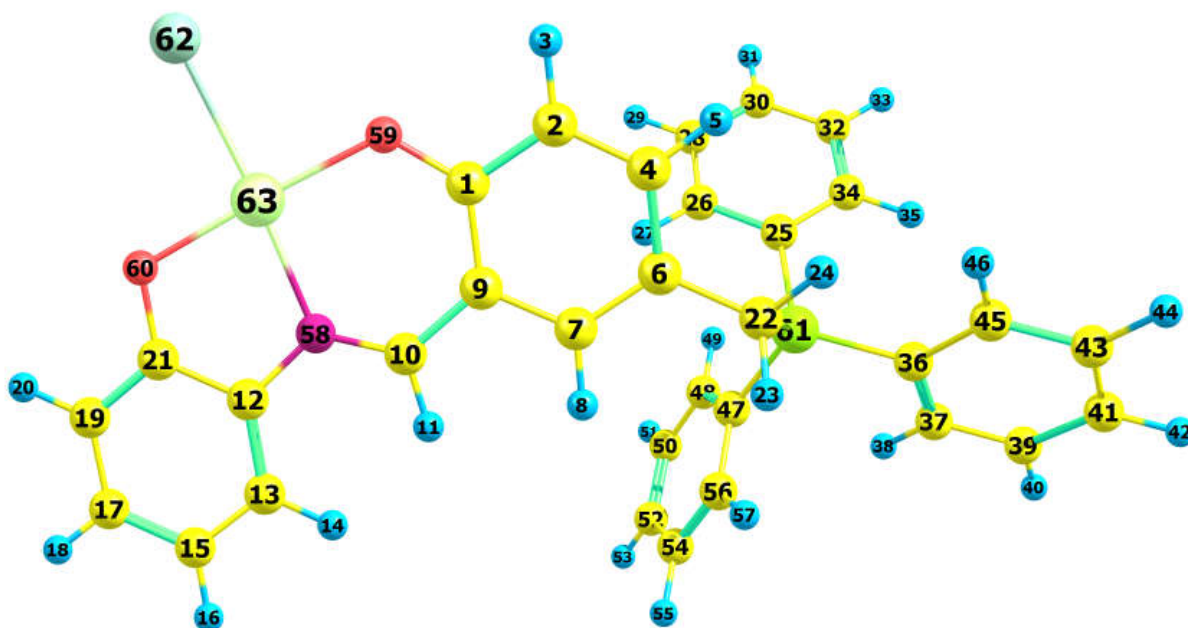
**Table S1.** NMR data of Cinnamate derivatives

	3a	Methyl cinnamate (Obtained as a white solid)
		<sup>1</sup> H NMR (400 MHz, CDCl <sub>3</sub> ) δ: 7.70 (1H, d, j=16.0 Hz), 7.51-7.54 (2H, m), 7.37-7.40 (3H, m), 6.45 (1H, d, j=16.0 Hz), 3.81 (3H, s)
		<sup>13</sup> C NMR (100.6 MHz, CDCl <sub>3</sub> ) δ: 167.55, 145.00, 134.50, 130.42, 129.01, 128.19, 117.92, 51.82
	3b	Methyl (E)-3-(p-tolyl)acrylate (Obtained as a pale yellow solid)
		<sup>1</sup> H NMR (400 MHz, CDCl <sub>3</sub> ) δ: 7.67 (1H, d, j=16.0 Hz), 7.42 (2H, d, j=7.9 Hz), 7.19 (2H, d, j=7.9 Hz), 6.40 (1H, d, j=16.0 Hz), 3.80 (3H, s), 2.37 (3H, s)
		<sup>13</sup> C NMR (100.6 MHz, CDCl <sub>3</sub> ) δ: 167.78, 145.02, 140.87, 131.80, 129.77, 128.21, 116.84, 51.79, 21.61.
	3c	Methyl (E)-3-(4-methoxyphenyl)acrylate (obtained as a white solid)
		<sup>1</sup> H NMR (400 MHz, CDCl <sub>3</sub> ) δ: 7.65 (1H, d, j=15.9 Hz), 7.47 (2H, d, j=8.8 Hz), 6.90 (2H, d, j=8.8 Hz), 6.31 (1H, d, j=15.9 Hz), 3.84 (3H, s), 3.79 (3H, s)
		<sup>13</sup> C NMR (100.6 MHz, CDCl <sub>3</sub> ) δ: 167.92, 161.54, 144.68, 129.87, 127.27, 115.41, 114.47, 55.52, 51.73.
	3d	Methyl (E)-3-(4-acetylphenyl)acrylate (obtained as a yellow solid)
		<sup>1</sup> H NMR (400 MHz, CDCl <sub>3</sub> ) δ: 7.97 (2H, d, j=8.2 Hz), 7.71 (1H, d, j=16.1 Hz), 7.61 (2H, d, j=8.2 Hz), 6.53 (1H, d, j=16.1 Hz), 3.82 (3H, s), 2.62 (3H, s)
		<sup>13</sup> C NMR (100.6 MHz, CDCl <sub>3</sub> ) δ: 197.31, 166.94, 143.31, 138.71, 138.05, 128.87, 128.16, 120.34, 51.92, 26.70.
	3e	Butyl cinnamate (obtained as a pale yellow oil)
		<sup>1</sup> H NMR (400 MHz, CDCl <sub>3</sub> ) δ: 7.68 (1H, d, j=16.0 Hz), 7.51-7.55 (2H, m), 7.37-7.40 (3H, m), 6.44 (1H, d, j=16.0 Hz), 4.21 (2H, t, j=6.7 Hz), 1.65-1.73 (2H, m), 1.41-1.49 (2H, m), 0.97 (3H, t, j=7.4 Hz)
		<sup>13</sup> C NMR (100.6 MHz, CDCl <sub>3</sub> ) δ: 167.25, 144.69, 134.62, 130.34, 129.01, 128.19, 118.44, 64.58, 30.92, 19.35, 13.90.
	3f	Butyl (E)-3-(p-tolyl)acrylate (obtained as a pale yellow oil)
		<sup>1</sup> H NMR (400 MHz, CDCl <sub>3</sub> ) δ: 7.66 (1H, d, j=16.0 Hz), 7.42 (2H, d, j=8.1 Hz), 7.19 (2H, d, j=7.8 Hz), 6.40 (1H, d, j=16.0 Hz), 4.20 (2H, t, j=6.7 Hz), 2.37 (3H, s), 1.65-1.73 (2H, m), 1.39-1.49 (2H, m), 0.97 (3H, t, j=7.4 Hz)
		<sup>13</sup> C NMR (100.6 MHz, CDCl <sub>3</sub> ) δ: 167.45, 144.68, 140.74, 131.89, 129.74, 128.18, 117.34, 64.48, 30.94, 21.60, 19.35, 13.90.
	3g	Butyl (E)-3-(4-methoxyphenyl)acrylate (obtained as a pale yellow oil)
		<sup>1</sup> H NMR (400 MHz, CDCl <sub>3</sub> ) δ: 7.63 (1H, d, j=15.9 Hz), 7.47 (2H, d, j=8.6 Hz), 6.89 (2H, d, j=8.6 Hz), 6.31 (1H, d, j=15.9 Hz), 4.19 (2H, t, j=6.7 Hz), 3.83 (3H, s), 1.64-1.72 (2H, m), 1.38-1.48 (2H, m), 0.96 (3H, t, j=7.4 Hz)
		<sup>13</sup> C NMR (100.6 MHz, CDCl <sub>3</sub> ) δ: 167.59, 161.46, 144.34, 129.83, 127.36, 115.93, 114.44, 64.41, 55.51, 30.96, 19.36, 13.91.
	3h	Butyl (E)-3-(4-acetylphenyl)acrylate (obtained as a yellow oil)
		<sup>1</sup> H NMR (400 MHz, CDCl <sub>3</sub> ) δ: 7.94 (2H, d, j=8.2 Hz), 7.66 (1H, d, j=16.0 Hz), 7.58 (2H, d, j=8.2 Hz), 6.50 (1H, d, j=16.0 Hz), 4.20 (2H, t, j=6.7 Hz), 2.59 (3H, s), 1.65-1.70 (2H, m), 1.37-1.47 (2H, m), 0.94 (3H, t, j=7.4 Hz)
		<sup>13</sup> C NMR (100.6 MHz, CDCl <sub>3</sub> ) δ: 197.35, 166.64, 143.03, 138.88, 138.03, 128.91, 128.19, 120.91, 64.74, 30.80, 26.75, 19.26, 13.81.

**Table S2.** NMR data of Stylbene derivatives

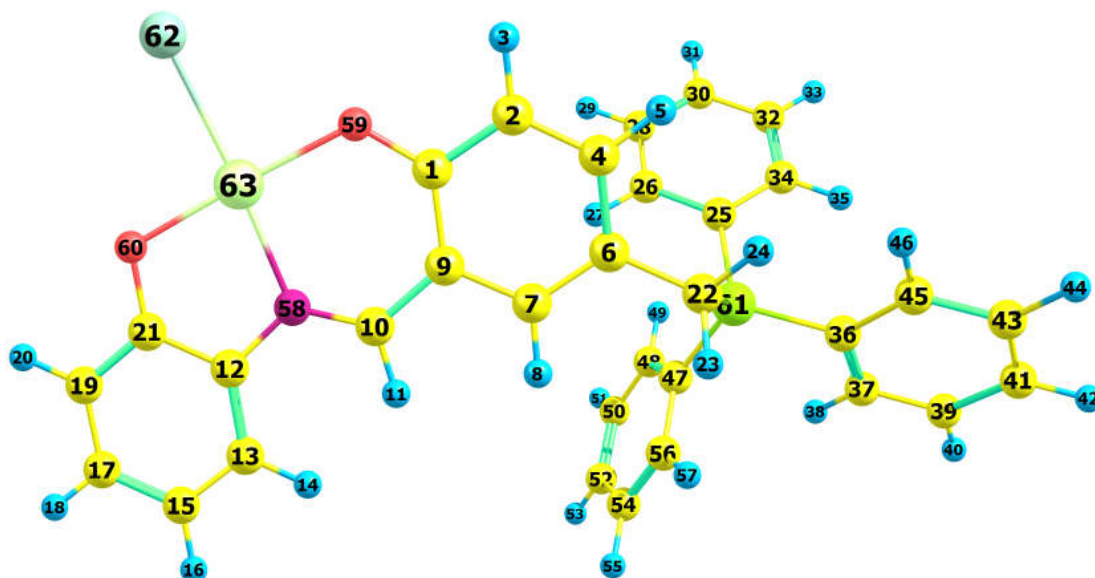
	<b>4a</b>	(E)-stylbene (Obtained as a white solid)
		$^1\text{H NMR}$ (400 MHz, $\text{CDCl}_3$ ) $\delta$ : 7.50-7.57 (4H, m), 7.34-7.41 (4H, m), 7.27-7.31 (2H, m), 7.13 (2H, s)
		$^{13}\text{C NMR}$ (100.6 MHz, $\text{CDCl}_3$ ) $\delta$ : 137.47, 128.83, 127.76, 126.66.
	<b>4b</b>	(E)-1-methyl-4-styrylbenzene (Obtained as a white solid)
		$^1\text{H NMR}$ (400 MHz, $\text{CDCl}_3$ ) $\delta$ : 7.52 (2H, d, $j=7.7$ Hz), 7.43 (2H, d, $j=7.9$ Hz), 7.34-7.39 (2H, m), 7.24-7.28 (1H, m), 7.18 (2H, d, $j=7.8$ Hz), 7.04-7.14 (2H, m), 2.38 (3H, s).
		$^{13}\text{C NMR}$ (100.6 MHz, $\text{CDCl}_3$ ) $\delta$ : 137.66, 137.65, 134.69, 129.54, 128.79, 128.76, 127.84, 127.54, 126.57, 126.53, 21.40.
	<b>4c</b>	(E)-1-methoxy-4-styrylbenzene (Obtained as a white solid)
		$^1\text{H NMR}$ (400 MHz, $\text{CDCl}_3$ ) $\delta$ : 7.50 (2H, d, $j=7.6$ Hz), 7.46 (2H, d, $j=8.7$ Hz), 7.33-7.38 (2H, m), 7.23 (1H, d, $j=7.3$ Hz), 6.95-7.10 (2H, m), 6.91 (2H, d, $j=8.7$ Hz), 3.84 (3H, s).
		$^{13}\text{C NMR}$ (100.6 MHz, $\text{CDCl}_3$ ) $\delta$ : 159.44, 137.79, 130.29, 128.78, 128.35, 127.86, 127.35, 126.76, 126.39, 114.27, 55.47.
	<b>4d</b>	(E)-1-(4-styrylphenyl)ethan-1-one (Obtained as a yellow solid)
		$^1\text{H NMR}$ (400 MHz, $\text{CDCl}_3$ ) $\delta$ : 7.95 (2H, d, $j=8.3$ Hz), 7.59 (2H, d, $j=8.3$ Hz), 7.54 (2H, d, $j=7.4$ Hz), 7.35-7.40 (2H, m), 7.30-7.32 (1H, m), 7.21-7.28 (1H, m), 7.11-7.16 (1H, m), 2.61 (3H, s).
		$^{13}\text{C NMR}$ (100.6 MHz, $\text{CDCl}_3$ ) $\delta$ : 197.45, 142.17, 136.83, 136.08, 131.62, 129.03, 128.95, 128.47, 127.59, 126.96, 126.64, 26.74.
	<b>4e</b>	(E)-1-chloro-4-styrylbenzene (Obtained as a white solid)
		$^1\text{H NMR}$ (400 MHz, $\text{CDCl}_3$ ) $\delta$ : 7.51 (2H, d, $j=7.4$ Hz), 7.44 (2H, d, $j=8.4$ Hz), 7.38 (2H, d, $j=7.4$ Hz), 7.33-7.35 (2H, m), 7.27-7.31 (1H, m), 7.01-7.11 (2H, m).
		$^{13}\text{C NMR}$ (100.6 MHz, $\text{CDCl}_3$ ) $\delta$ : 137.12, 135.99, 133.32, 129.46, 128.99, 128.88, 128.02, 127.80, 127.51, 126.69.
	<b>4f</b>	(E)-1-chloro-4-(4-methylstyryl)benzene (Obtained as a white solid)
		$^1\text{H NMR}$ (400 MHz, $\text{CDCl}_3$ ) $\delta$ : 7.39-7.44 (4H, m), 7.31 (2H, d, $j=8.5$ Hz), 7.17 (2H, d, $j=7.9$ Hz), 6.98-7.08 (2H, m), 2.36 (3H, s).
		$^{13}\text{C NMR}$ (100.6 MHz, $\text{CDCl}_3$ ) $\delta$ : 137.98, 136.19, 134.35, 133.07, 129.60, 129.39, 128.95, 127.68, 126.61, 126.51, 21.42.
	<b>4g</b>	(E)-1-chloro-4-(4-methoxystyryl)benzene (Obtained as a white solid)
		$^1\text{H NMR}$ (400 MHz, $\text{CDCl}_3$ ) $\delta$ : 7.44 (2H, d, $j=8.7$ Hz), 7.41 (2H, d, $j=8.5$ Hz), 7.31 (2H, d, $j=8.4$ Hz), 7.01-7.06 (1H, m), 6.89-6.94 (3H, m), 3.83 (3H, s).
		$^{13}\text{C NMR}$ (100.6 MHz, $\text{CDCl}_3$ ) $\delta$ : 159.63, 136.32, 132.83, 129.93, 128.98, 128.93, 127.93, 127.53, 125.40, 114.33, 55.48.
	<b>4h</b>	(E)-1-(4-(4-chlorostyryl)phenyl)ethan-1-one (Obtained as a pale yellow solid)
		$^1\text{H NMR}$ (400 MHz, $\text{CDCl}_3$ ) $\delta$ : 7.95 (2H, d, $j=8.2$ Hz), 7.57 (2H, d, $j=8.3$ Hz), 7.46 (2H, d, $j=8.4$ Hz), 7.35 (2H, d, $j=8.4$ Hz), 7.07-7.19 (2H, m), 2.61 (3H, s).
		$^{13}\text{C NMR}$ (100.6 MHz, $\text{CDCl}_3$ ) $\delta$ : 197.67, 141.85, 136.38, 135.45, 134.19, 130.32, 129.23, 129.14, 128.28, 128.20, 126.79, 26.84.

**Table S3.** Calculated bond length in optimized structure of complex 1



<b>R(1-2)</b>	1.426	<b>R(12-13)</b>	1.405	<b>R(22-61)</b>	1.86	<b>R(36-45)</b>	1.407	<b>R(48-49)</b>	1.084
<b>R(1-9)</b>	1.439	<b>R(12-21)</b>	1.421	<b>R(25-26)</b>	1.408	<b>R(36-61)</b>	1.818	<b>R(48-50)</b>	1.397
<b>R(1-59)</b>	1.306	<b>R(12-58)</b>	1.422	<b>R(25-34)</b>	1.405	<b>R(37-38)</b>	1.085	<b>R(50-51)</b>	1.085
<b>R(2-3)</b>	1.085	<b>R(13-14)</b>	1.085	<b>R(25-61)</b>	1.815	<b>R(37-39)</b>	1.396	<b>R(50-52)</b>	1.397
<b>R(2-4)</b>	1.38	<b>R(13-15)</b>	1.393	<b>R(26-27)</b>	1.084	<b>R(39-40)</b>	1.085	<b>R(52-53)</b>	1.086
<b>R(4-5)</b>	1.087	<b>R(15-16)</b>	1.085	<b>R(26-28)</b>	1.395	<b>R(39-41)</b>	1.398	<b>R(52-54)</b>	1.399
<b>R(4-6)</b>	1.417	<b>R(15-17)</b>	1.407	<b>R(28-29)</b>	1.085	<b>R(41-42)</b>	1.086	<b>R(54-55)</b>	1.085
<b>R(6-7)</b>	1.386	<b>R(17-18)</b>	1.087	<b>R(28-30)</b>	1.399	<b>R(41-43)</b>	1.399	<b>R(54-56)</b>	1.395
<b>R(6-22)</b>	1.51	<b>R(17-19)</b>	1.391	<b>R(30-31)</b>	1.086	<b>R(43-44)</b>	1.085	<b>R(56-57)</b>	1.085
<b>R(7-8)</b>	1.087	<b>R(19-20)</b>	1.086	<b>R(30-32)</b>	1.397	<b>R(43-45)</b>	1.396	<b>R(58-63)</b>	2.006
<b>R(7-9)</b>	1.42	<b>R(19-21)</b>	1.414	<b>R(32-33)</b>	1.085	<b>R(45-46)</b>	1.085	<b>R(59-63)</b>	2.021
<b>R(9-10)</b>	1.438	<b>R(21-60)</b>	1.329	<b>R(32-34)</b>	1.397	<b>R(47-48)</b>	1.404	<b>R(60-63)</b>	2.028
<b>R(10-11)</b>	1.089	<b>R(22-23)</b>	1.095	<b>R(34-35)</b>	1.084	<b>R(47-56)</b>	1.407	<b>R(62-63)</b>	2.42
<b>R(10-58)</b>	1.302	<b>R(22-24)</b>	1.093	<b>R(36-37)</b>	1.405	<b>R(47-61)</b>	1.817		

**Table S4.** Calculated bond angle in optimized structure of complex **1**



A(2-1-9)	117.1	A(12-13-14)	120.8	A(25-34-32)	119.9	A(42-41-43)	119.9
A(2-1-59)	117.1	A(12-13-15)	120.1	A(25-34-35)	120.6	A(41-43-44)	120.3
A(1-2-3)	117.3	A(21-12-58)	113.9	A(25-61-36)	109.9	A(41-43-45)	120.2
A(1-2-4)	122	A(12-21-19)	118.4	A(25-61-47)	109.8	A(44-43-45)	119.5
A(9-1-59)	125.8	A(12-21-60)	120.6	A(27-26-28)	119.3	A(43-45-46)	118.9
A(1-9-7)	119	A(12-58-63)	111.4	A(26-28-29)	119.5	A(48-47-56)	119.8
A(1-9-10)	124.8	A(14-13-15)	119.1	A(26-28-30)	120.2	A(48-47-61)	121
A(1-59-63)	124.3	A(13-15-16)	119.8	A(29-28-30)	120.3	A(47-48-49)	120.7
A(3-2-4)	120.6	A(13-15-17)	119.8	A(28-30-31)	119.9	A(47-48-50)	119.9
A(2-4-5)	119.1	A(16-15-17)	120.4	A(28-30-32)	120.1	A(56-47-61)	119.2
A(2-4-6)	121.3	A(15-17-18)	119.8	A(31-30-32)	120	A(47-56-54)	120
A(5-4-6)	119.6	A(15-17-19)	120.7	A(30-32-33)	120.3	A(47-56-57)	121.1
A(4-6-7)	117.7	A(18-17-19)	119.5	A(30-32-34)	120.2	A(49-48-50)	119.4
A(4-6-22)	120.3	A(17-19-20)	121.2	A(33-32-34)	119.5	A(48-50-51)	119.5
A(7-6-22)	122	A(17-19-21)	120.4	A(32-34-35)	119.5	A(48-50-52)	120.2
A(6-7-8)	119.6	A(20-19-21)	118.4	A(37-36-45)	119.8	A(51-50-52)	120.3
A(6-7-9)	122.8	A(19-21-60)	121	A(37-36-61)	120	A(50-52-53)	120
A(6-22-23)	112.1	A(21-60-63)	110.8	A(36-37-38)	120.6	A(50-52-54)	120.1
A(6-22-24)	110.5	A(23-22-24)	106.8	A(36-37-39)	119.9	A(53-52-54)	119.9
A(6-22-61)	116.1	A(23-22-61)	105.4	A(45-36-61)	120.3	A(52-54-55)	120.3
A(8-7-9)	117.6	A(24-22-61)	105.4	A(36-45-43)	119.9	A(52-54-56)	120.1
A(7-9-10)	116.1	A(22-61-25)	111	A(36-45-46)	121.2	A(55-54-56)	119.6
A(9-10-11)	115.2	A(22-61-36)	107.7	A(36-61-47)	109	A(54-56-57)	119
A(9-10-58)	126.9	A(22-61-47)	109.4	A(38-37-39)	119.5	A(58-63-59)	94.2
A(11-10-58)	117.9	A(26-25-34)	119.8	A(37-39-40)	119.5	A(58-63-60)	83.2
A(10-58-12)	124.7	A(26-25-61)	119.9	A(37-39-41)	120.2	A(58-63-62)	176
A(10-58-63)	123.9	A(25-26-27)	120.8	A(40-39-41)	120.3	A(59-63-60)	177.4
A(13-12-21)	120.6	A(25-26-28)	119.8	A(39-41-42)	120	A(59-63-62)	89.9
A(13-12-58)	125.5	A(34-25-61)	120.3	A(39-41-43)	120.1	A(60-63-62)	92.7

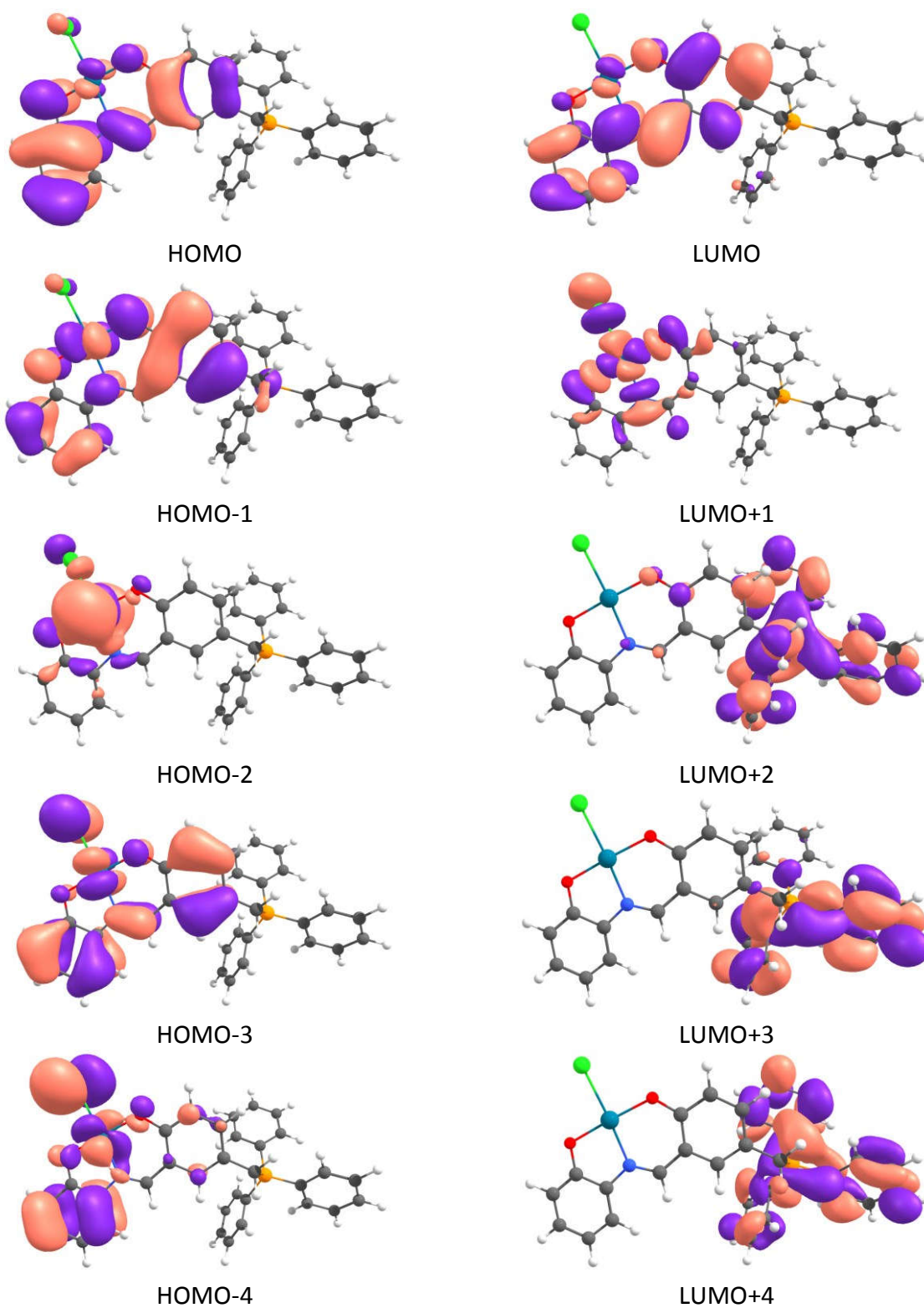


**Figure S1.** Contour map of the frontier molecular orbital of complex **1**



**Table S5.** Frontier molecular orbital composition in the ground state structure of complex **1**

MO	eV	Pd	Imine bond	Cl	Aminophenol ring	Benzyl ring	PPh <sub>3</sub>
LUMO+4	-1.67	0	0	0	0	1	98
LUMO+3	-1.8	0	0	0	0	2	97
LUMO+2	-1.89	0	1	0	1	-5	104
LUMO+1	-2.08	53	11	10	9	16	0
LUMO	-2.26	<b>3</b>	<b>37</b>	<b>0</b>	<b>20</b>	<b>35</b>	<b>5</b>
HOMO	-5.61	<b>3</b>	<b>7</b>	<b>1</b>	<b>71</b>	<b>17</b>	<b>0</b>
HOMO-1	-5.9	17	5	1	20	56	1
HOMO-2	-6.69	87	2	4	5	2	0
HOMO-3	-6.71	20	7	13	28	31	1
HOMO-4	-6.98	21	1	40	32	5	0

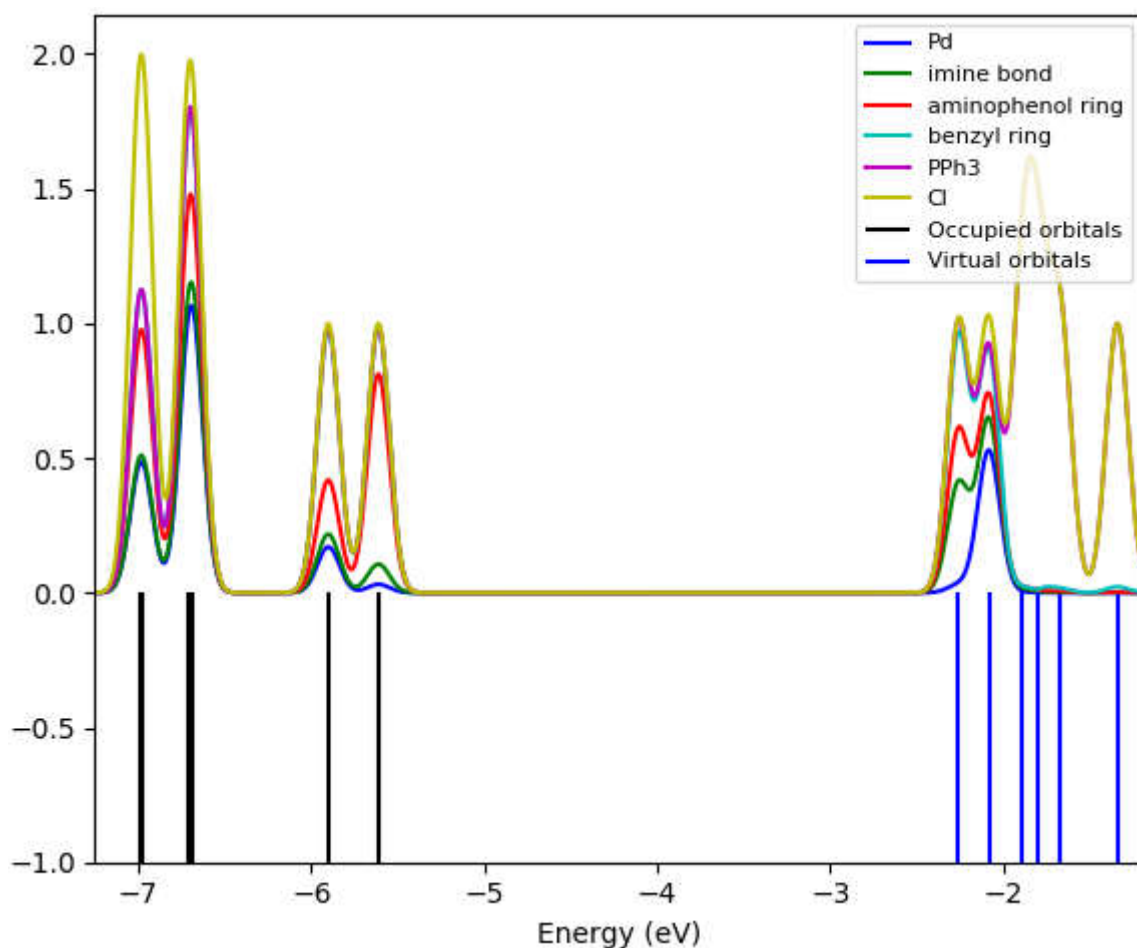


**Figure S2.** Density of states level energy for Frontier molecular orbital of complex **1**



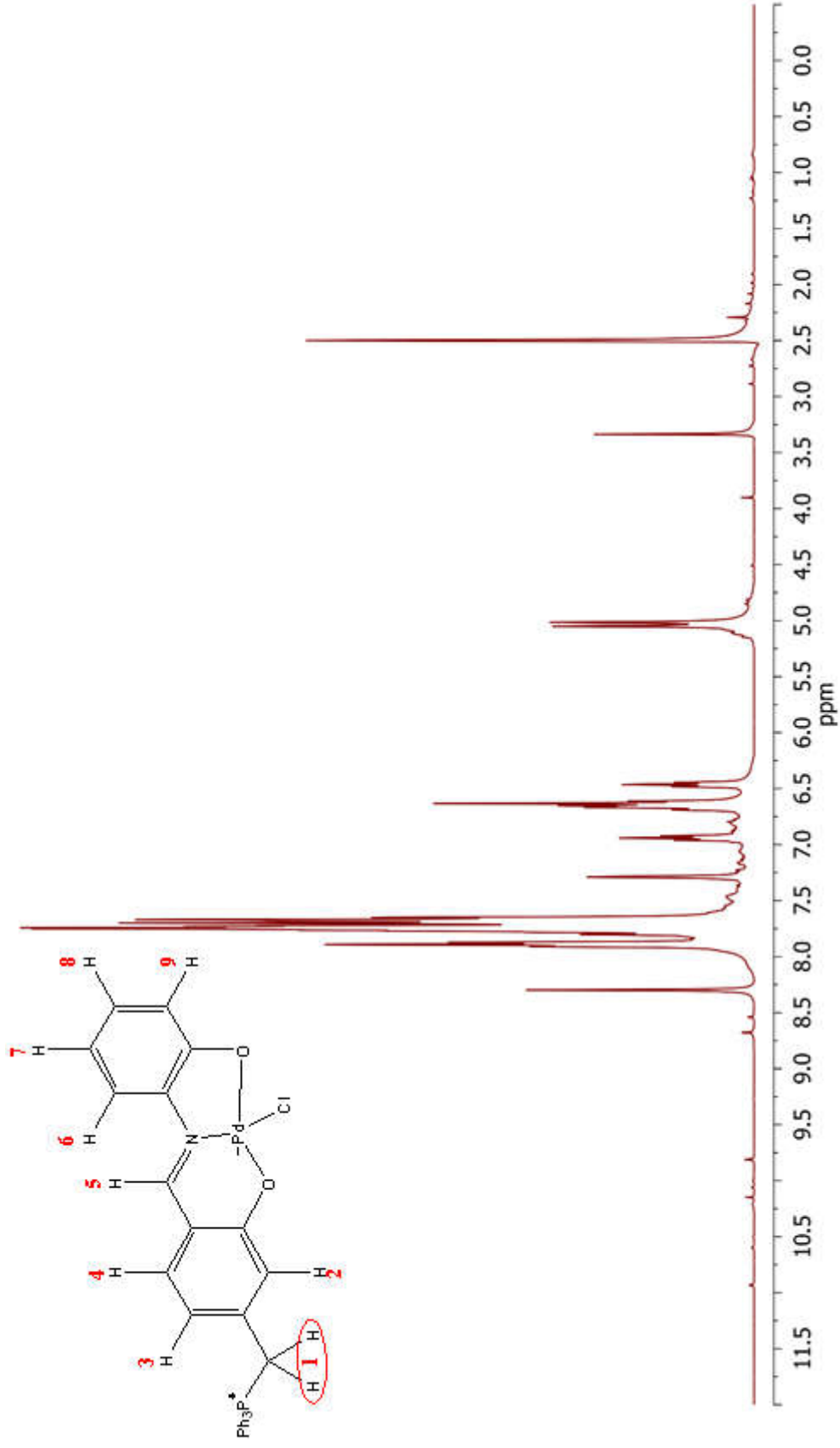


**Figure S3.**  $^1\text{H-NMR}$  spectrum of zwitterionic complex **1**

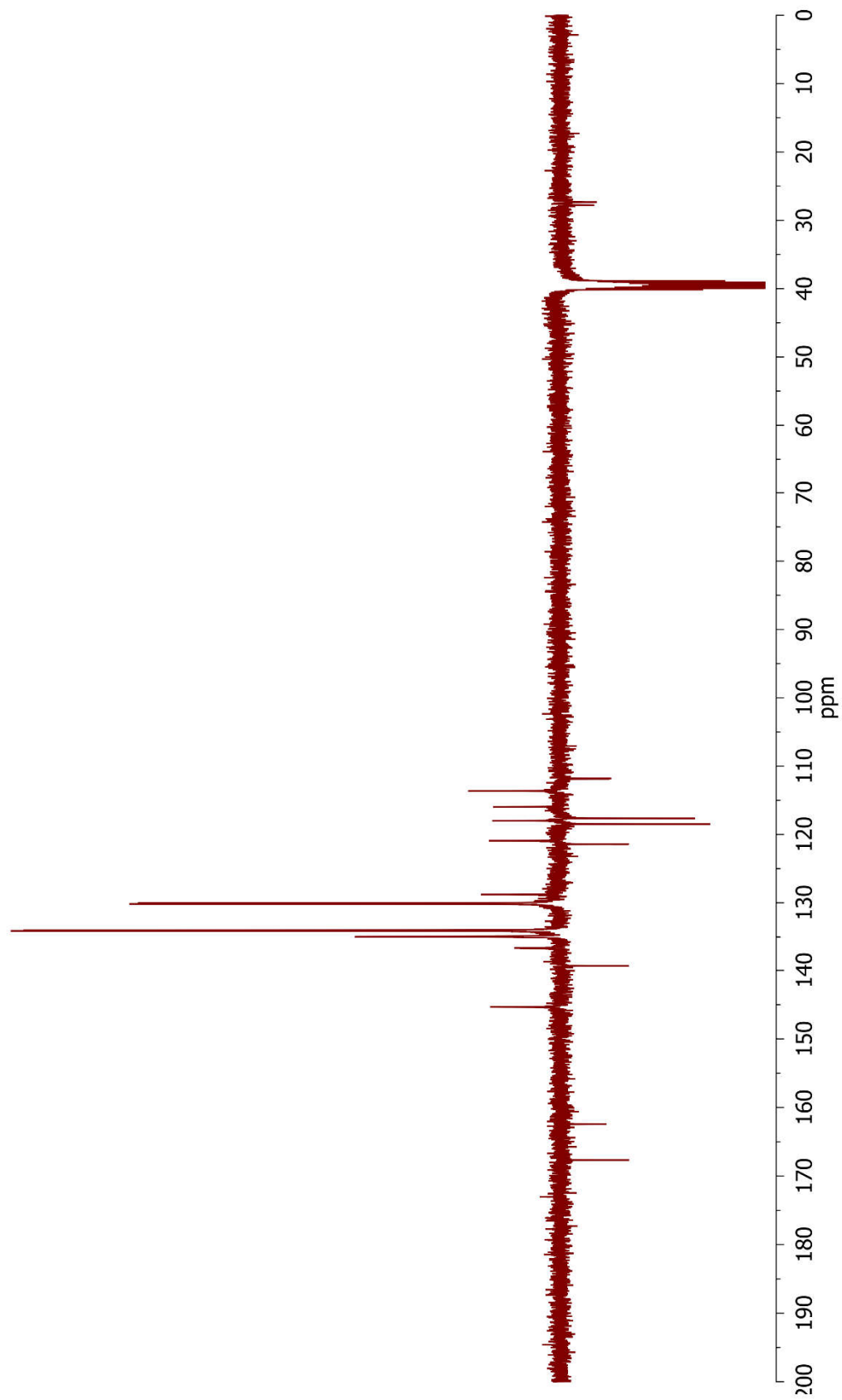


**Figure S4.**  $^{13}\text{C}$ -NMR spectrum of zwitterionic complex **1**

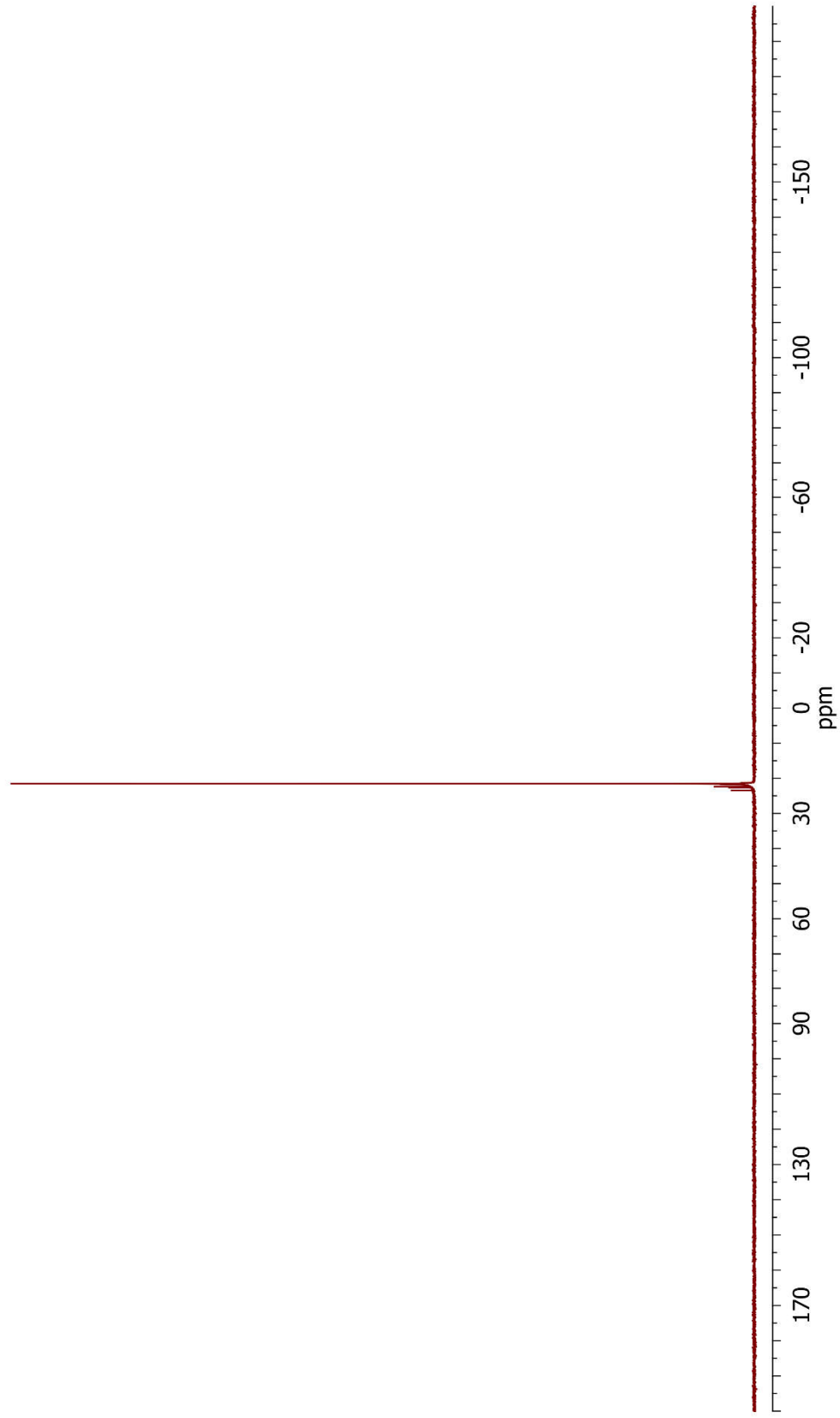


**Figure S5.**  $^{31}\text{P}$ -NMR spectrum of zwitterionic complex **1**

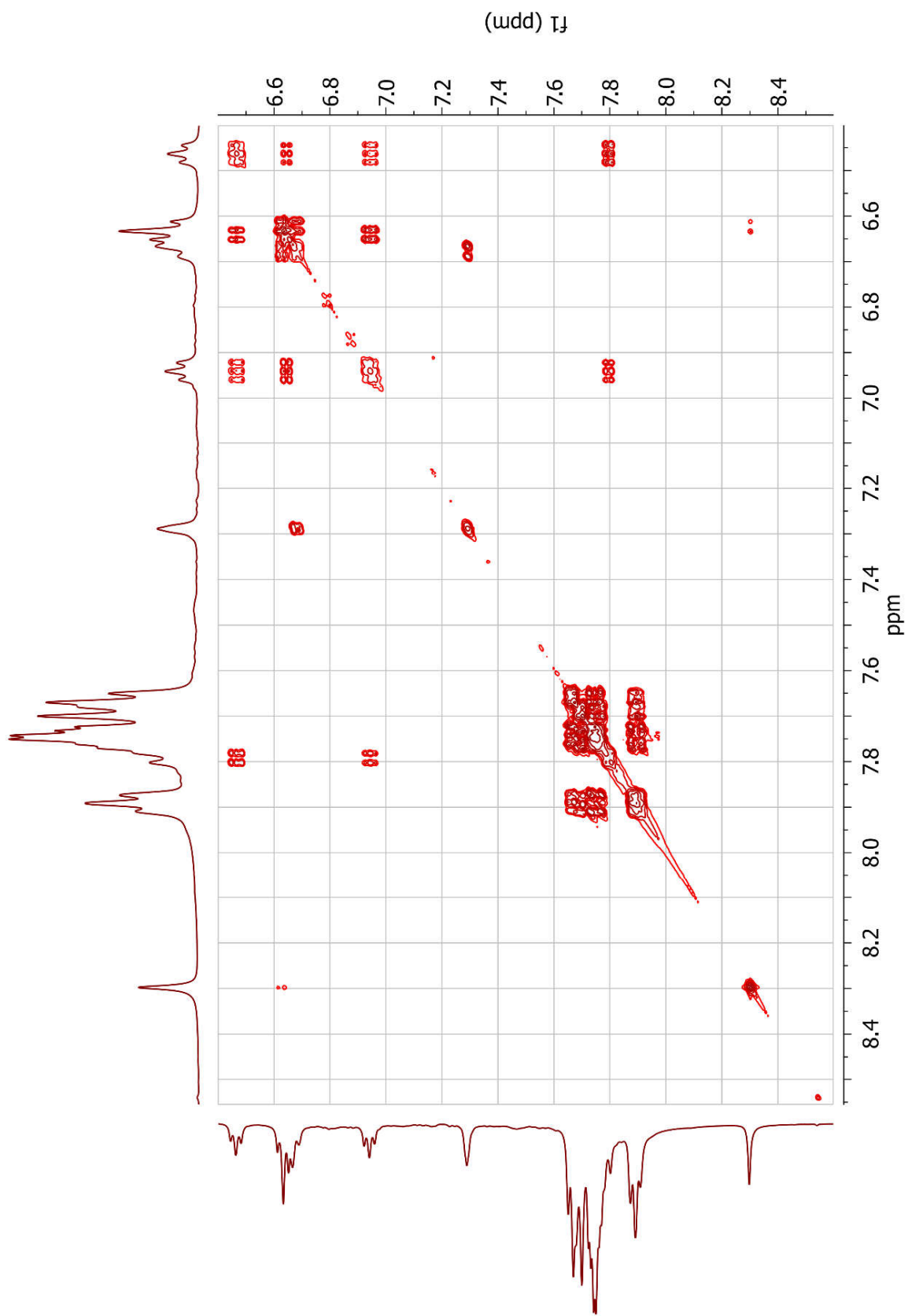


**Figure S6.**  $^1\text{H}$ - $^1\text{H}$  COSY NMR spectrum of zwitterionic complex **1**

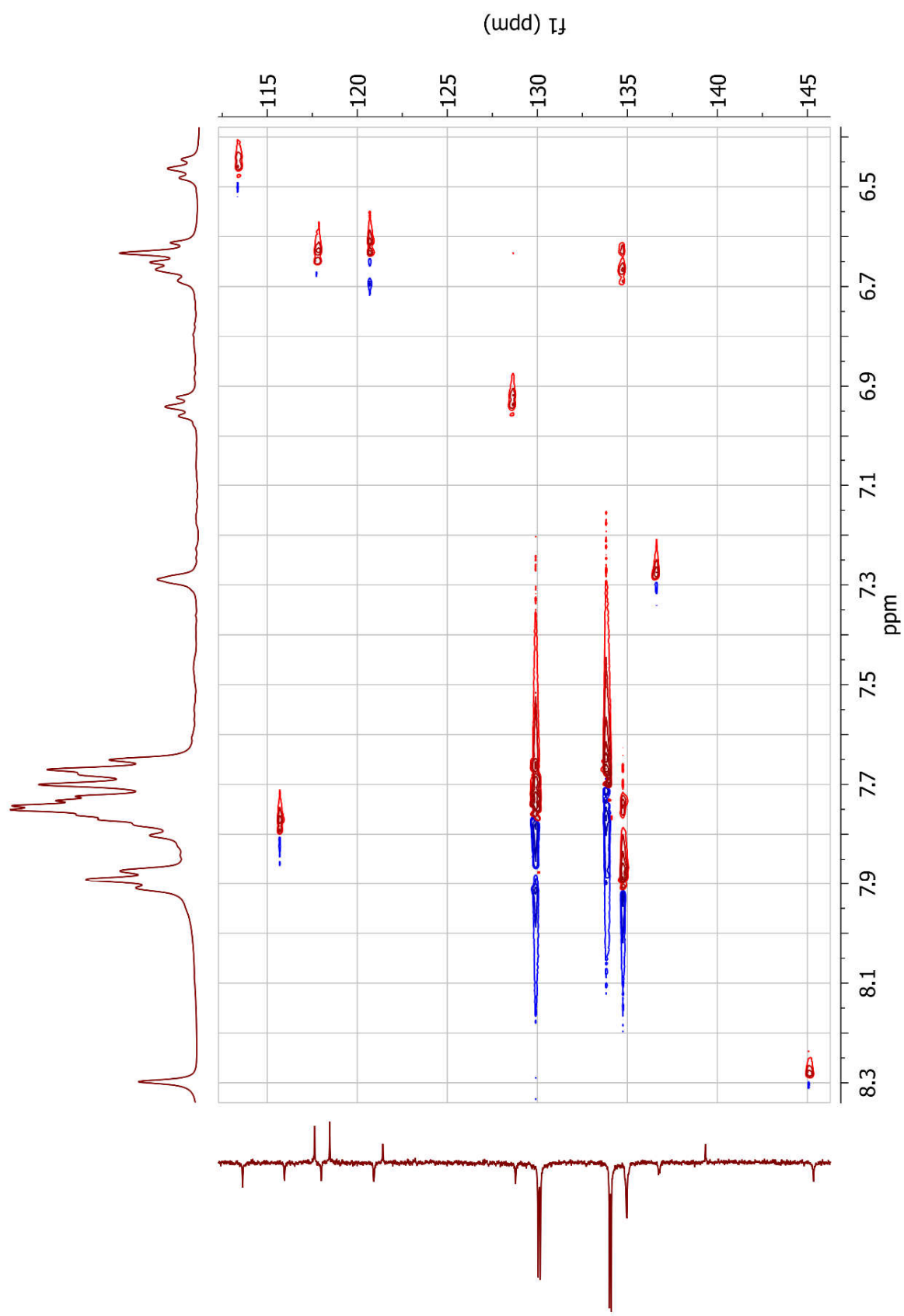


**Figure S7.**  $^1\text{H}$ - $^{13}\text{C}$  HSQC NMR spectrum of zwitterionic complex **1**

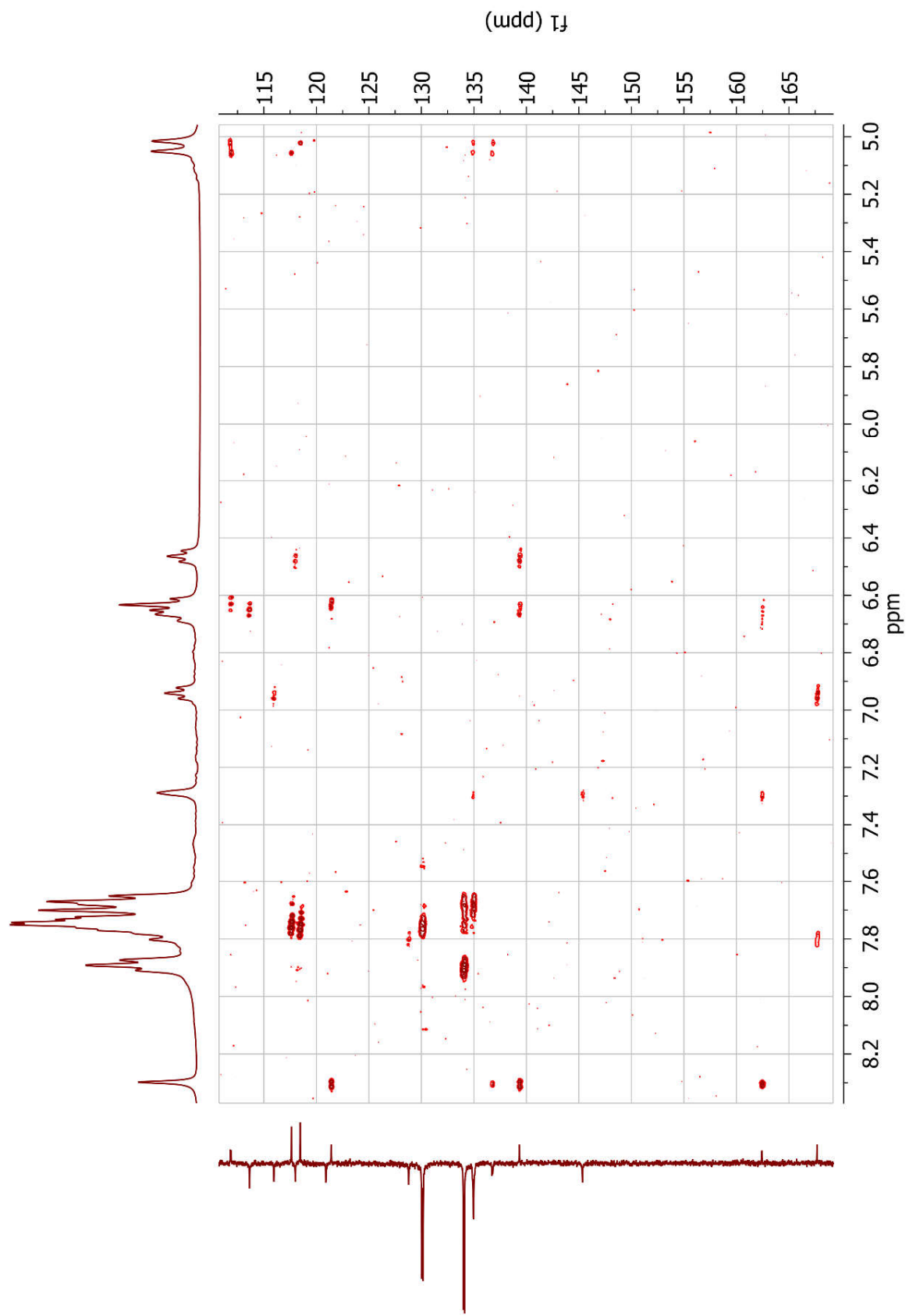


**Figure S8.**  $^1\text{H}$ - $^{13}\text{C}$  HMB NMR spectrum of zwitterionic complex **1**

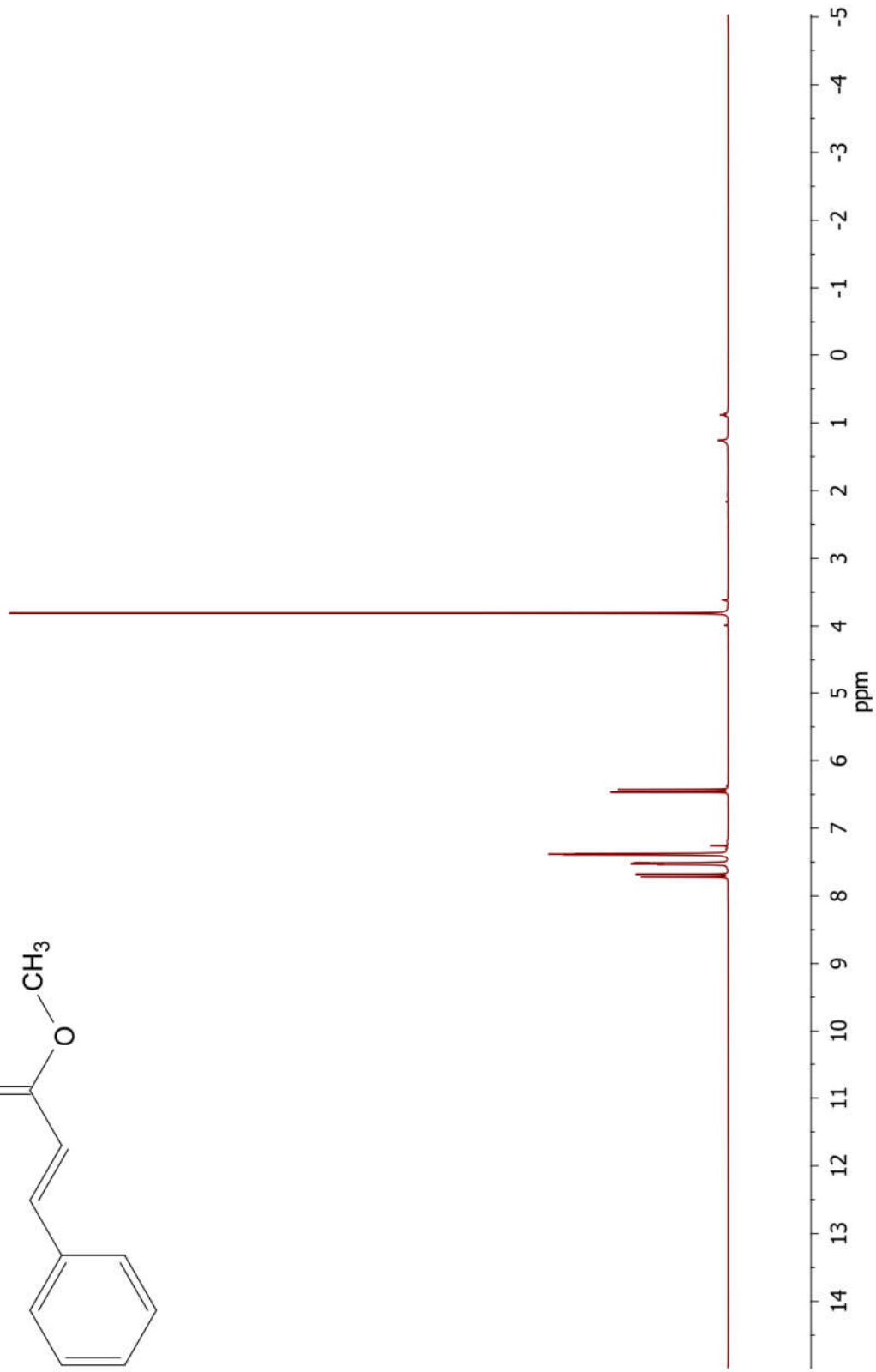
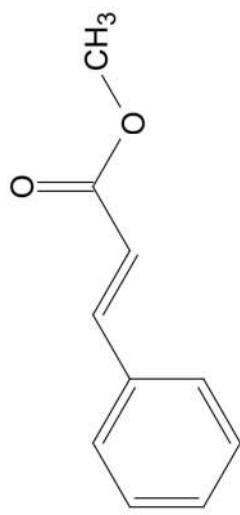


Figure S9. <sup>1</sup>H-NMR spectrum of **3a**

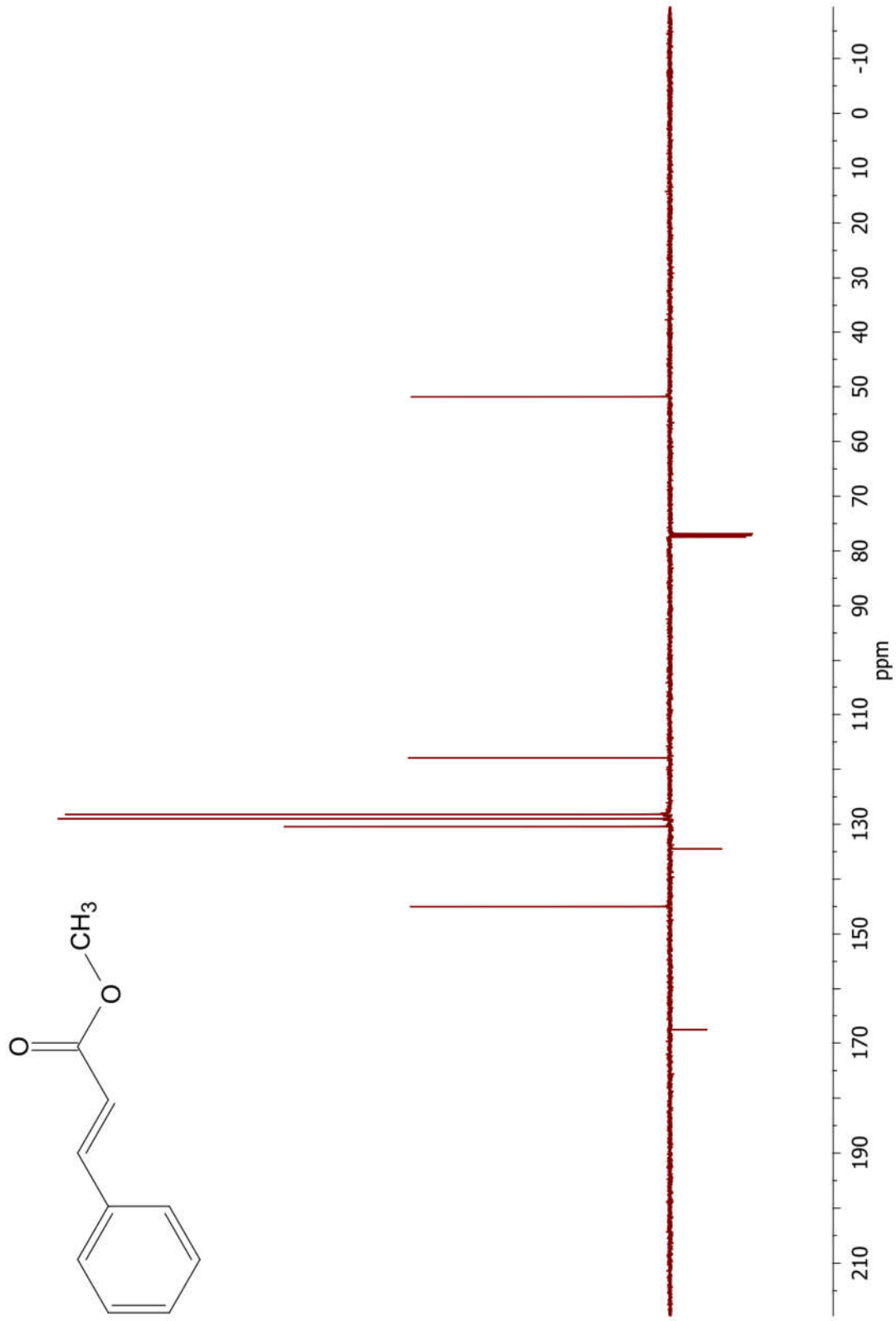


Figure S10. <sup>13</sup>C-NMR spectrum of 3a



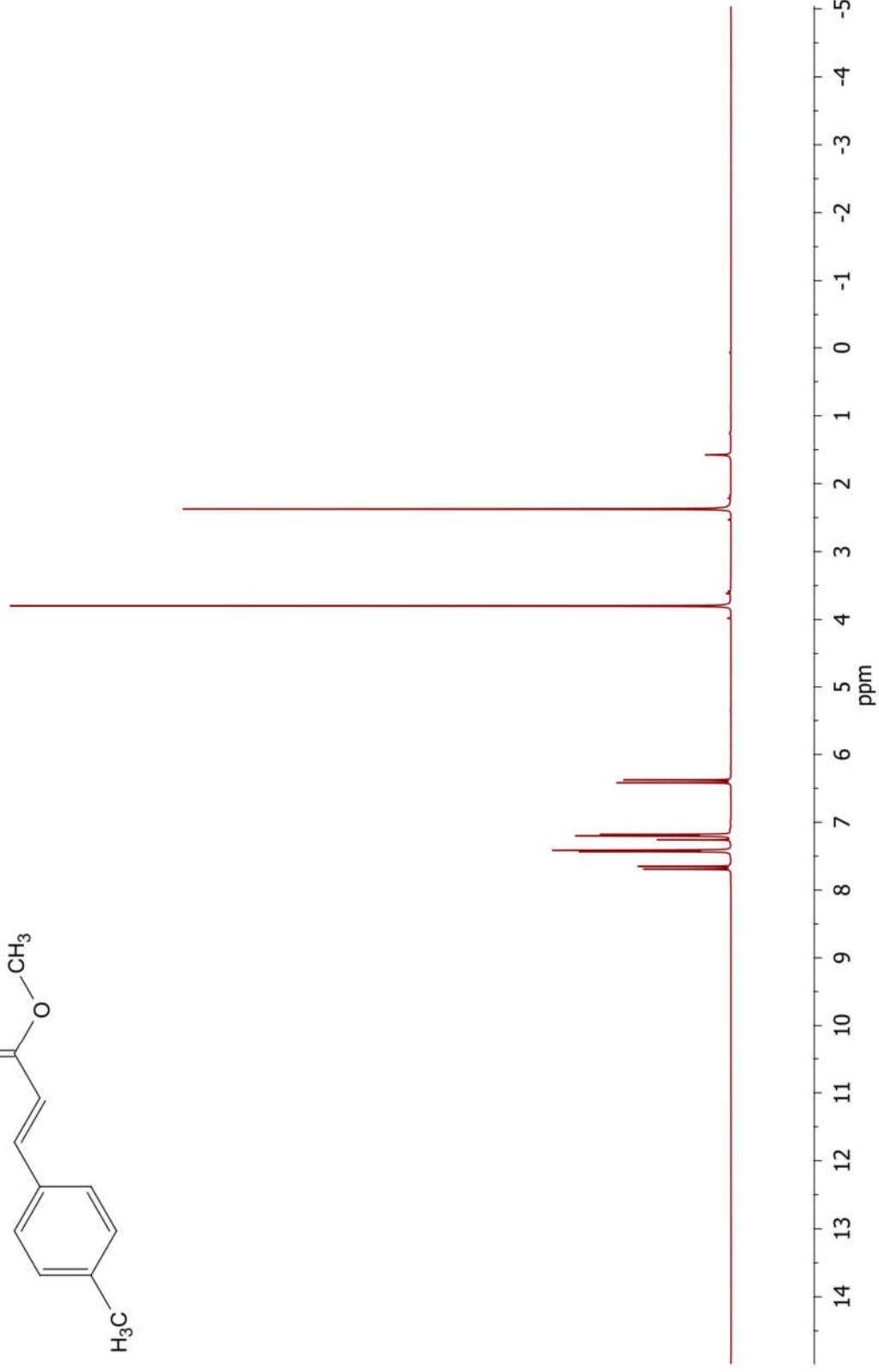
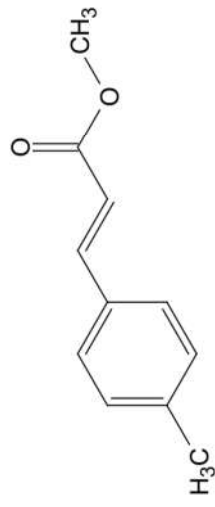


Figure S11. <sup>1</sup>H-NMR spectrum of **3b**

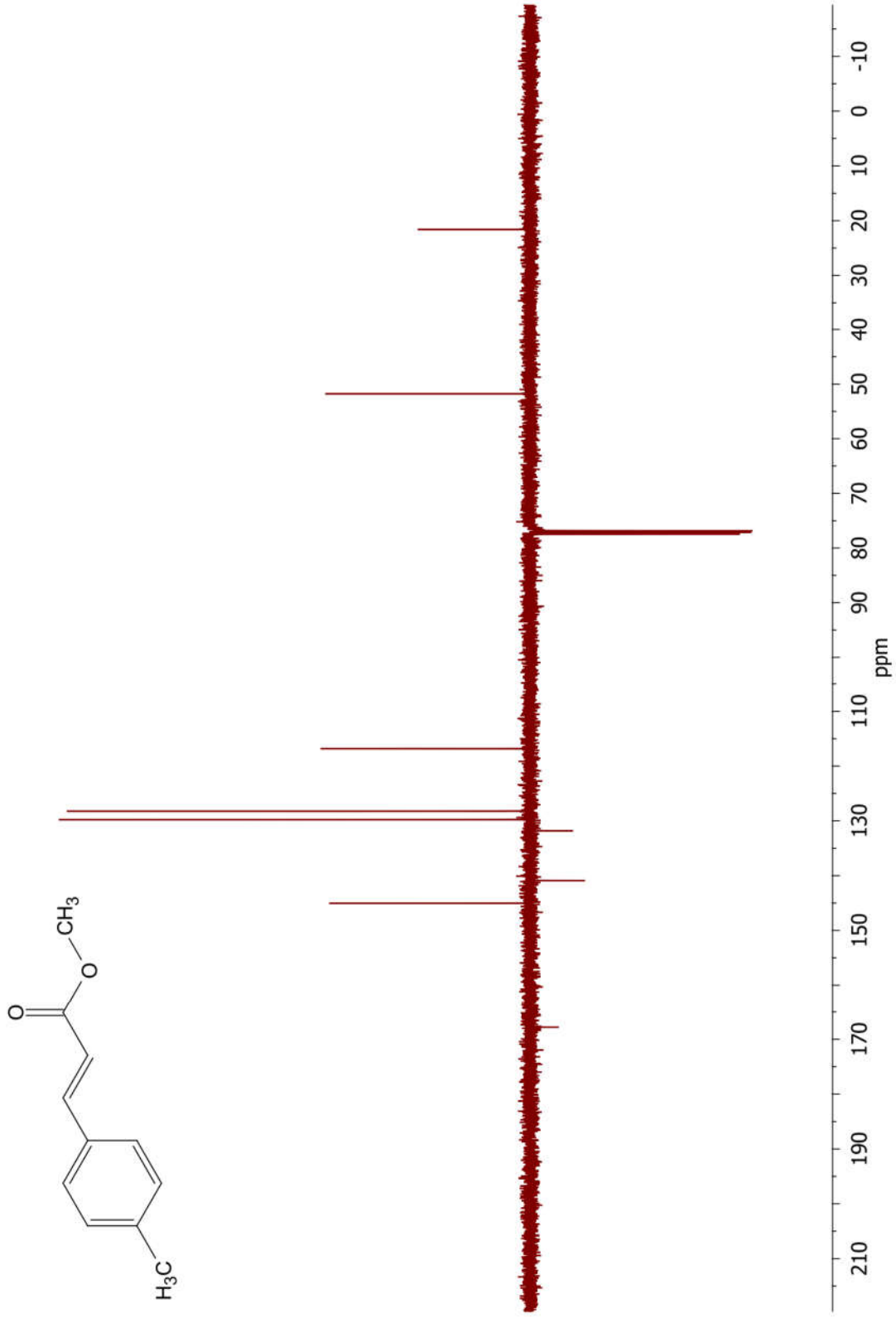


Figure S12. <sup>13</sup>C-NMR spectrum of 3b

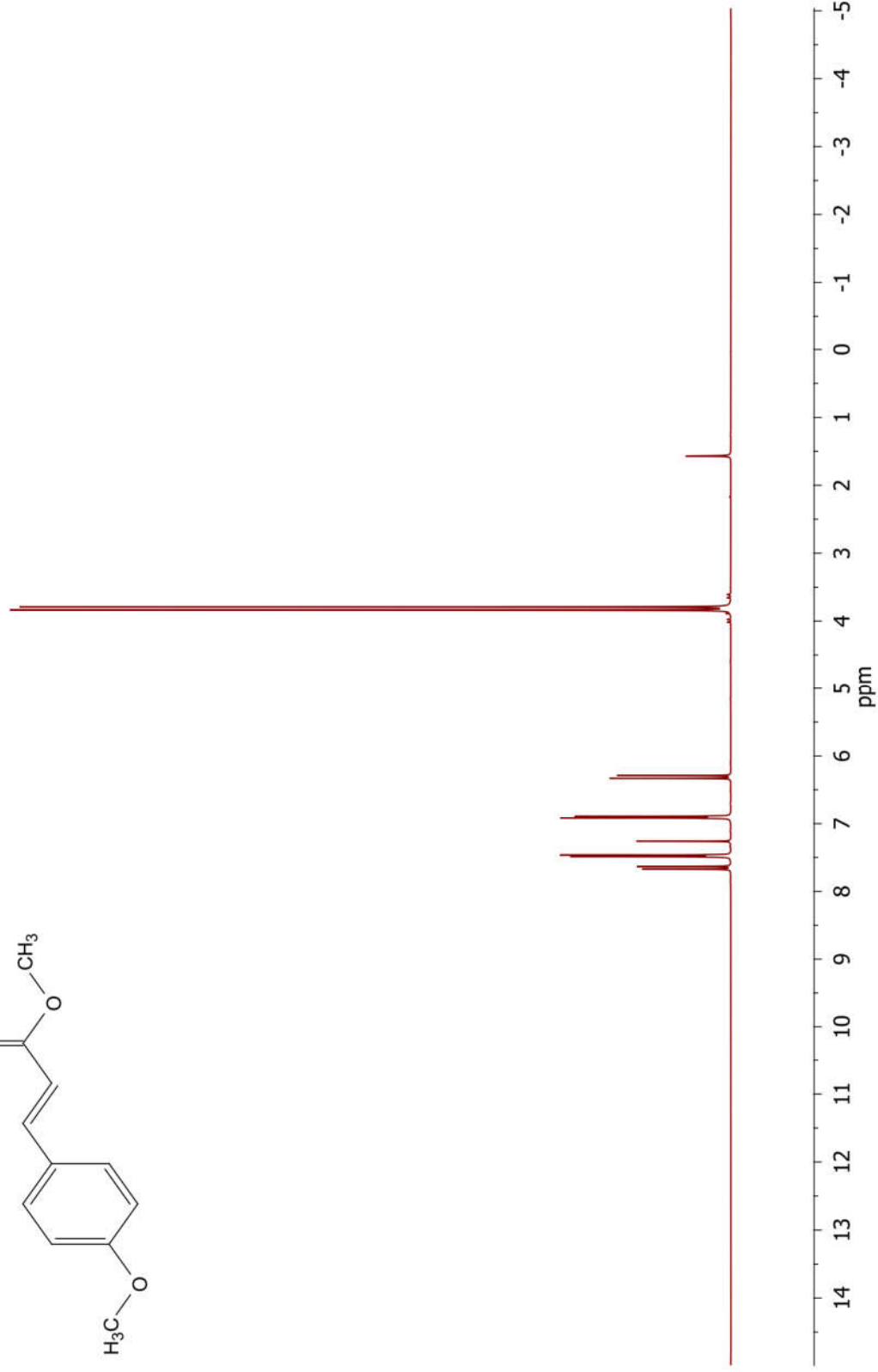
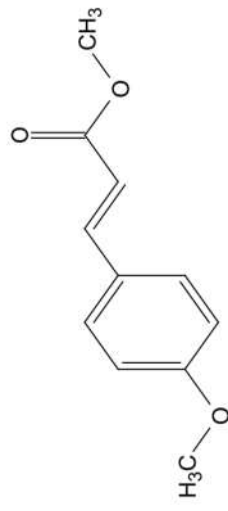
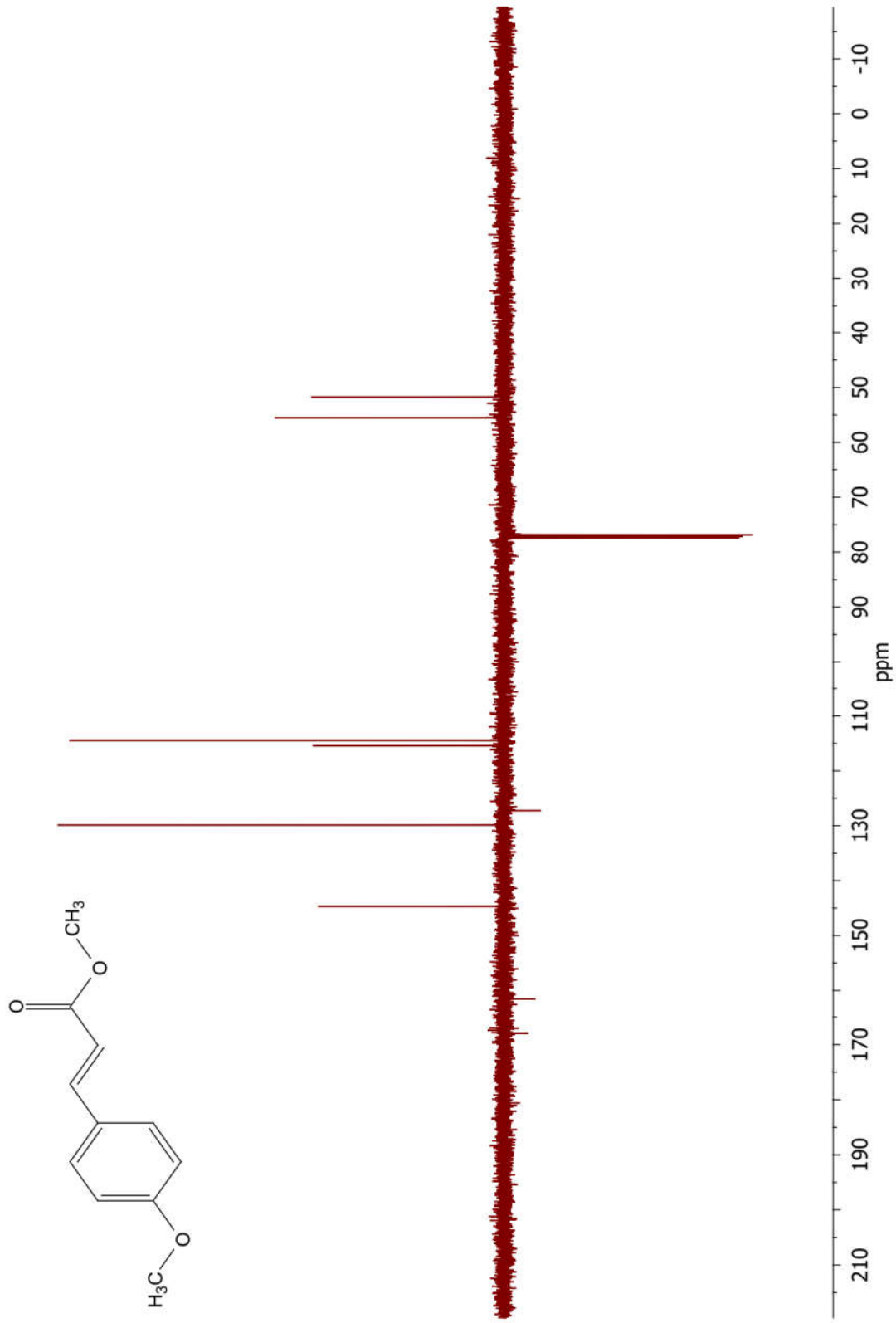
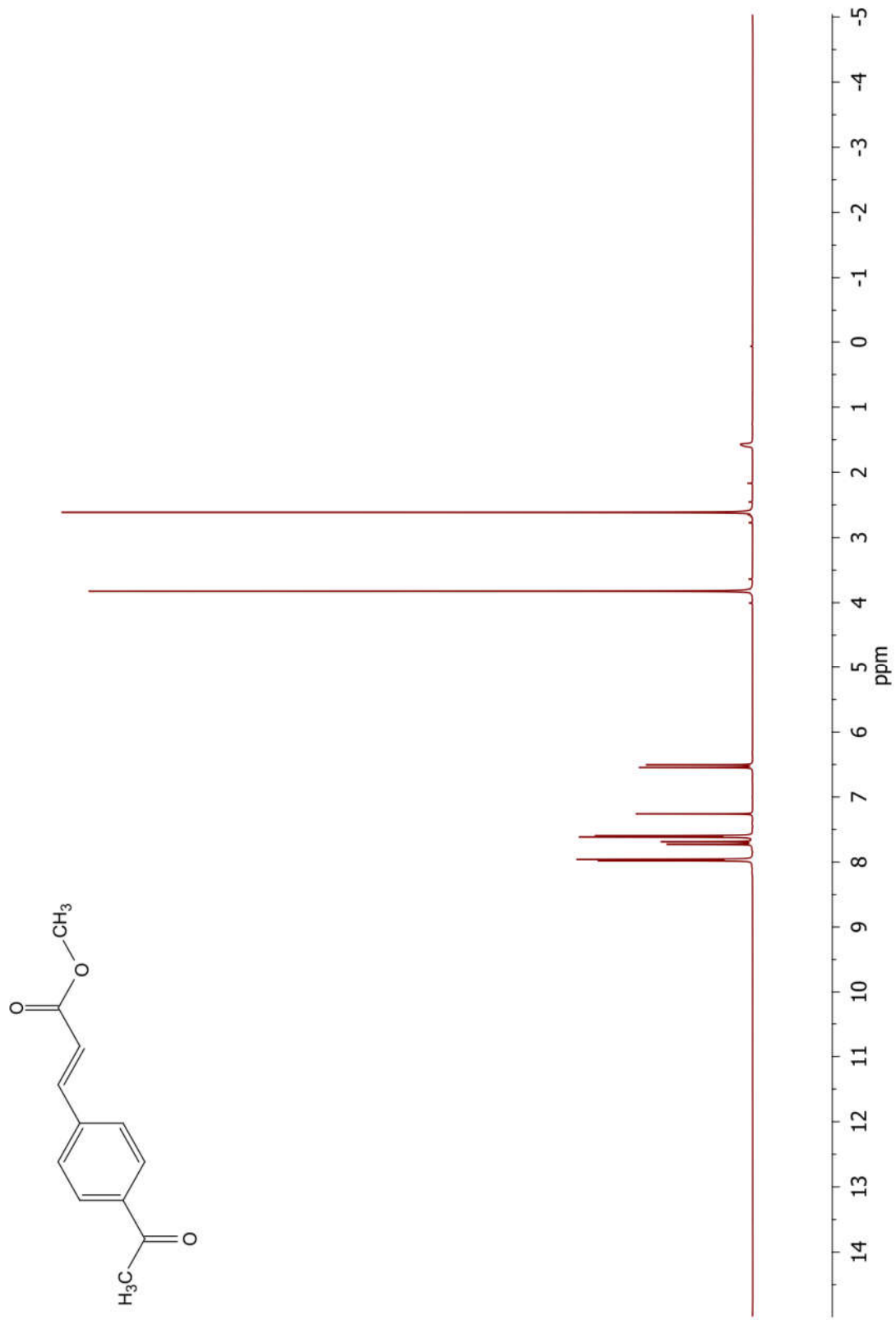


Figure S13. <sup>1</sup>H-NMR spectrum of **3c**



**Figure S14.** <sup>13</sup>C-NMR spectrum of **3c**



**Figure S15.**  $^1\text{H-NMR}$  spectrum of **3d**

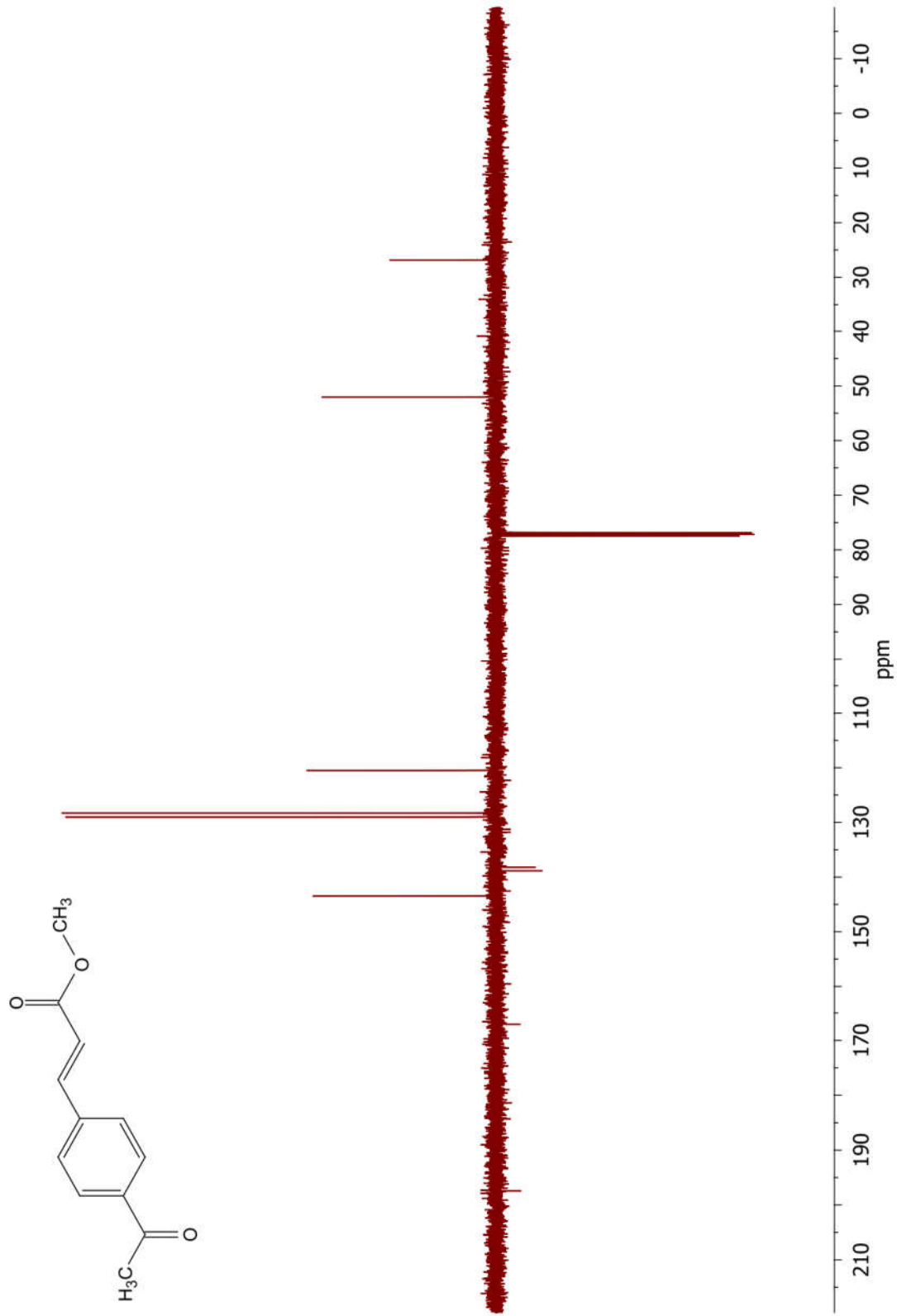


**Figure S16.**  $^{13}\text{C}$ -NMR spectrum of **3d**

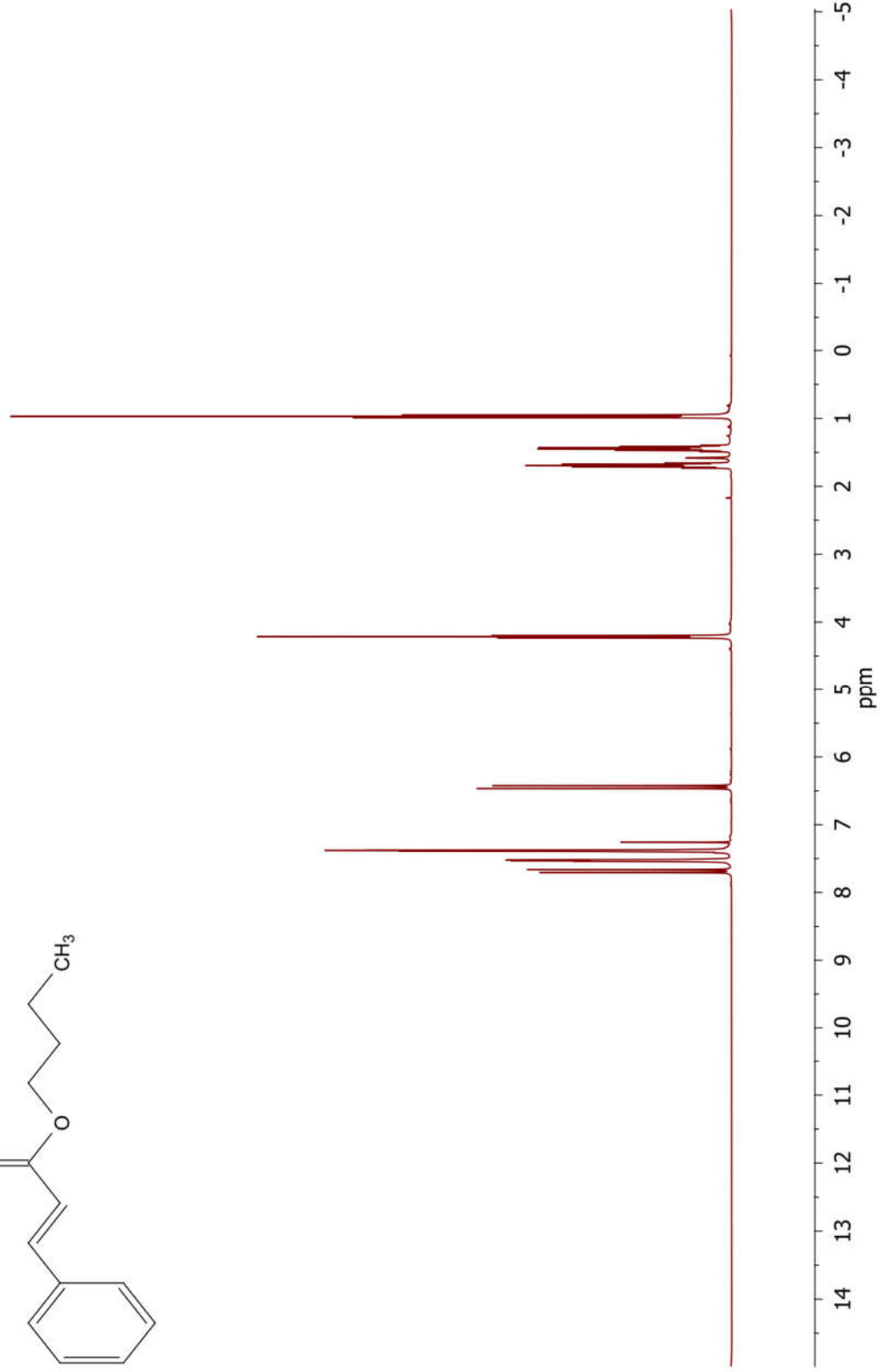
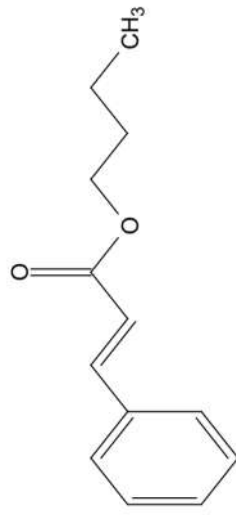
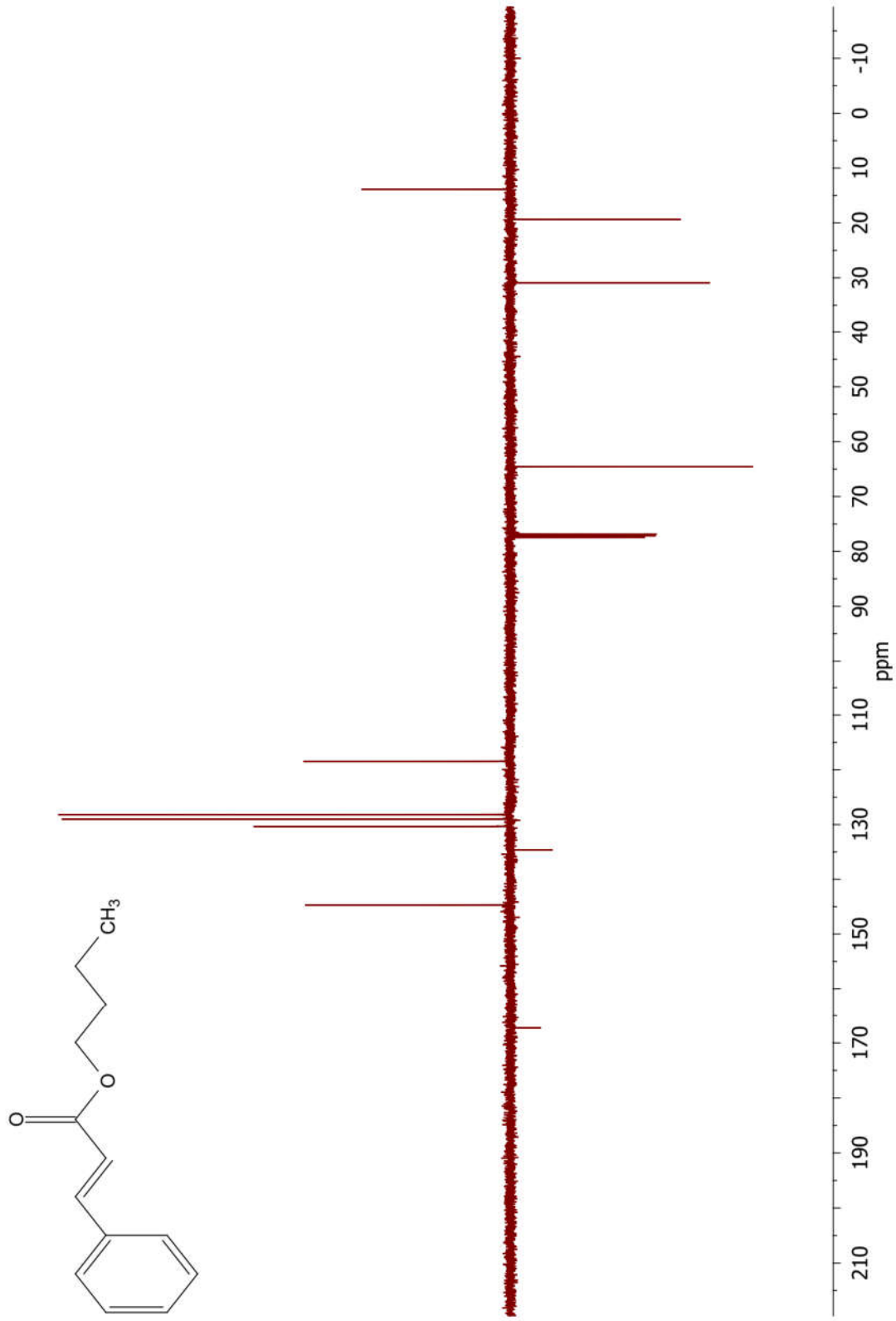


Figure S17. <sup>1</sup>H-NMR spectrum of 3e



**Figure S18.**  $^{13}\text{C}$ -NMR spectrum of **3e**



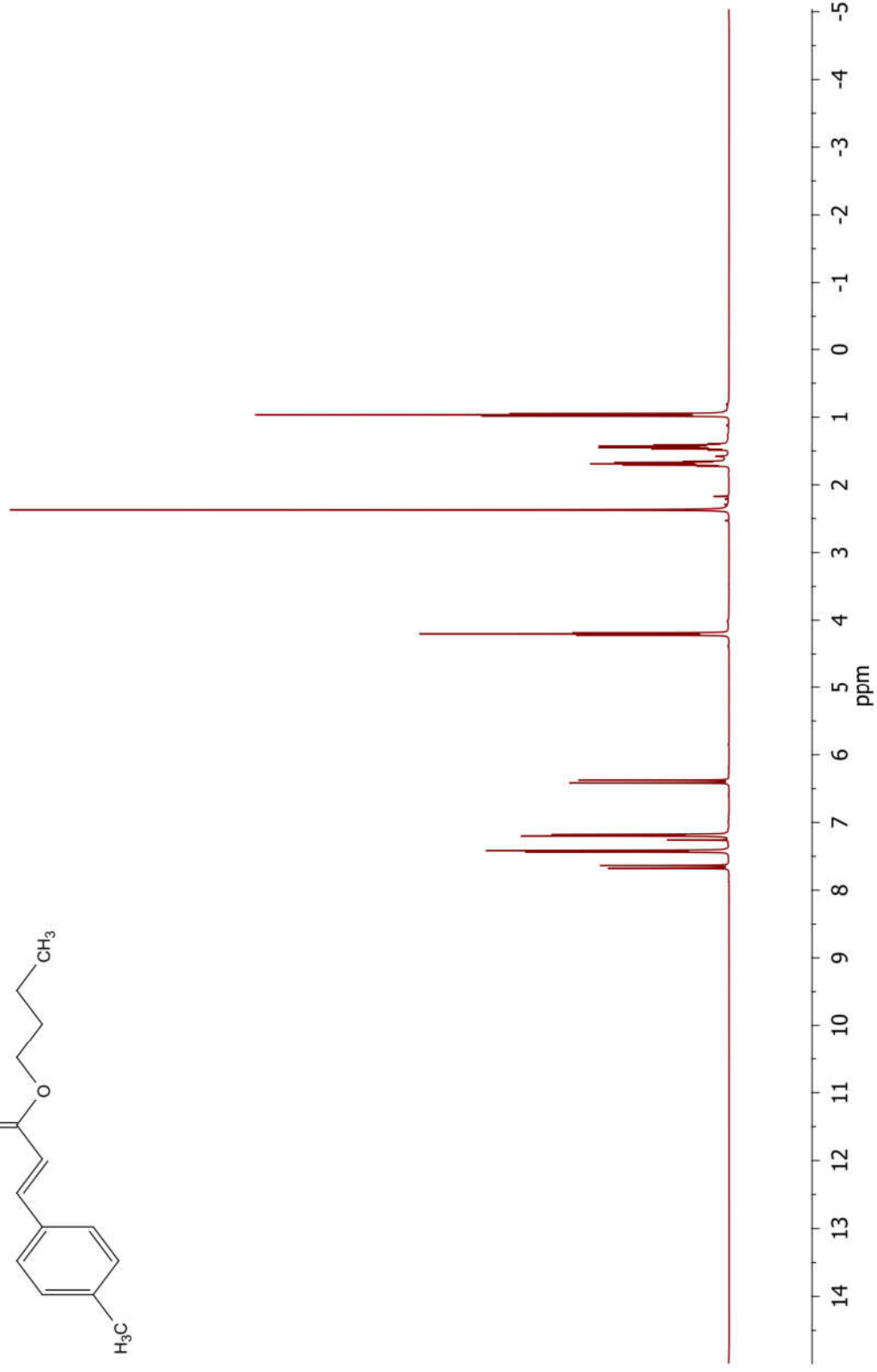
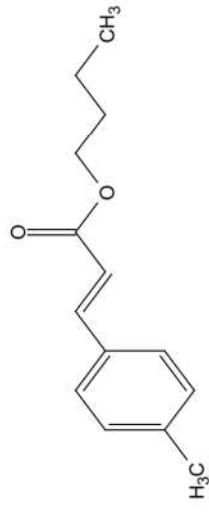


Figure S19. <sup>1</sup>H-NMR spectrum of 3f

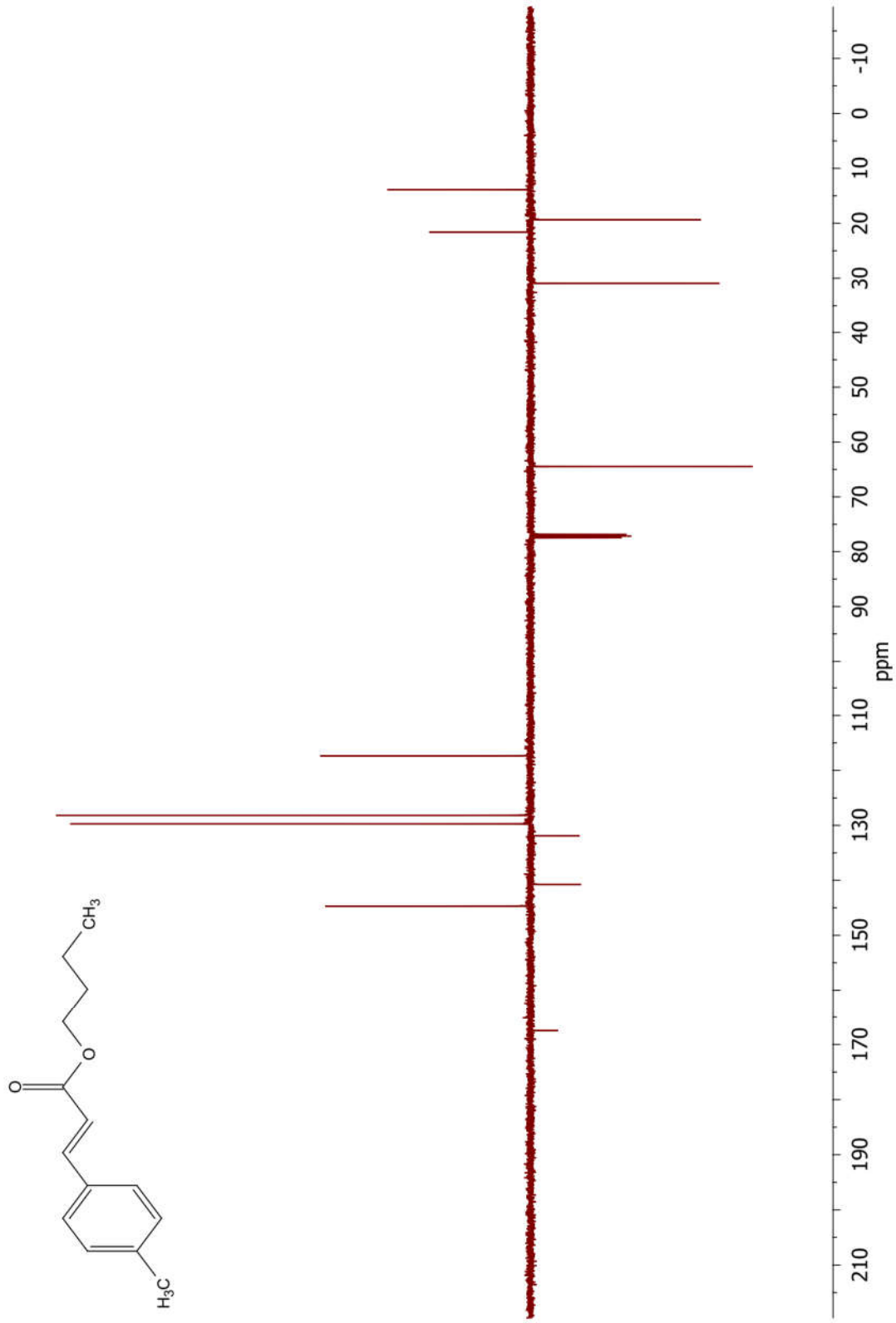


Figure S20.  $^{13}\text{C}$ -NMR spectrum of **3f**

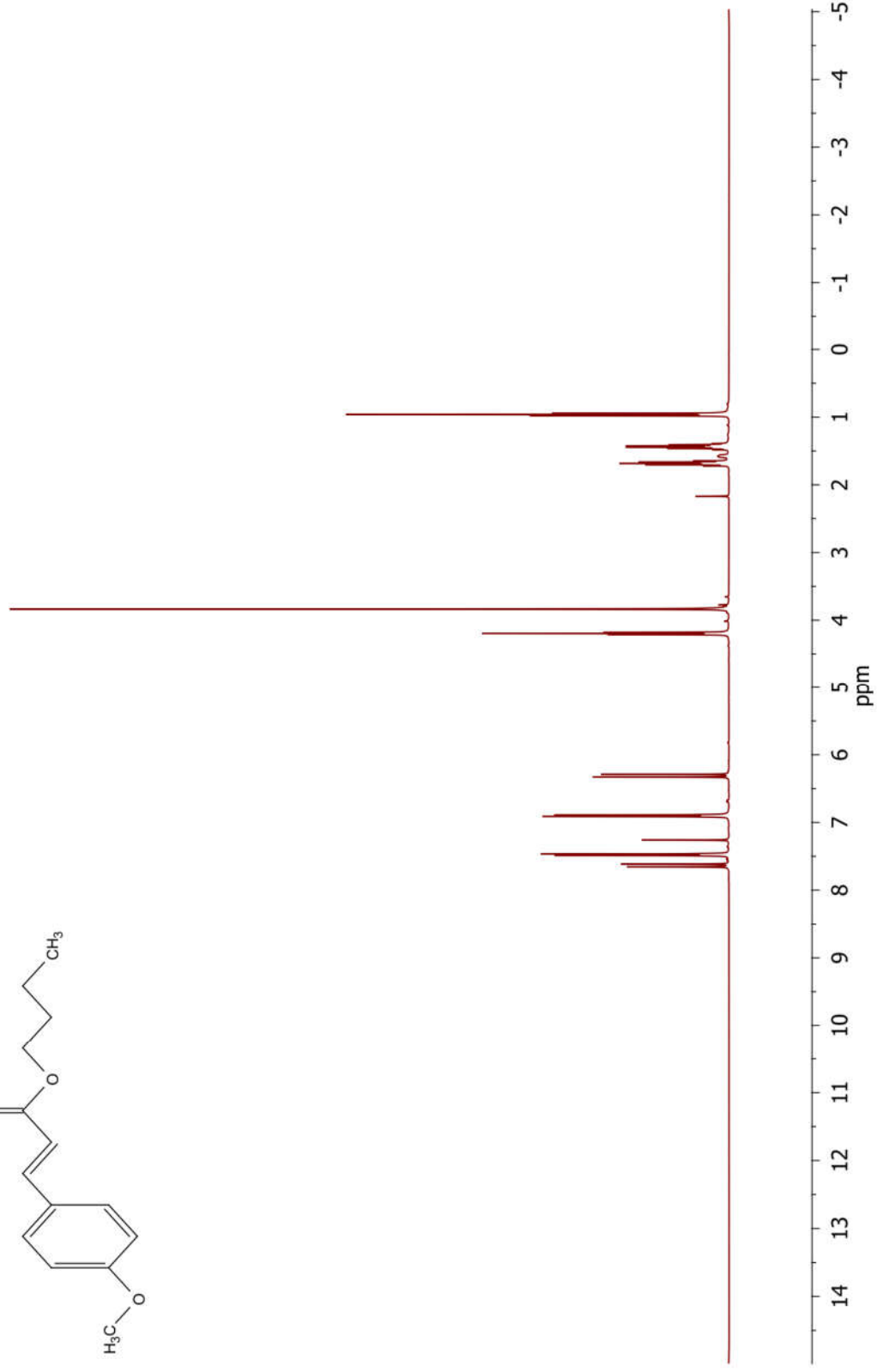
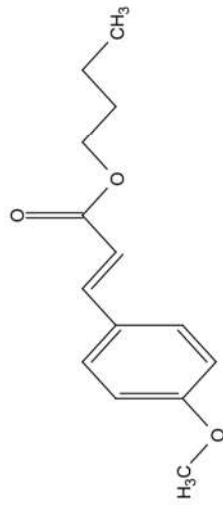
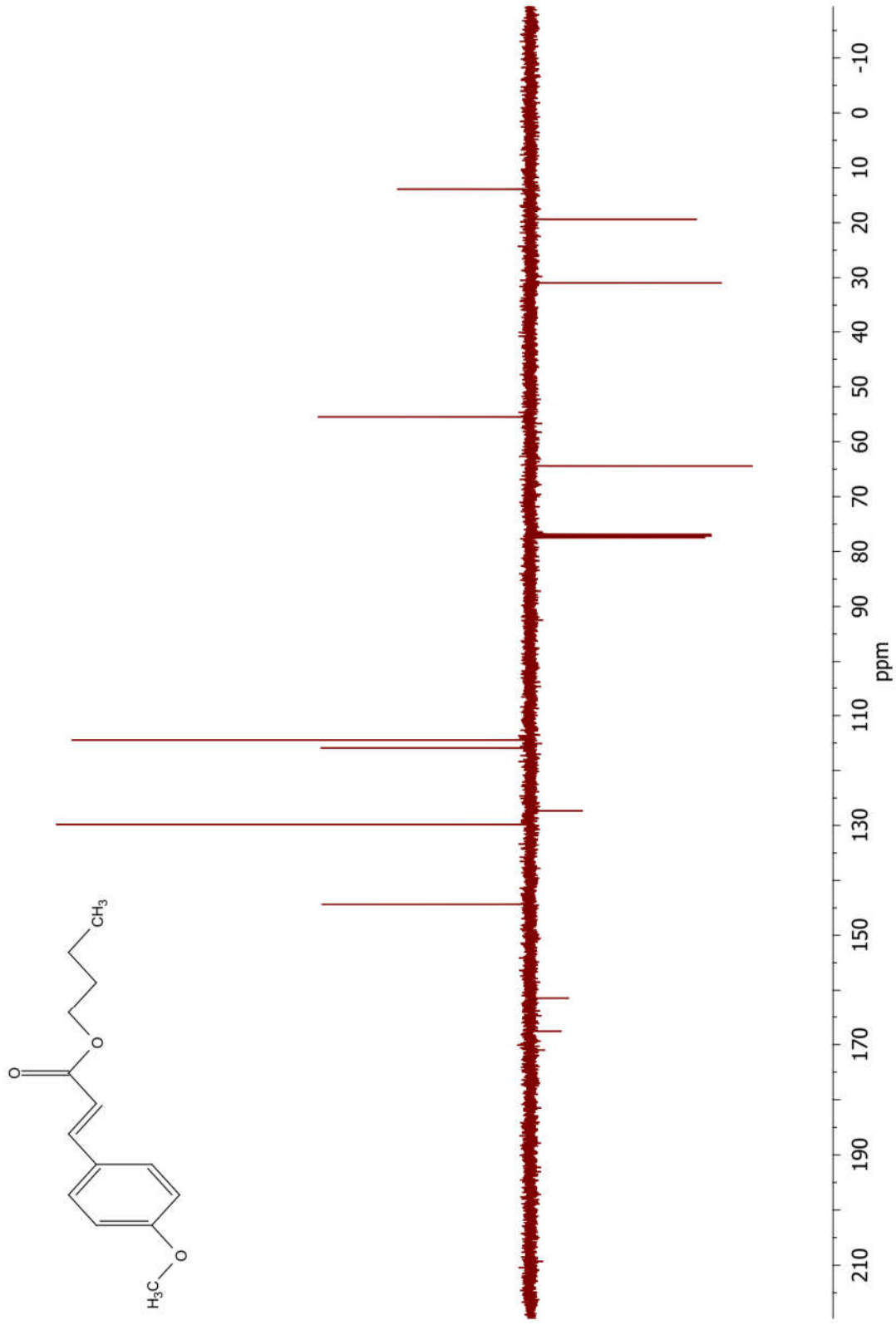


Figure S21. <sup>1</sup>H-NMR spectrum of 3g



**Figure S22.**  $^{13}\text{C}$ -NMR spectrum of **3g**

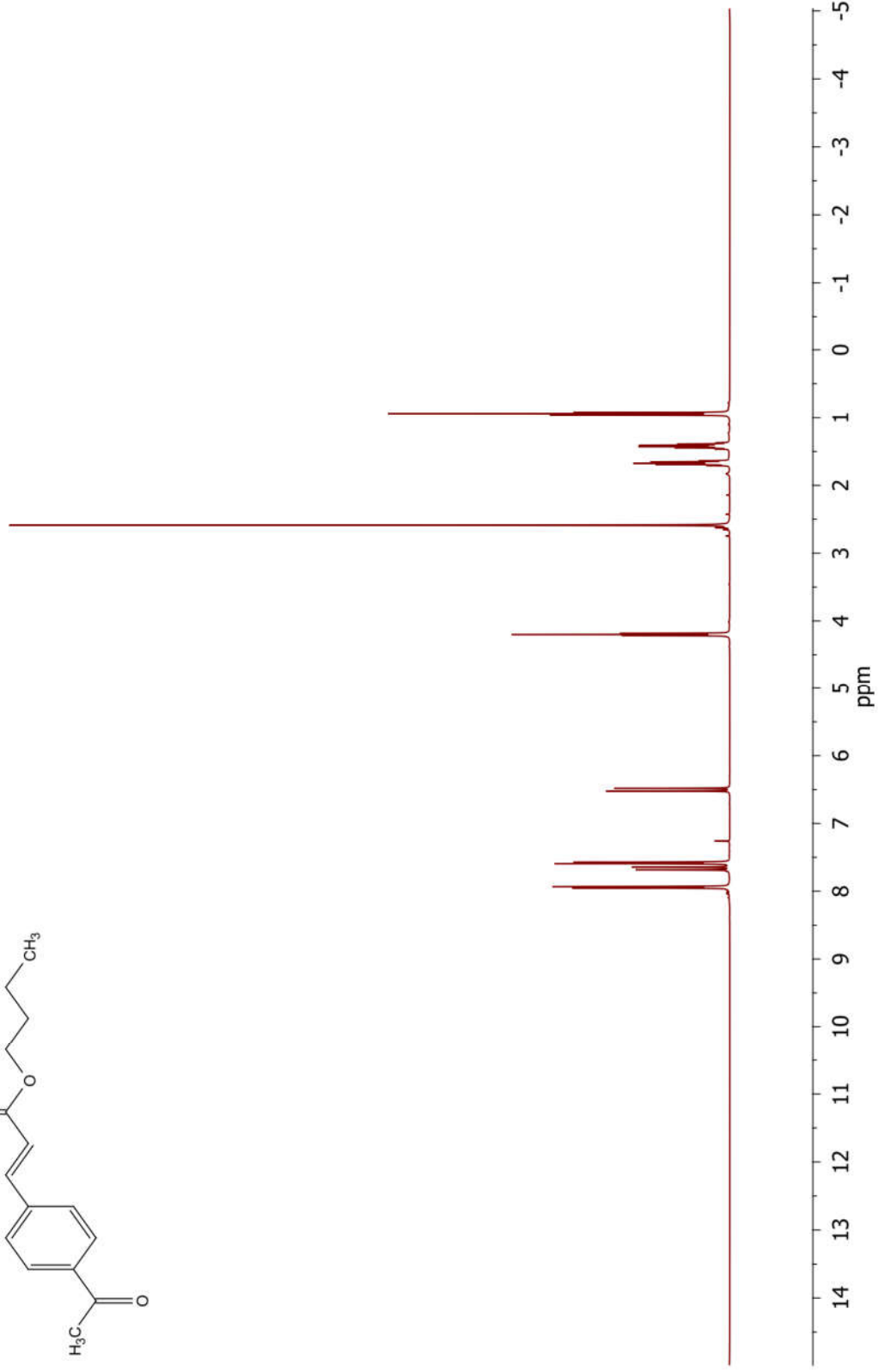
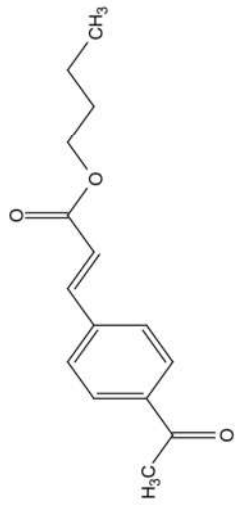
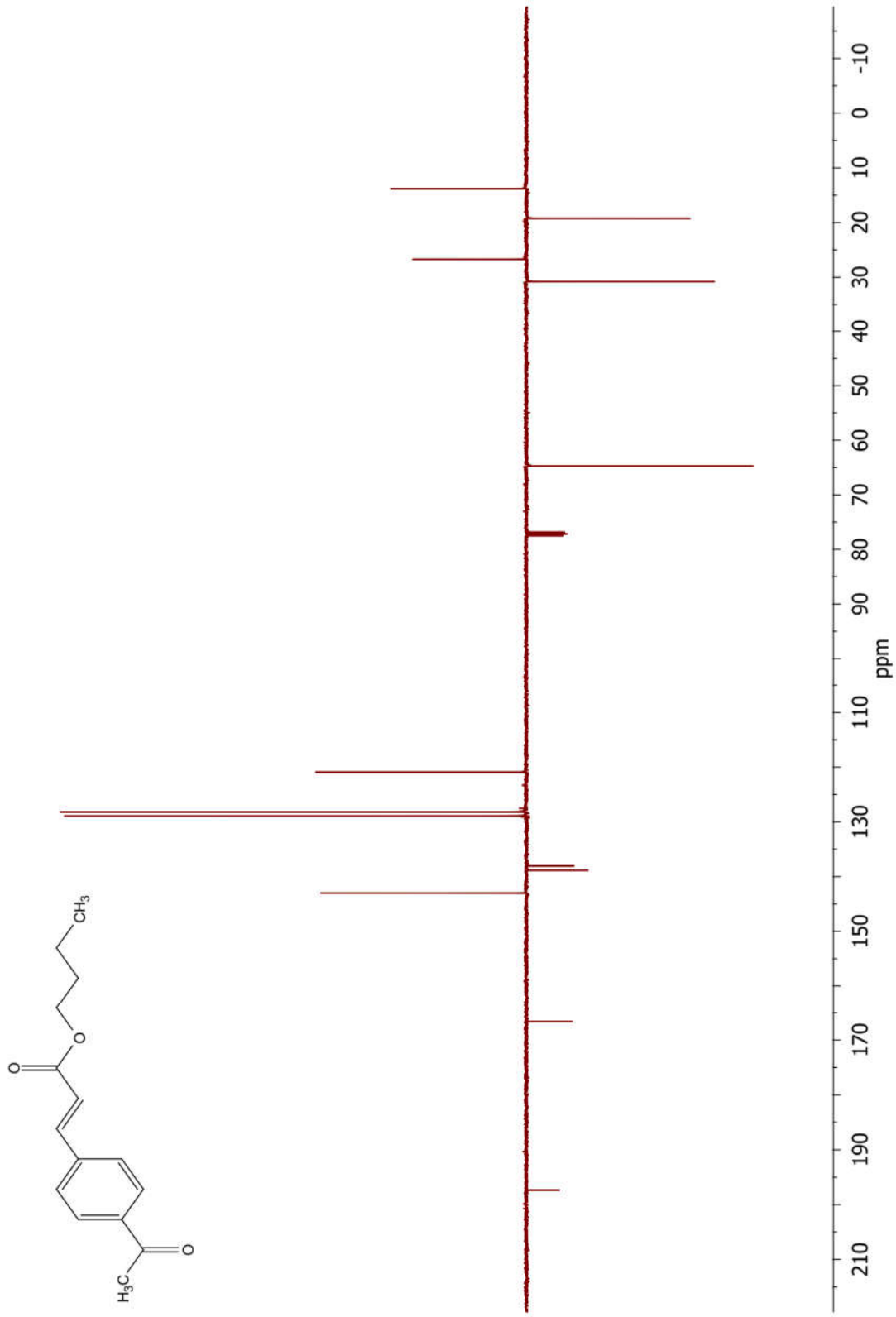


Figure S23.  $^1\text{H-NMR}$  spectrum of 3h



**Figure S24.** <sup>13</sup>C-NMR spectrum of **3h**

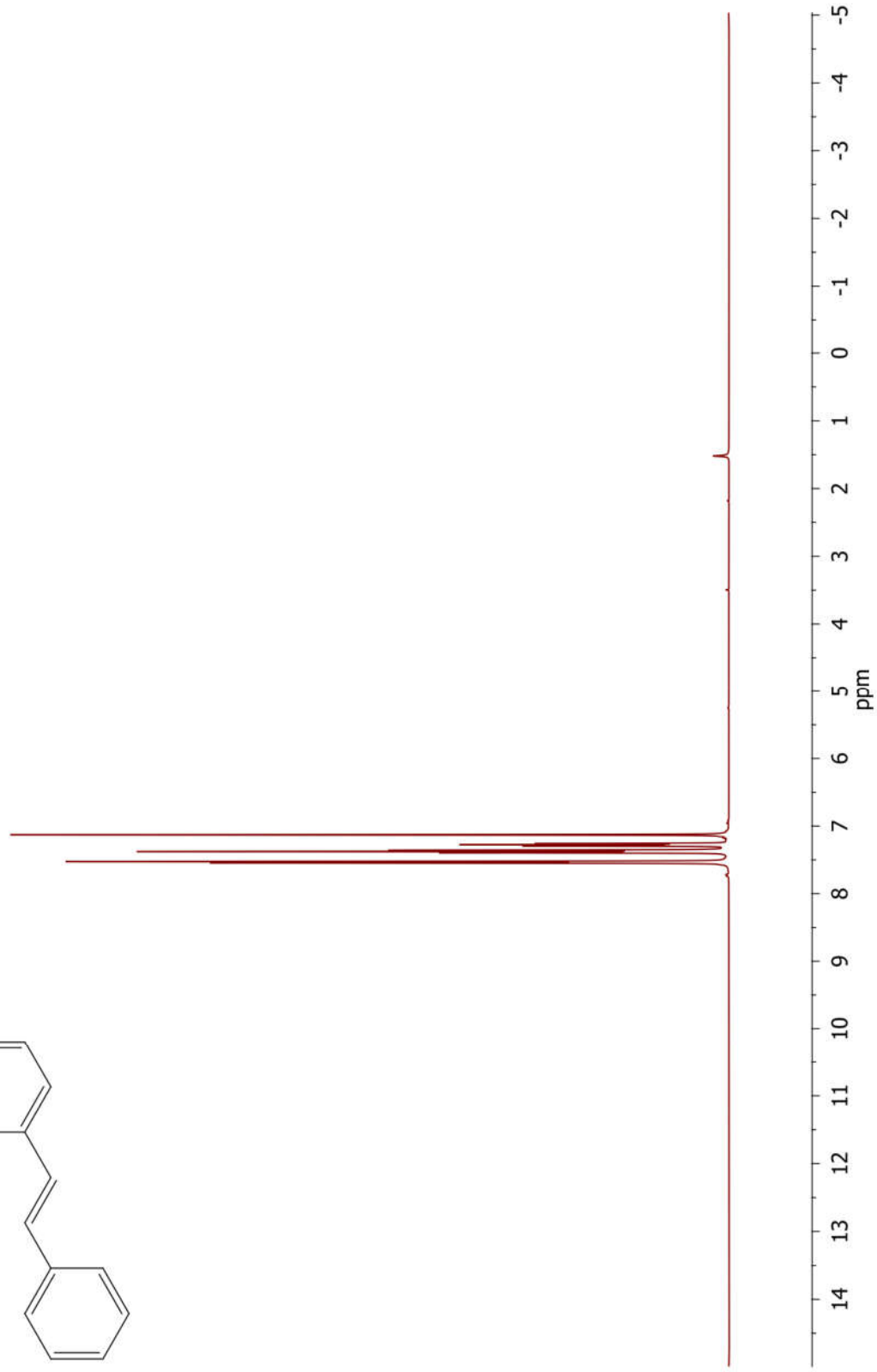
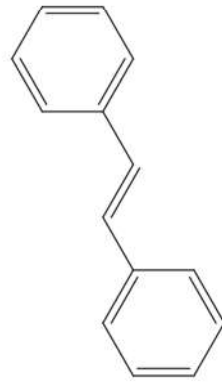
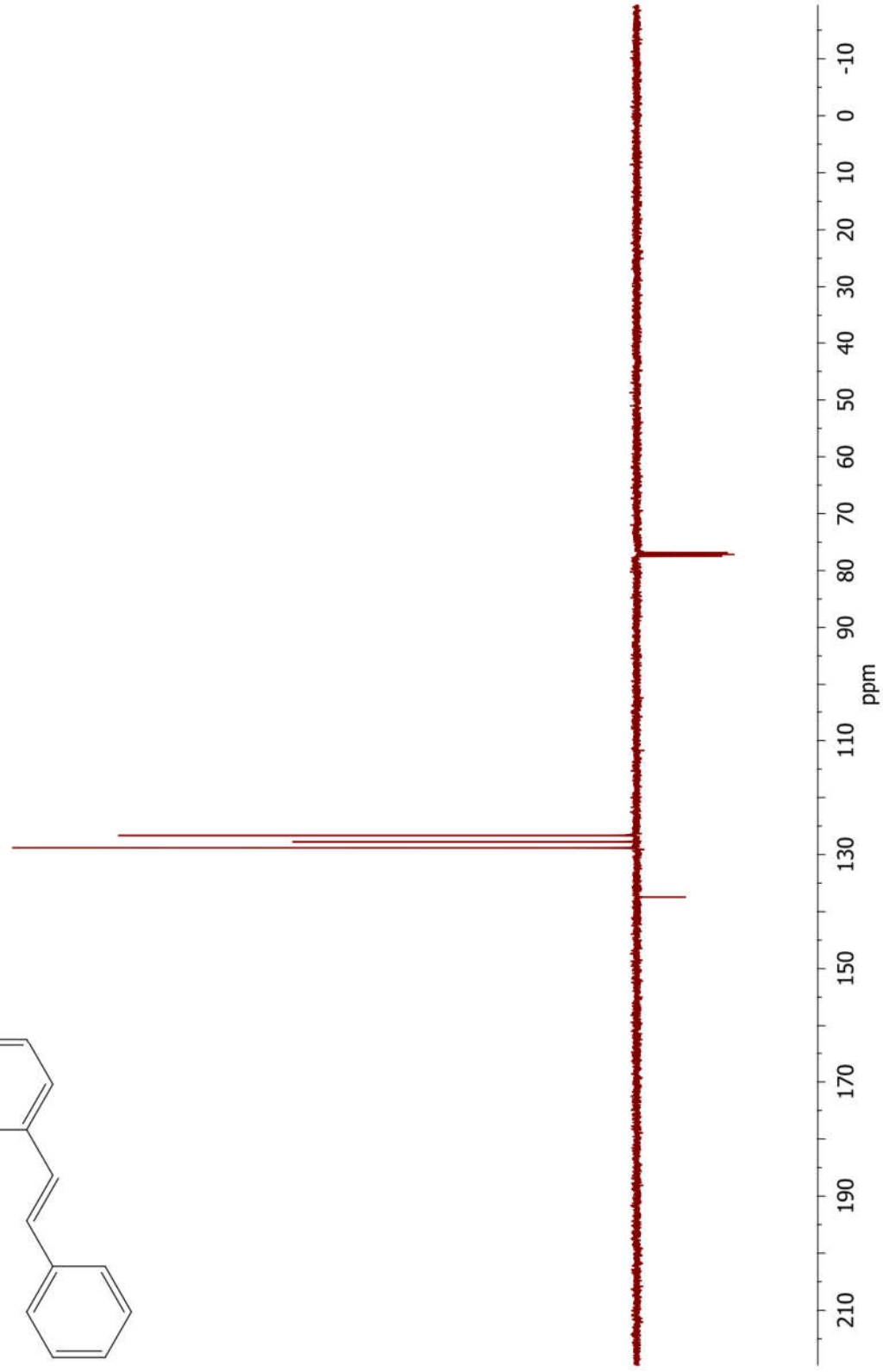
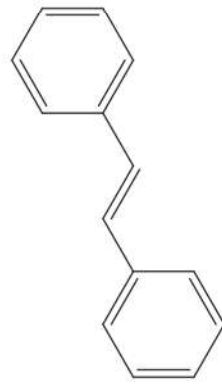


Figure S25. <sup>1</sup>H-NMR spectrum of 4a



**Figure S26.**  $^{13}\text{C}$ -NMR spectrum of **4a**



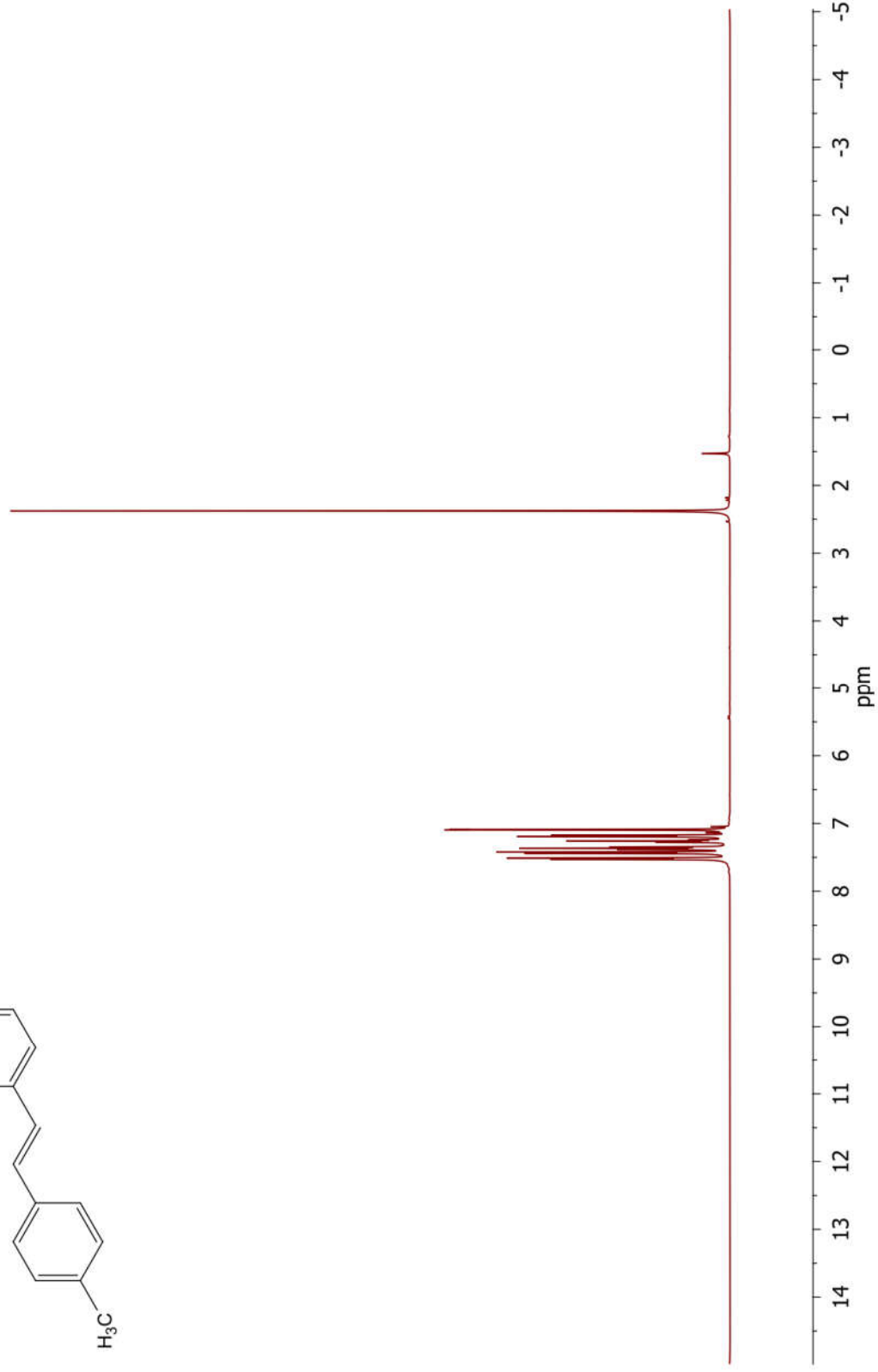
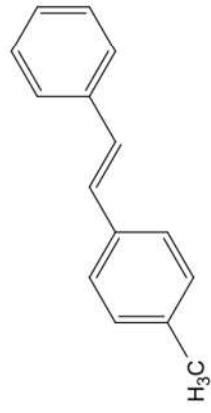


Figure S27. <sup>1</sup>H-NMR spectrum of 4b

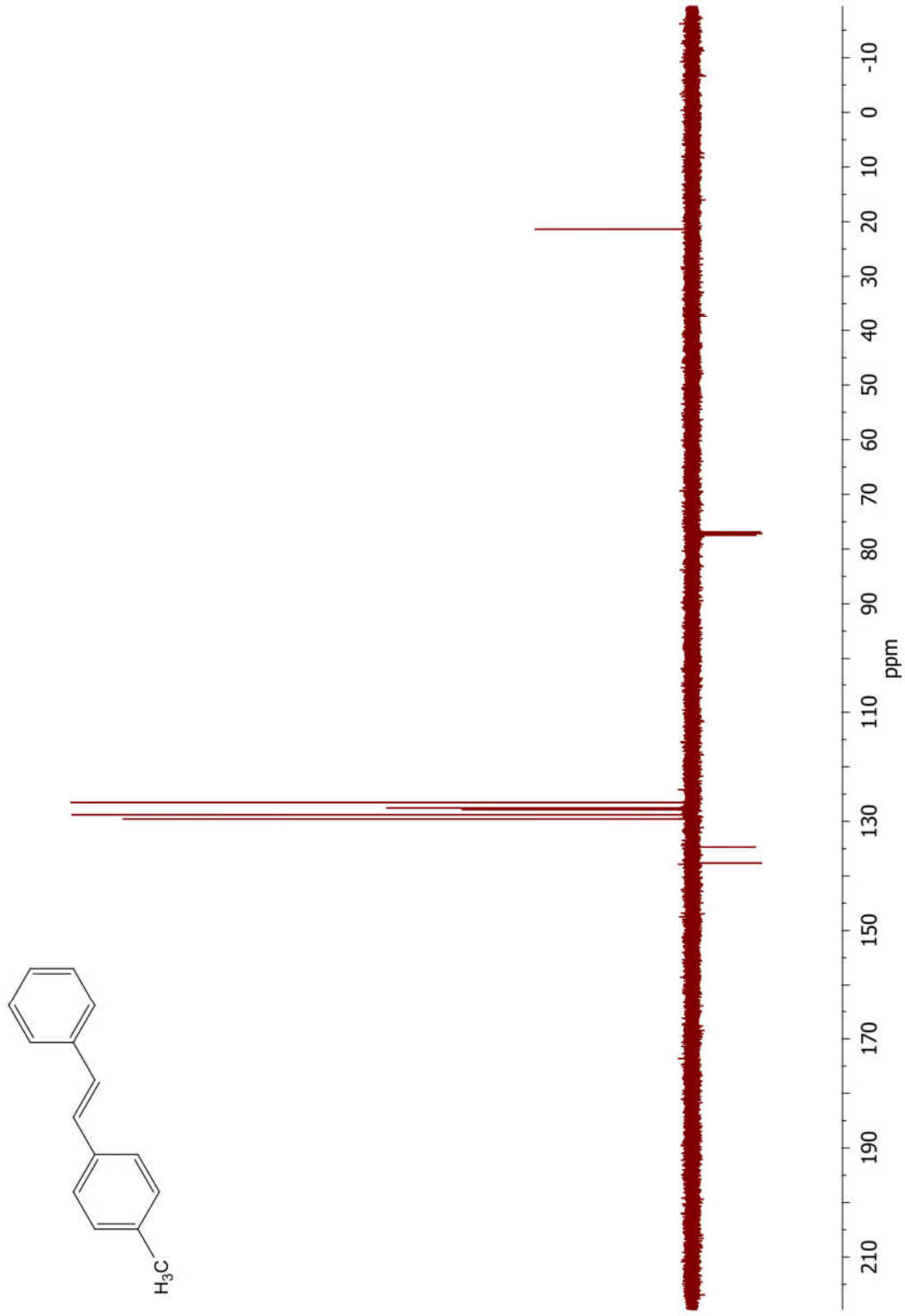


Figure S28. <sup>13</sup>C-NMR spectrum of 4b

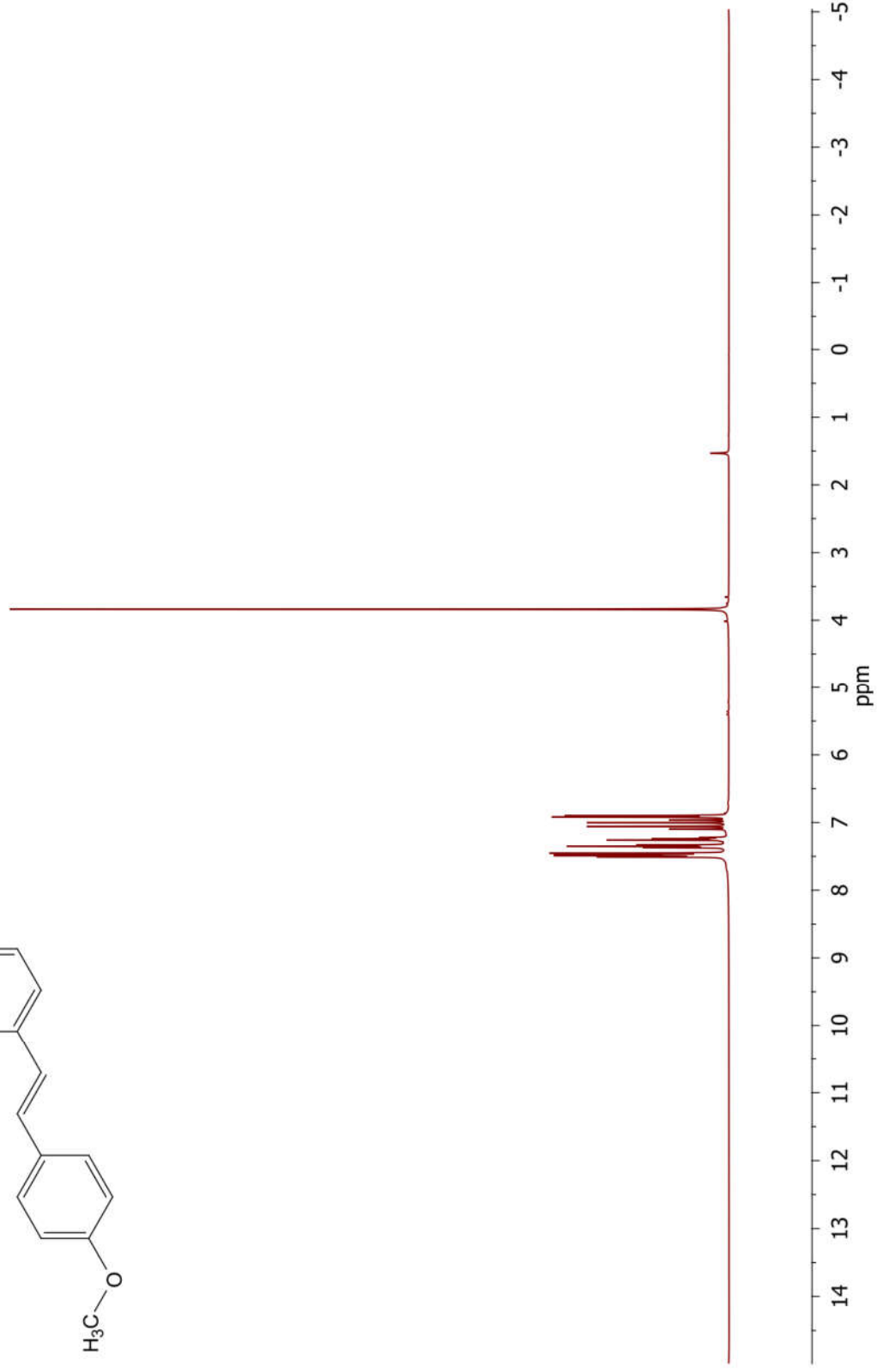
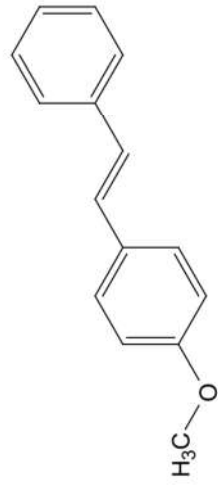
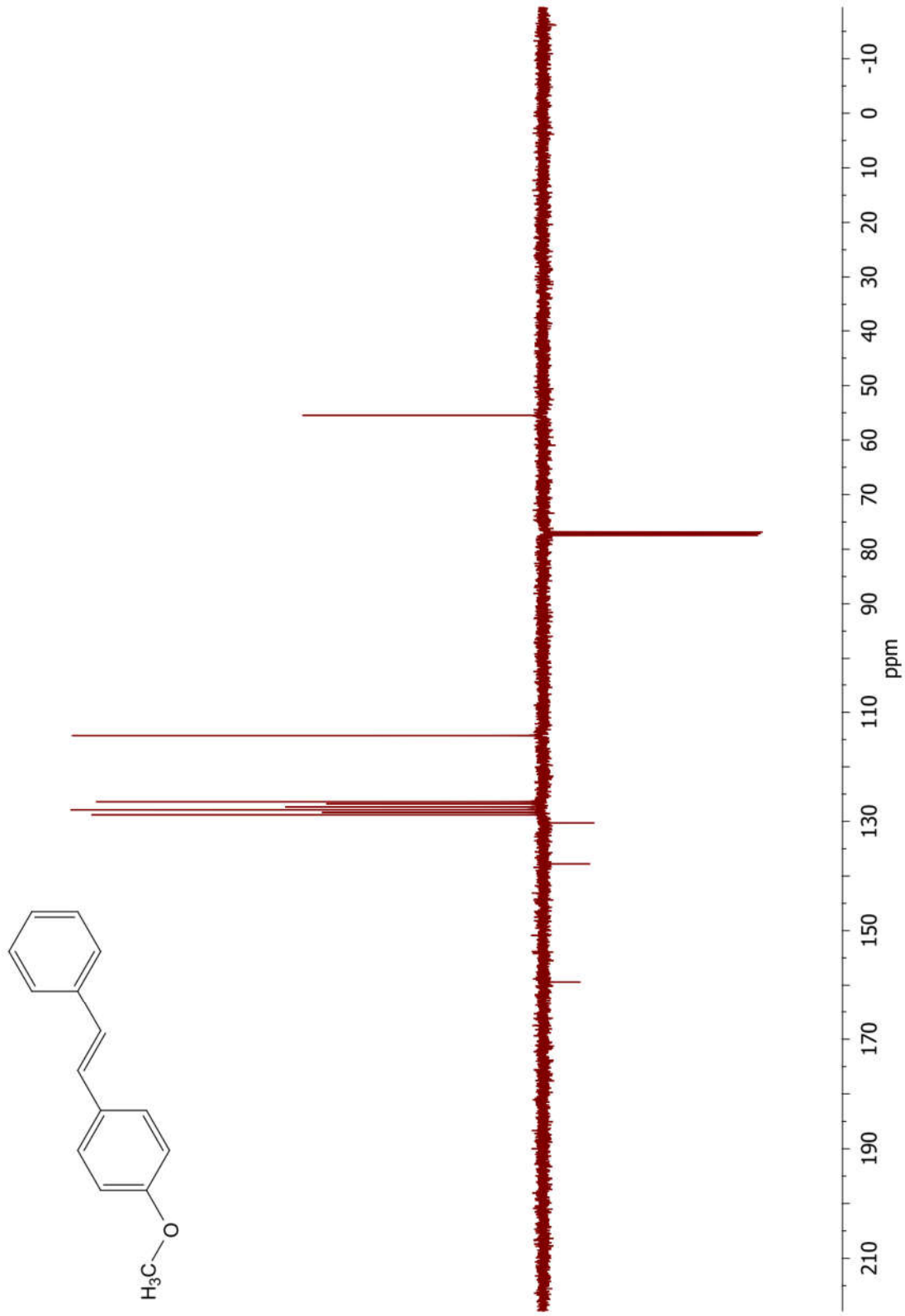


Figure S29. <sup>1</sup>H-NMR spectrum of 4c



**Figure S30.**  $^{13}\text{C}$ -NMR spectrum of **4c**

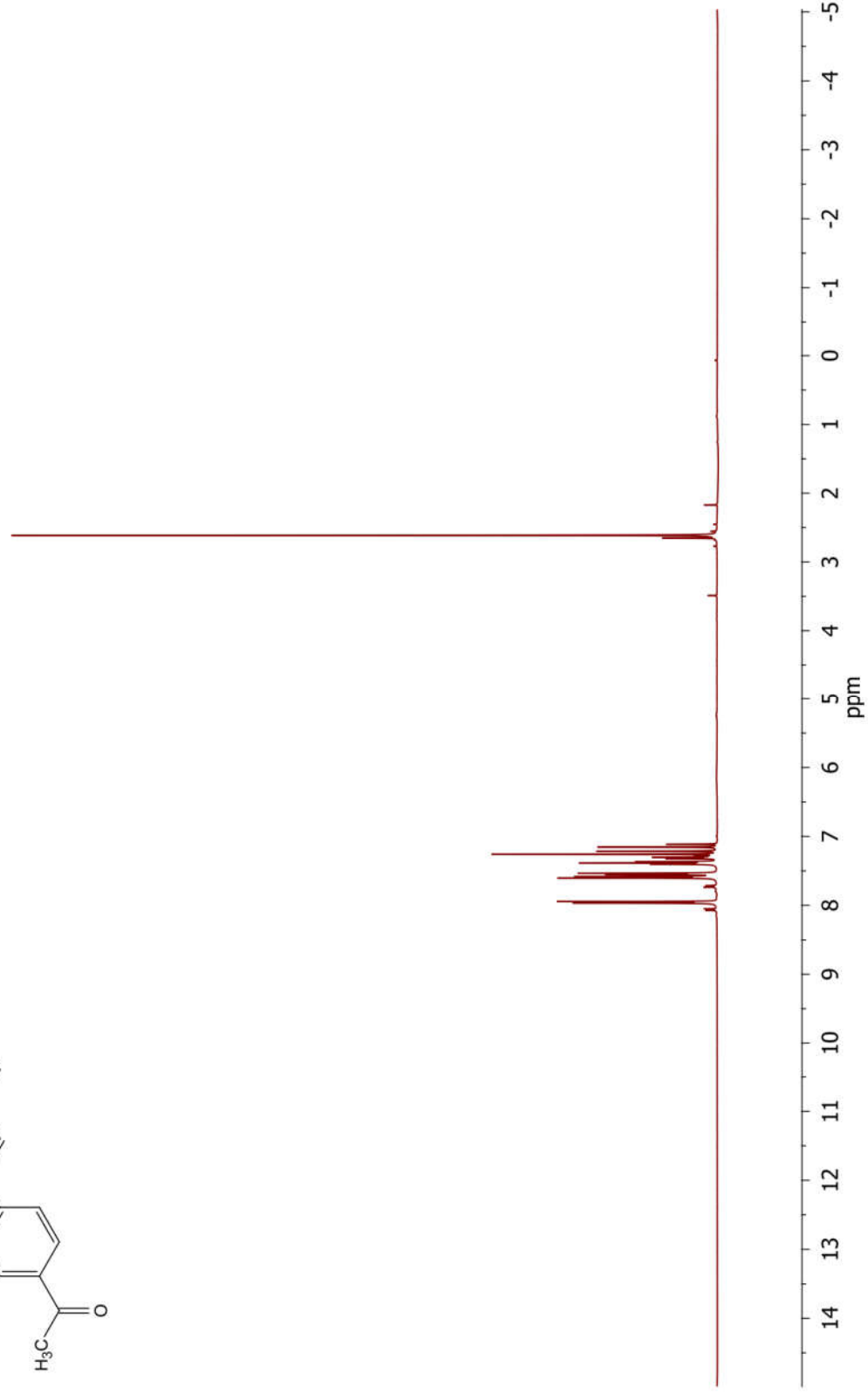
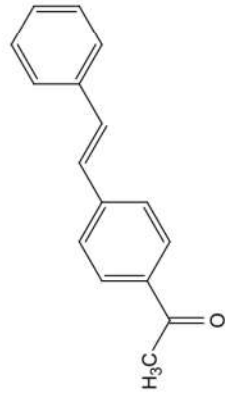


Figure S31. <sup>1</sup>H-NMR spectrum of 4d

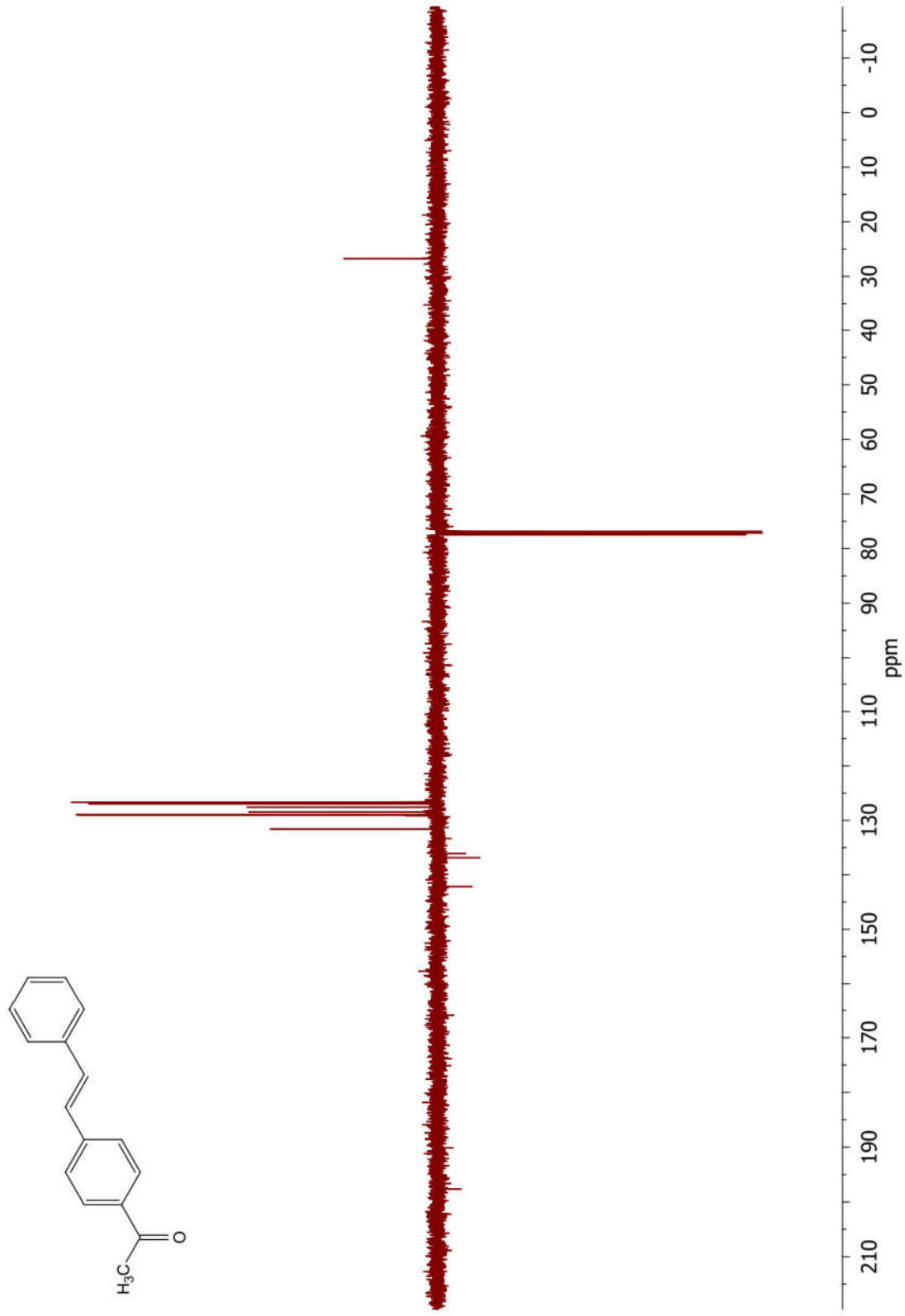


Figure S32.  $^{13}\text{C}$ -NMR spectrum of 4d

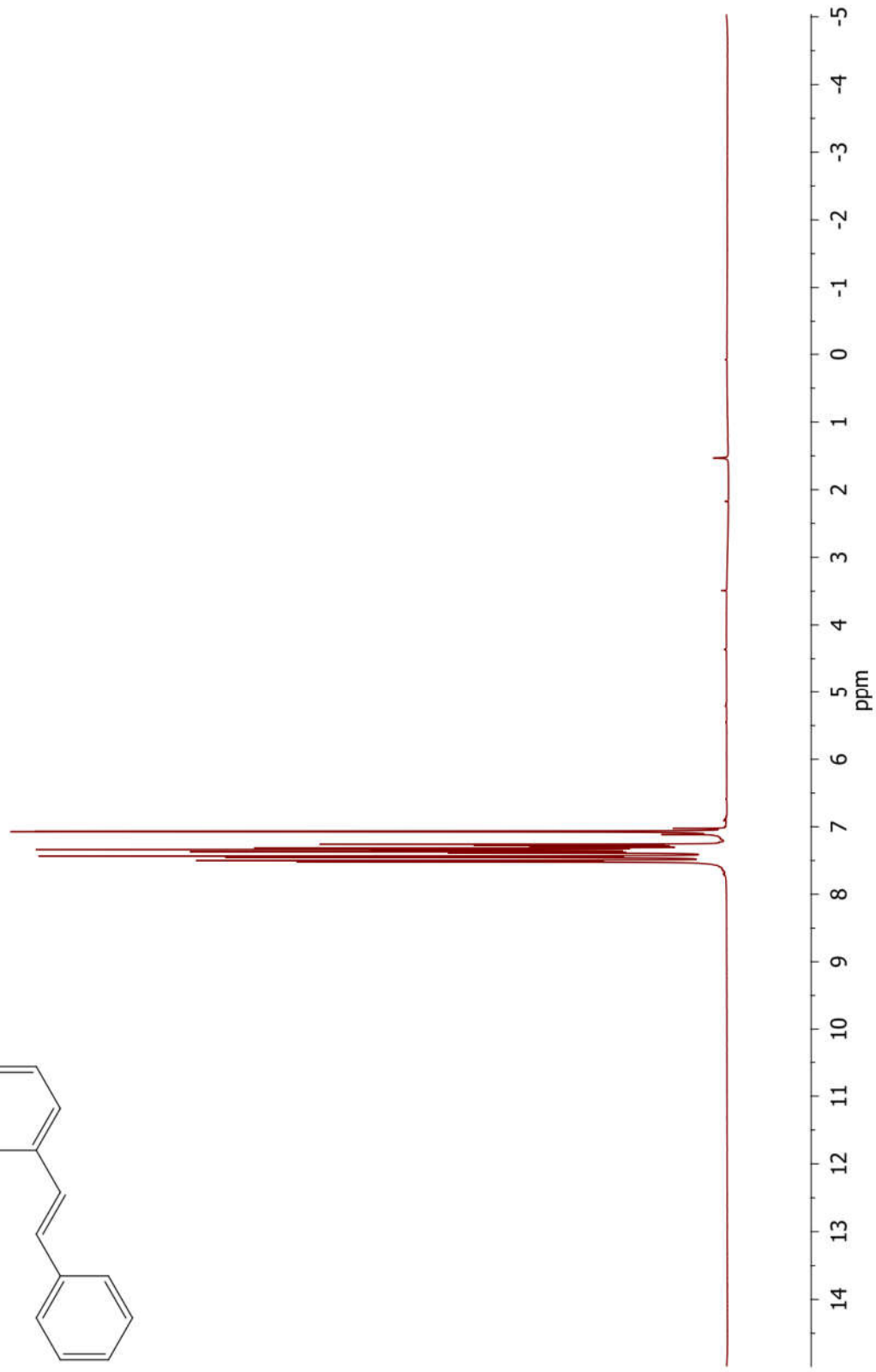
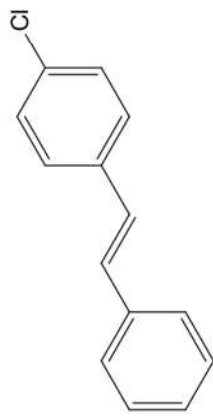


Figure S33. <sup>1</sup>H-NMR spectrum of **4e**

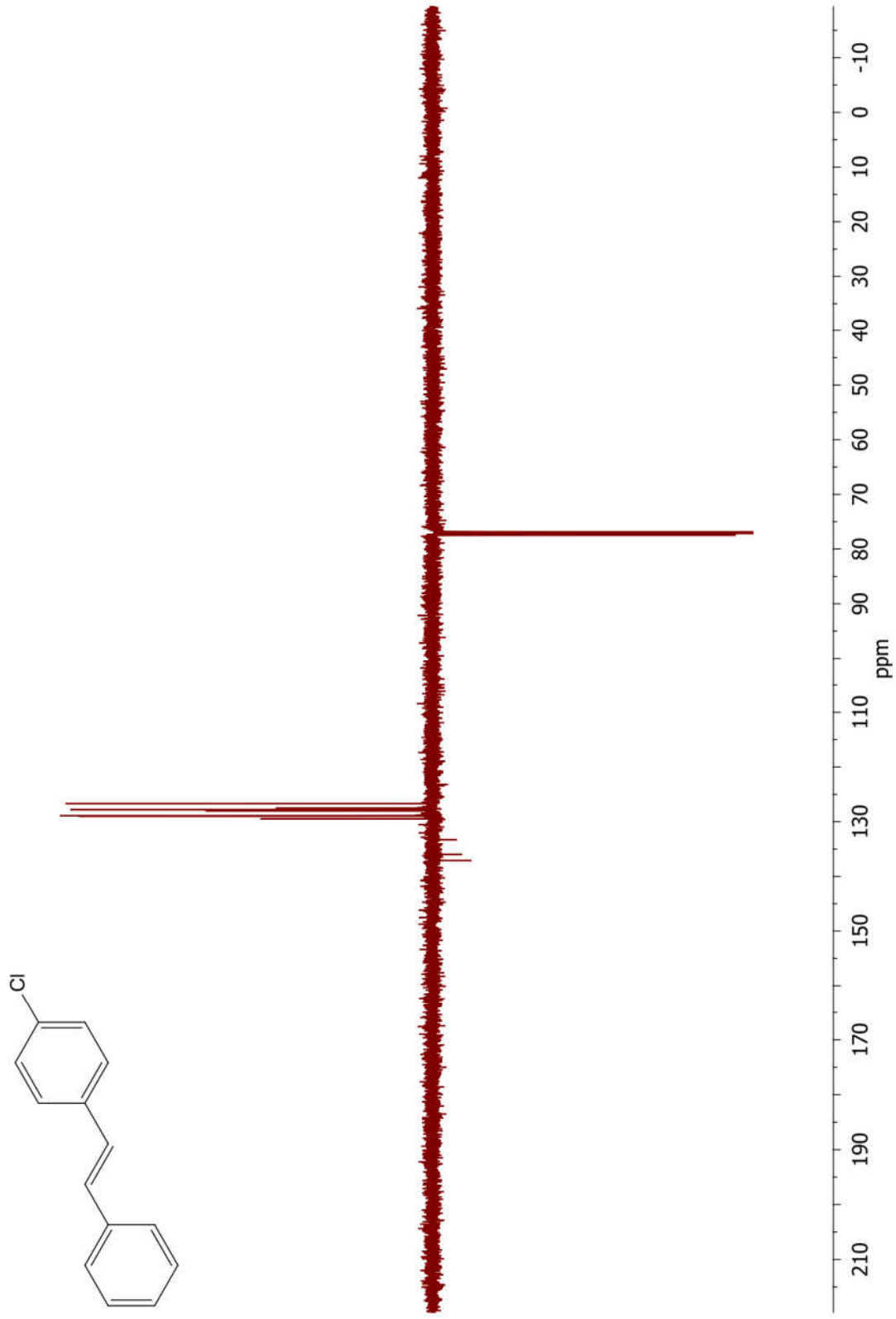


Figure S34. <sup>13</sup>C-NMR spectrum of 4e



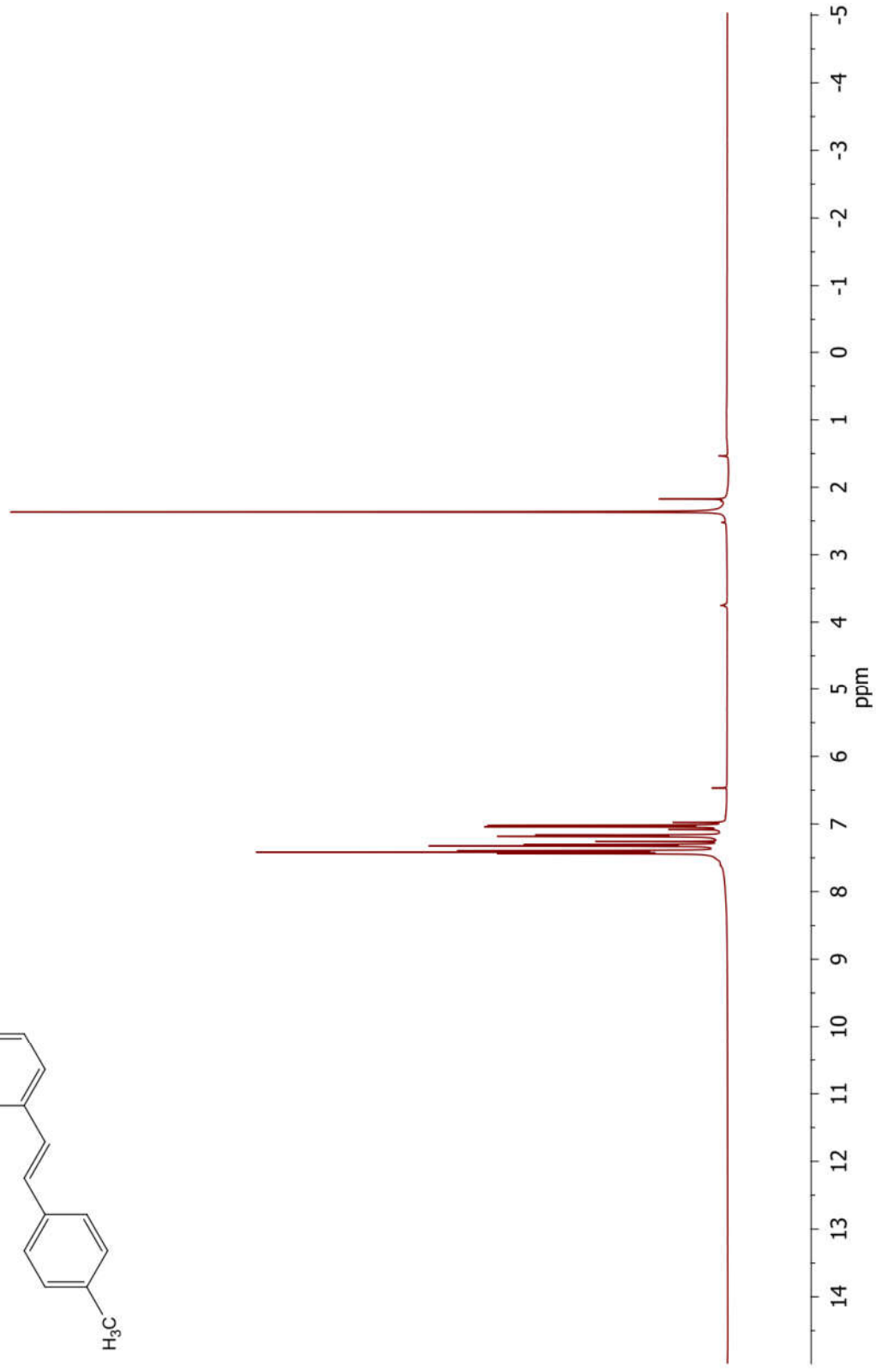
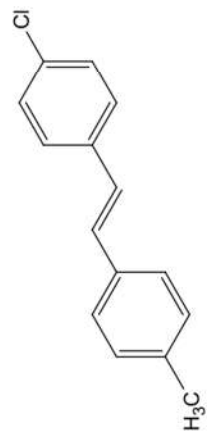


Figure S35. <sup>1</sup>H-NMR spectrum of 4f

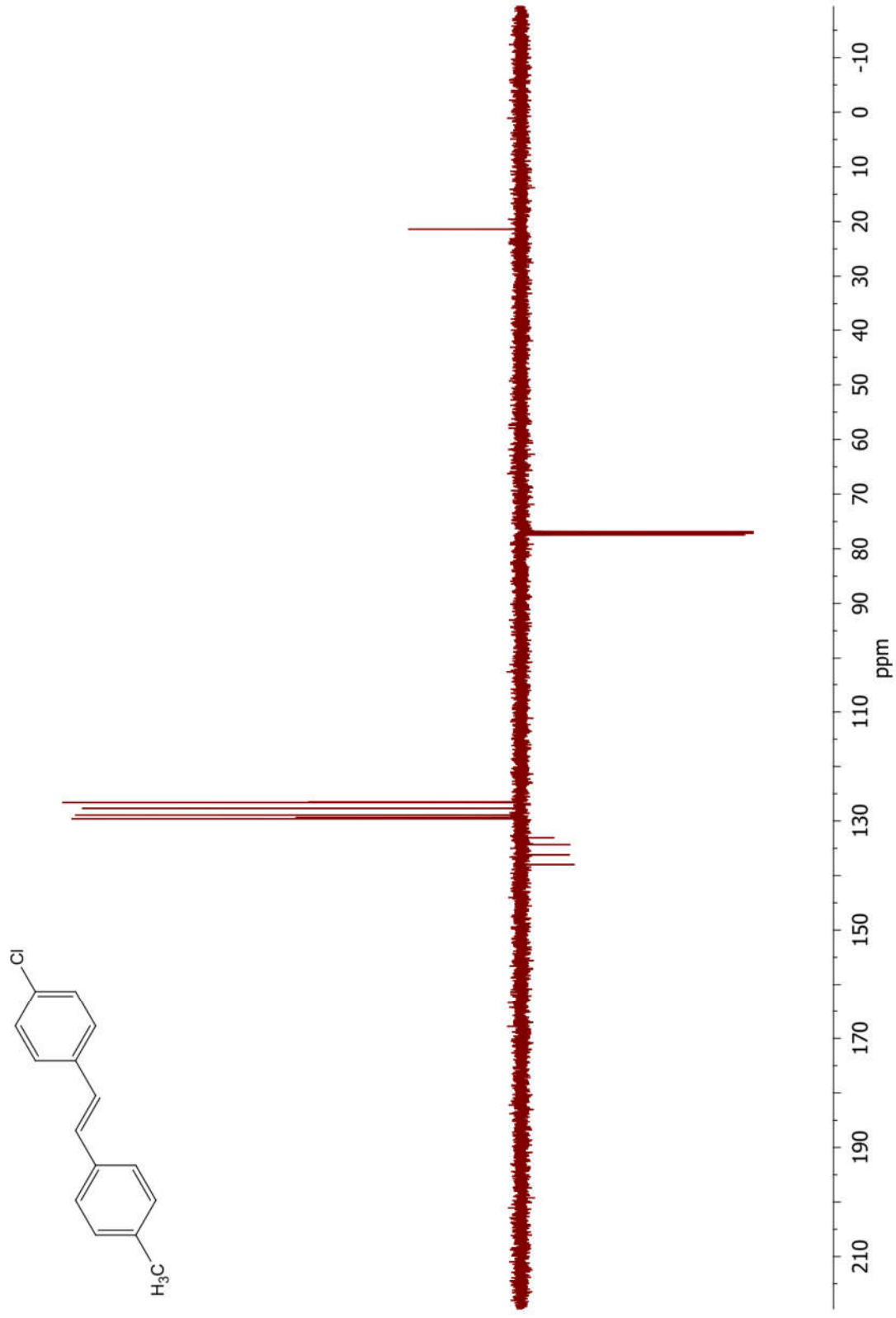


Figure S36. <sup>13</sup>C-NMR spectrum of 4f

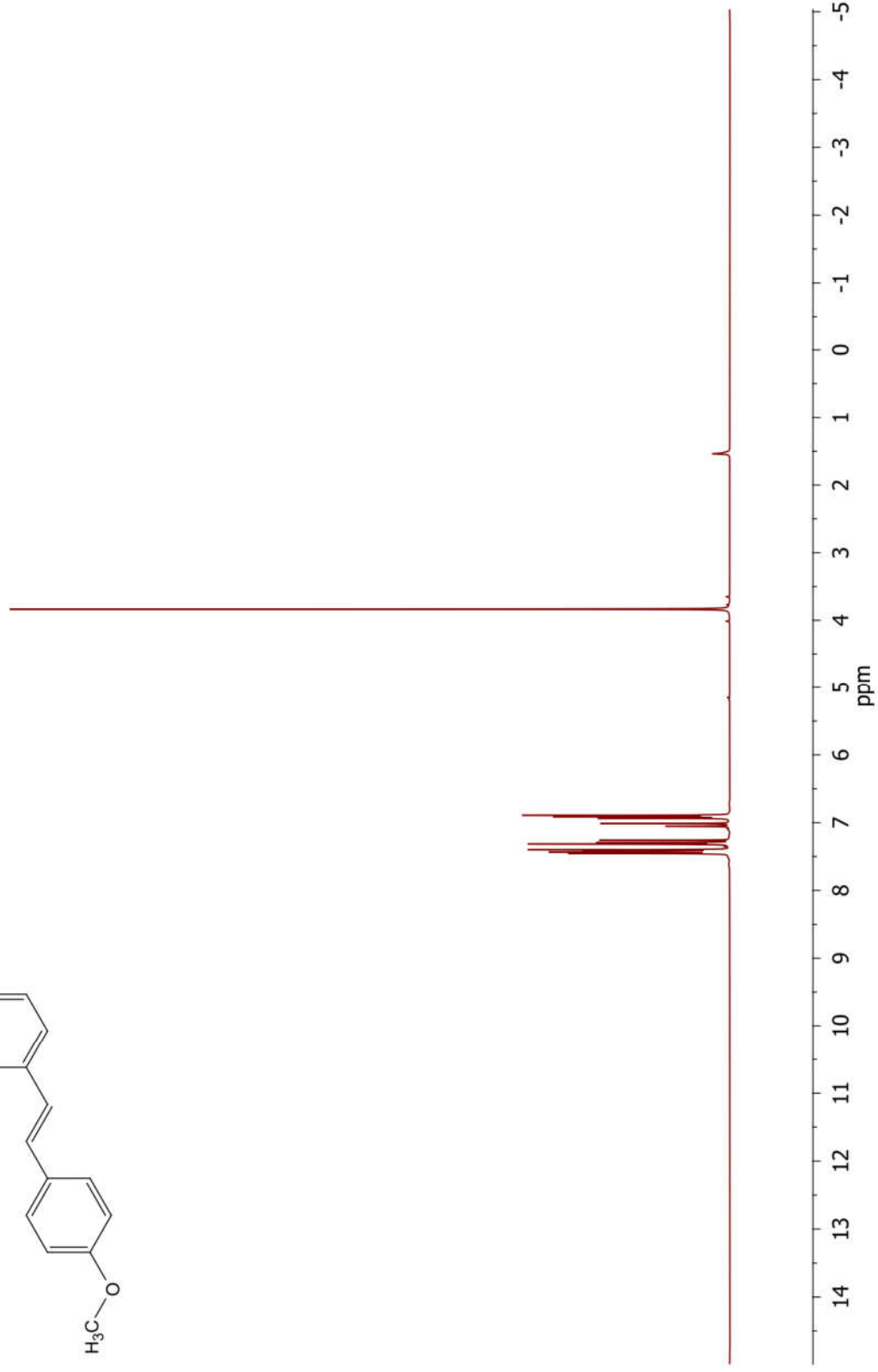
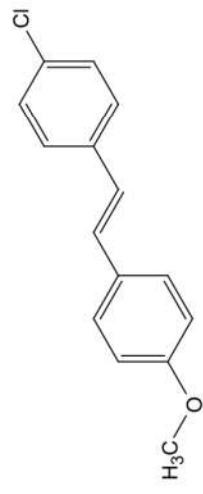
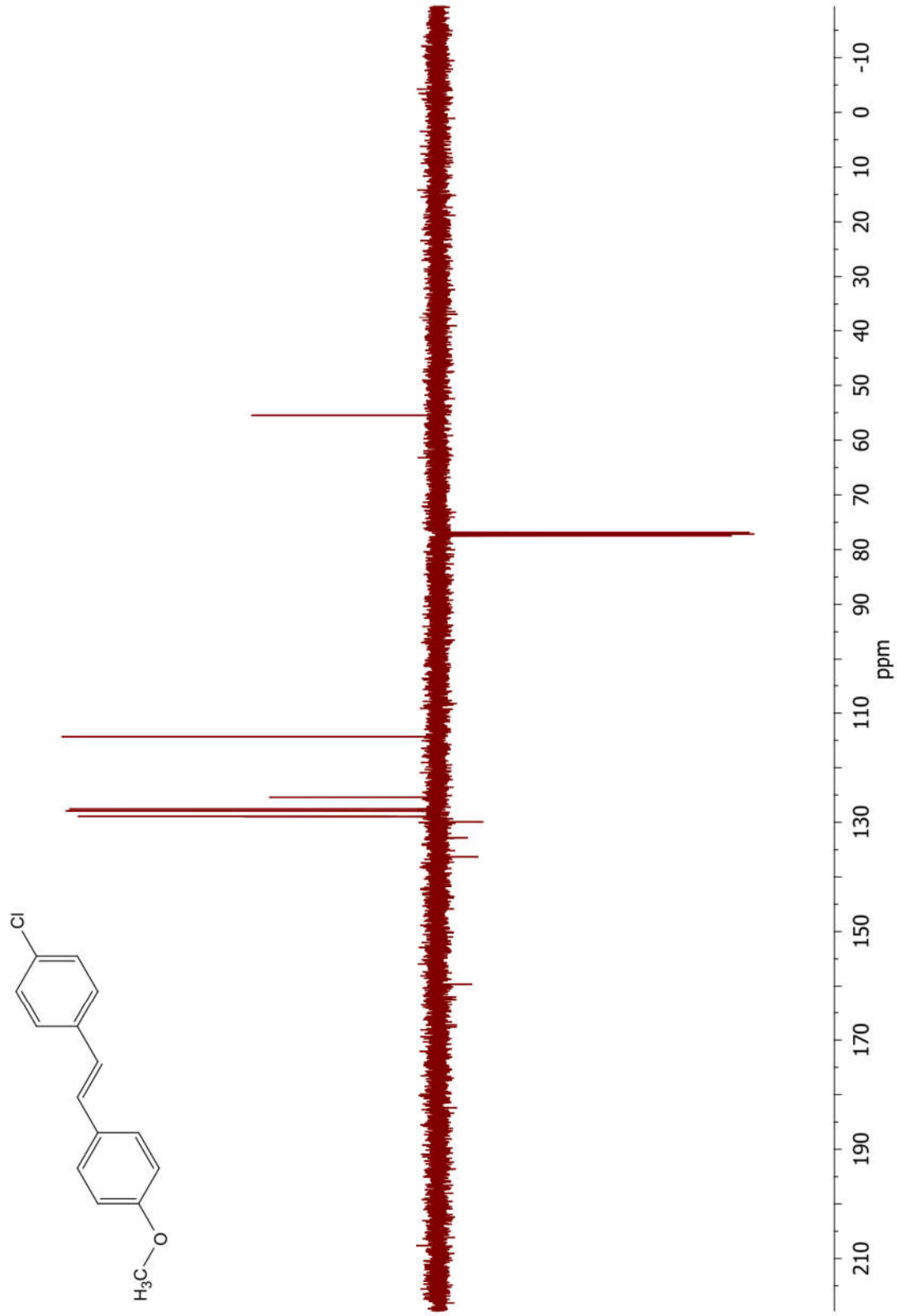


Figure S37. <sup>1</sup>H-NMR spectrum of 4g



**Figure S38.**  $^{13}\text{C}$ -NMR spectrum of **4g**

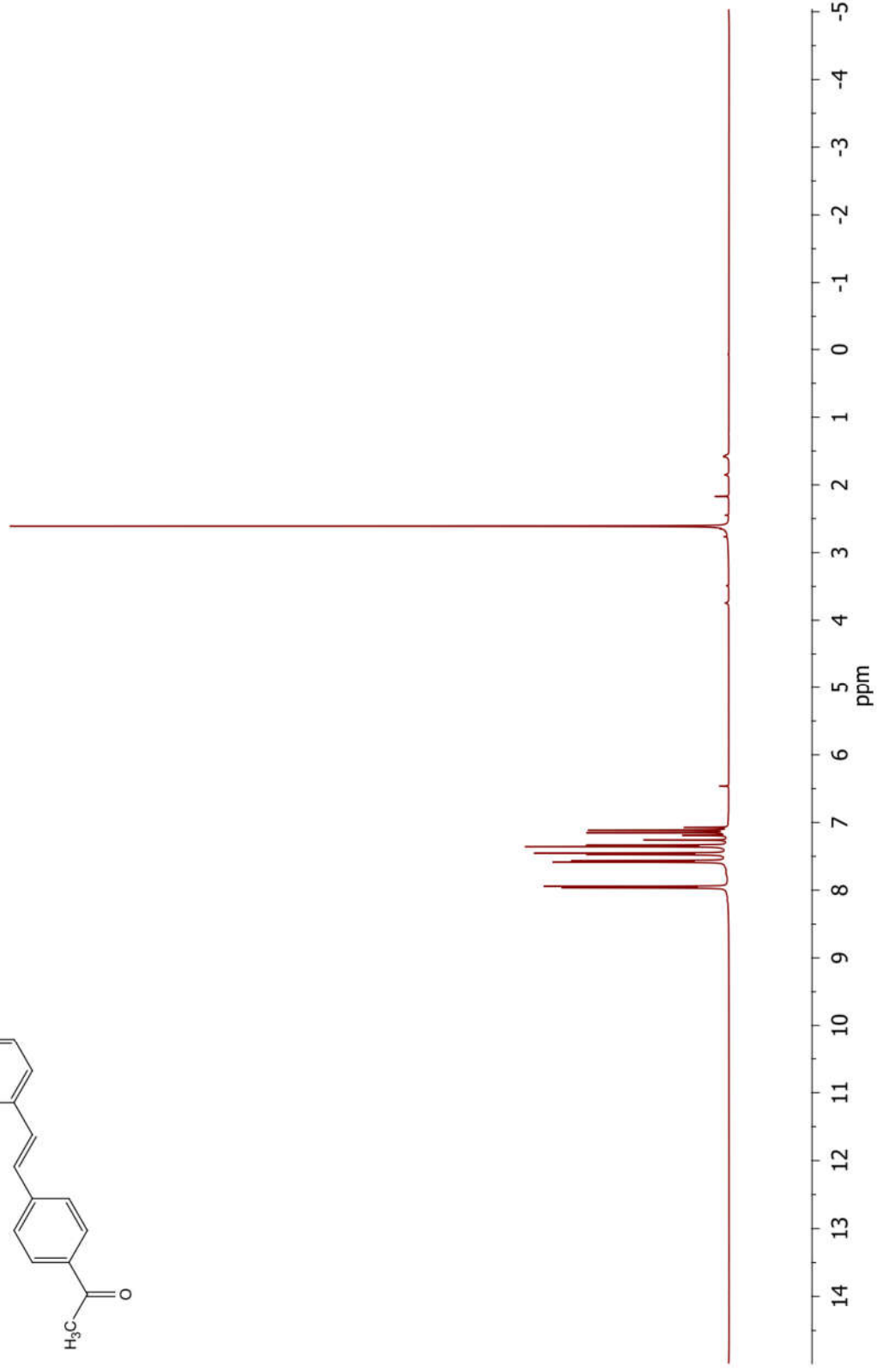
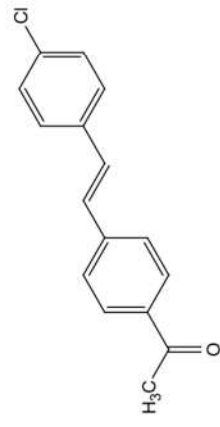


Figure S39. <sup>1</sup>H-NMR spectrum of 4h

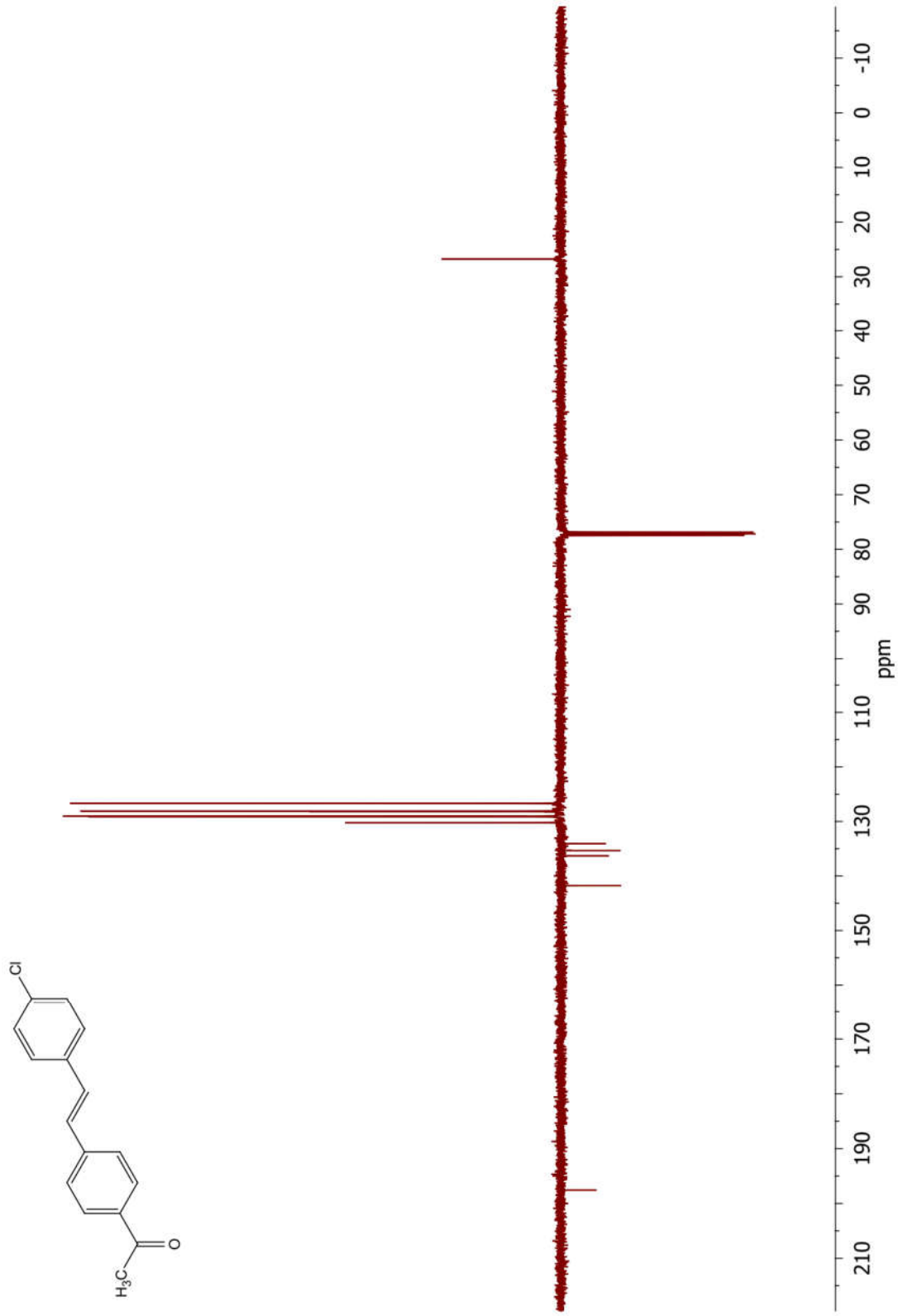


Figure S40. <sup>13</sup>C-NMR spectrum of 4h